NASA Technical Memorandum 85936

V/STOL Wind-Tunnel Testing

David G. Koenig, Ames Research Center, Moffett Field, California

National Aeronautics and
Space Administration

Ames Research Center
Moffett Field, California 94035

V/STOL WIND-TUNNEL TESTING

David G. Koenig
NASA Ames Research Center, Moffett Field, California 94035, U.S.A.

SUMMARY

Factors influencing effective program planning for V/STOL wind-tunnel testing are discussed. The planning sequence itself, which includes a short checklist of considerations that could enhance the value of the tests, is also described. Each of the considerations, choice of wind tunnel, type of model installation, model development and test operations is discussed, and examples of appropriate past and current V/STOL test programs are provided. A short survey of the moderate to large subsonic wind tunnels is followed by a review of several model installations, from two-dimensional to large-scale models of complete aircraft configurations. Model sizing, power simulation, and planning are treated, including three areas in test operations: data-acquisition systems, acoustic measurements in wind tunnels, and flow surveying.

SYMBOLS

A	aspect ratio, b^2/S, nozzle or jet area, m^2 ($in.^2$)
A_L	lifting element area $[n(\pi/4)D_L{}^2]$, m^2 (ft^2)
A_M	momentum area of aircraft ($\pi b^2/4$), m^2 (ft^2)
A_N	area of powered lift element, fully expanded; or equivalent nozzle area, m^2 (ft^2)
A_T	cross-sectional area of wind-tunnel test section, m^2 (ft^2)
b	wing span, m (ft)
B	test section width, m (ft)
c	wing chord, cm or m (in. or ft)
$\bar{c}$	mean aerodynamic chord, m (ft)
c_n	section normal force coefficient
c_p	pressure coefficient, $(p - p_\infty)/q$
C_{corr}	corrected coefficients
C_D	drag coefficient, total if not otherwise indicated, drag/(qS)
C_{DA}	aerodynamic drag coefficient, C_D (total) less effects of thrust and ram drag
C_J	jet thrust/qS
C_L	lift coefficient, total, (L/q)S
C_{LA}	aerodynamic lift coefficient C_L (total) less effects of thrust
C_{LAERO}	same as C_{LA}
C_m	total moment coefficient, moment/q $S\bar{c}$
C_{m_A}	aerodynamic moment coefficient less effects of thrust and ram drag
C_{meas}	measured coefficients
C_{si}	see Fig. 71
C_u	jet momentum coefficient $(m_j/q) \cdot (V_j/S)$
d	jet exit diameter ($\approx D_o$)
D	equivalent surface diameter of the suck-down plate, m (ft)
D_e	equivalent exit diameter, diameter of a circle whose area equals the sum of the areas of all jets, m (ft)
D_L	diameter of lifting element, m (ft)
D_n	diameter of nozzle, m (ft)
D_o	outside diameter of annular nozzle slot (the investigation of Ref. 35), m (ft)
F_x	force parallel to free stream, N (lb)
h	ground height, m (ft)
H	test section height, m (ft)
i_t	tail incidence, deg
IGE	in ground effect
K	angle-of-attack correction factor used in Ref. 52, $[3.537 - 1.256(1 - M^2)^{1/2}$
l	length, m (ft)
L	lift, N (lb)
m_j	mass rate of flow of jet, kg/sec (lb/m/sec)
M	Mach number
n	number of lifting elements
NPR	nozzle pressure ratio
OGE	out-of-ground effect
OASPL	overall sound pressure level
p	local static pressure, N/m^2 (lb/ft^2)
Pt	total pressure, N/m^2 (lb/ft^2)
P_∞	free-stream static, N/m^2 (lb/ft^2)
P_o	free-stream total pressure, N/m^2 (lb/ft^2)
PNL	perceived noise level
q	dynamic pressure, free stream unless noted otherwise, $1/2\ \rho V^2$, N/m^2 (lb/ft^2)
s	distance along jet, m (in.)
S	wing reference area, m^2 (ft^2)
SPL	sound pressure level
T	static thrust, N (lb)
Tc	thrust coefficient, [thrust/(q × fan area)]
V_B	moving belt speed, m/sec (ft/sec)

V_e	effective velocity ratio, $[qo/(T/2A_N)]^{1/2}$
V'_e	value of V_e at which the jet impinges on the floor, (see Fig. 66)
V_j	jet velocity, m/sec (ft/sec)
V_o	free-stream velocity, m/sec (ft/sec)
w_p	primary weight rate of flow, kg/sec (lb·m/sec)
w_s	secondary weight rate of flow, kg/sec (lb·m/sec)
x	streamwise or longitudinal dimension, m (ft)
y	spanwise dimension, m (ft)
z	vertical dimension, m (ft)
α	angle of attack, deg
α_g	geometric angle of attack, deg
β_v	deflector vane setting with respect to fan axis, deg
Γ	vortex circulation strength
δ_j	jet deflection, deg
Δ	difference or change in a parameter
Λ	wing sweep, deg
ρ	mass density of air

Subscripts:

c	corrected
e	effective
i	inlet
n	nozzle
o	free-stream conditions
u	uncorrected

1. INTRODUCTION

Wind-tunnel testing continues to be a key activity in aircraft development. It has been particularly necessary in the development of V/STOL aircraft because our understanding of the complex flow patterns affecting a powered-lifting system and formulations of prediction theories, has continued to lag the requirement to design and build a V/STOL aircraft. Our present ability to predict details of aircraft performance and of stability and control relies heavily on the use of integral flow modeling combined with paneling methods based on potential-flow assumptions. The solutions and computer codes that apply the methods must be efficient enough to be used with aircraft design optimization techniques. As computer capability improves, computational fluid dynamics (CFD) will be used.

In any case, wind-tunnel testing will figure in many stages of the aircraft development from the initial conception of the thrust-vectoring method using quasi-two-dimensional or semispan installations to testing of full or scaled models of the aircraft configuration. Even though we do not have complete and reliable computation methods with which to supplant wind-tunnel testing, they will, in whatever stage of development, be an integral part of the testing phase as means of correlating test results and, possibly, helping to restrict the size of the test matrix.

As indicated by the other lecturers in this series, and in the overviews on V/STOL concepts given in Refs. 1-3, it is a continuing objective in V/STOL development to make efficient use of all available on-board energy for meeting requirements in maneuverability, maximum speed, range, and short field lengths (at an affordable cost). The techniques in testing must be chosen carefully if it is to be ensured that the aircraft designer has well-documented test data (which verify predictions) providing him with sufficient information for preliminary design of the advanced version of the aircraft. At the same time, it is hoped that all the test data can be sufficiently documented using the proper instrumentation to make it valuable as a data base to be used for general aerodynamic study.

Because of these considerations, this lecture will concentrate on methodology with which an experimentalist must be intimately familiar in order to plan and complete a successful V/STOL wind-tunnel test program. The approach draws heavily on some of the factors mentioned in Refs. 4 and 5, and it is assumed that the reader can become familiar with the many other papers on V/STOL wind-tunnel testing, many of which will be cited throughout the lecture. It will also be assumed that the basics of Pope and Harper (Ref. 6) and of Pope and Goin (Ref. 7) are available. The lecture is organized into the following sections: planning: an introductory section outlining the development of a program; wind tunnels: a brief review of typical, moderate-to-large size, testing facilities; V/STOL testing installations: a discussion of options or categories of wind-tunnel installations; model development: a consideration of model sizing criteria, possible power systems, and construction techniques; test operations: a discussion of data acquisition systems, acoustic testing, and flow visualization.

Treatment is limited primarily to fixed-wing (V/STOL) testing as opposed to rotor-wing (helicopter) testing. The author assumes V/STOL also applies to the tilt rotor or even to such designs as the X-wing (which will not be mentioned), but there will be no treatment of rotary-wing testing.

2. PLANNING AND PRETEST PREPARATION

Before all the available tools for V/STOL wind-tunnel testing are evaluated in detail, the essential objectives of the program must be considered, and, to a certain extent, the data analysis be addressed. Unfortunately, such factors as budgets, time restrictions, continual technological advancements, and military/commercial objectives prohibit writing this part in a textbook fashion, particularly for an aircraft development program. This is true for most new experimental efforts, but is particularly true in V/STOL wind-tunnel testing, where the amount of available testing time can be severely restricted because of high wind-tunnel operational costs and costs required to support on-site testing.

The planning sequence will be discussed briefly as follows:

1. Objectives of all testing
2. Test parameters to be considered
3. Model design
4. Wing-tunnel installation
5. Instrumentation and data acquisition
6. Program management

2.1 Objectives

Definition of objectives for V/STOL wind-tunnel testing must include considerations in two areas: (1) establish the overall aerodynamic factors to be obtained from the test that will be essential to the program involved, and (2) obtain an overall feeling for and commitment of the support available for the program (financial and otherwise). For a development program, for example, this can mean obtaining a decision based on studies as to how significant additional aerodynamic lift is related to the aircraft mission weight and cost. Obviously the two are interrelated to the extent that in the end analysis, the available support establishes the complexity of the model and the type of wind tunnel that can be used. Examples of past wind-tunnel programs with various levels of each factor are shown below.

	Factor	
	Aerodynamic scope	Project support
Jet-in cross flow	Component tests	Minimal budget
USB large-scale tests	Complete model	Low budget
Tilt nacelle tests	Component tests	Low budget
Grumman 698	Complete	Large budget
AV-8B 40 by 80 tests	Complete aircraft configuration	Large budget

It should be understood that any of these cases could vary widely in model complexity and instrumentation requirements. The second factor, project support, will not be included in any further discussion but the principals in "aerodynamic scope" will be addressed. An additional item concerning the above test installations is the possible justification for large-scale testing. This will be addressed in a following section.

2.2 Test Parameters

For most wind-tunnel test planning, Margason (Ref. 5) has provided an excellent checklist defining the objectives of an investigation. As is usually the case for any wind-tunnel investigation of complete configurations, the test results will include aerodynamic forces and moments for performance and stability. These characteristics may include aerodynamic propulsion-induced effects for transition flight (Fig. 1) as well as hover. Throughout this flight regime the test parameters must be chosen to define the complete flight envelope with assurance that the thrust effects are obtained. The configuration variables should be chosen and the construction of the model planned so that significant variables, such as flap settings or nozzle deflections, can be evaluated. It is at this point that a judgment in the importance of exact duplication of all aircraft details be made. In planning for either a small wind-tunnel model or in large-scale testing (Ref. 4), this cannot be completely accomplished for a number of reasons; as a result, a concentrated effort should now be made to establish areas in which direct duplication of the full-scale aircraft are not essential for evaluating aircraft flight characteristics.

2.3 Choice of model

It is at this point that the model design factors, such as model size, facility availability and model systems, should be considered as part of the planning. This will be directly influenced by factors discussed in appropriate sections of this lecture. However, there are several general considerations that can be made at this point.

2.3.1 Model size

Anticipated scale effects can have varying significance on the choice of model size depending on how close to production the aircraft to be investigated is, how well defined the details of the final configuration are, and how significant the local areas of flow separation are in their effect on the data. For purposes of discussion, model scale will be referred to as small, less than 0.2 scale, moderate, 0.2-0.5, and large, larger than 0.5 scale. For exploratory investigations with simplified models and for low flap settings and angles of attack, and where accurate corrections are possible, small-scale models can be most economical and produce reliable wind-tunnel test results. This certainly was the case in the early AV-8B development (Ref. 8) in which a powered 0.15-scale model was developed by modifying an available flow-through nacelle model. The resulting comparison with large-scale tests (Fig. 2) showed good comparisons with full-scale data in the linear angle-of-attack range. As might be expected, control and flap lift were slightly lower for the small-scale (Ref. 9) tests. More factors about both the large- and small-scale investigations will be discussed later since they are classic examples of coordinating both large- and small-scale aerodynamic testing in V/STOL aircraft development.

As noted in Ref. 4, there have been several well-documented demonstrations of the significance of scale effects. These are reprinted in Figs. 3 through 7. For components of models, the actual size or local Reynolds numbers may be very small compared with that of the complete aircraft configuration. This was the case for the examples shown in Figs. 3-5, where the small-scale data indicated lower stalling angles for the inlet, deflector vanes, or leading-edge slats. On the other hand, there may be a "size effect" for the complete aircraft configuration such as the one for the small- and large-scale installations of Fig. 6 (deflected slipstream transport model). The large-scale model was powered by PW JT15D engines and tested in the Ames 40- by 80-Foot Wind Tunnel. The small-scale model was powered by ejector propulsion simulators, and the relative size and shape of the 40 x 80 test section were simulated. The differences in the two sets of

longitudinal characteristics, shown in Fig. 7, are probably not only scale effects but may be due to the nonsimilarity in both inlet and exit flow, particularly where jet efflux and its velocity profile effects the induced lift from the flap.

2.3.2 Power Systems

The previous example of the importance of simulating the jet efflux in any powered-lift test is one of many which can probably not be completely documented but in which wind-tunnel testing produced erroneous performance estimations of the aircraft flight characteristics. As is discussed in Sec. 5.2, the current trend is to attempt to simulate the actual engine flow including bypass ratio. The CMAPS (see Sec. 5.2.4) is such a device on which its full application potential is currently being evaluated. The ejectors, developed in the 1960s and which powered the smaller model of Fig. 6 produced a uniform exit flow but were limited in exit pressure ratio and did not simulate the inlet flow rate for a given thrust level. A very valuable workhorse has been the tip-driven fans which have been built in several sizes up to more than 12 in. The driving factor in the use of any of these propulsion simulators is the need to get high-pressure air into the model and, if the forces and movements of the entire lifting system are required, that air must be "jumped" across the sting or wind-tunnel balance. The flexible lines, coil, or other transfer means can have significant effects on the design and cost of the model. At this point, if large- or full-scale testing is contemplated, several schemes of building a large but subscale model such as that of Fig. 8 should be considered. In this case, a model was built using 2-J97 turbojet engines which were 0.7 scale of a two-engine fighter design (see Sec. 5.2). Planning for the power system must be integrated with other considerations, including the compatibility of the facility with the wind tunnel.

For rotary-wing projects, the power systems for some generic rotor tests are variable frequency electric motors. For example, the Ames 40 x 80 rotor test bed shown installed in Fig. 9 is driven by two 1,500 hp variable-frequency motors coupled together. Air-driven and hydraulic-powered motors are also used for small-scale rotor tests.

2.4 Wind-Tunnel Installation

At this point in the planning sequence, the investigator must have a working plan that includes the aerodynamic experiments needed to meet his objectives and must consider what model support and wind-tunnel test facilities are required. A table might be assembled similar to the one shown in Table 1 for in-flight jet noise simulation; it is described in Ref. 10. A section in this lecture covers typical wind-tunnel facilities that are available. Let it be stressed that for the particular demands of V/STOL testing, any choice should include consideration of the equipment and staff that could be made available to the program. Reference 11 or its equivalent will provide important parameters of candidate wind tunnels, but a meeting with the staff of each facility should be held to determine availability. Topics pertinent to V/STOL testing, among many other details should include:

1. Availability of electrical power or high pressure air.

2. Model motors and engine simulators available and maintenance required.

3. Capacity and currency of data-acquisition systems; the value of planned testing depends on reliable documentation of power for each test condition, and this is probably one of the most important topics in the planning.

4. Model support and balance hardware: for rotary-wing testing, few wind tunnels are currently equipped with all the support hardware needed — meaning added cost to the experimenter. For air-driven tests, rotary wing or otherwise, metering and air-transfer equipment are essential topics.

5. For acoustics tests, factors listed in Ref. 10 should be discussed.

6. For large- or full-scale testing, using gas turbine engines, specific items such as maintenance required, fuel, fire control, hydraulics, and start-stop requirements should be discussed. For the Ames 40 by 80, length of testing before temperature limits are reached is an important consideration, although planned improvements in ventilation will extend these limits.

After power systems and wind tunnels have been adequately considered, it is recommended that the combination of model scale or size and type of wind-tunnel support be readdressed. The important factor of magnitude of wall-constraint effects for all projected test conditions may never be answered until after the testing is complete but, as noted in Sec. 5.1., advancements in computational fluid dynamics (CFD) are taking an increasingly essential role in this area. Information that could serve as a guide has been accumulated using the Ames 40 by 80 for tests on widely varying V/STOL aircraft configurations. The resulting wind-tunnel and flight-test data correlations were used to obtain the charts shown in Fig. 10 (Ref. 4 with G698 data added). Data for both lift and momentum, as well as wing-span sizing, were obtained. The lines, representing possible size limits, have been somewhat arbitrarily drawn in the charts to represent guidelines for good wind-tunnel flight comparison under balanced conditions, and all data were obtained on complete lifting systems.

The possible acceptability of using partially complete models or component tests should be considered. Most wind tunnels now in operation have a full stock of the hardware needed for semispan mounts and, if not, it usually is relatively inexpensive to manufacture the needed parts. Where lateral and directional characteristics are not required, the semispan mount is an economical method of studying high-lift characteristics, power-component performances, and loading on all parts. There is enough well-documented testing experience to ensure quantitative measurements and to evaluate most questions concerning effective aspect ratio. As examples, the large- and small-scale installations shown in Figs. 11 and 12 were tested in the Ames 40 by 80 and 7 by 10 wind tunnels, respectively. Objectives of both tests were to evaluate the performance and spanwise effects both in hover and during transition (Refs. 12 and 13). For the 40 by 80 tests, even though the effective wing-span-to-tunnel-width ratio was about 0.4 the wind-tunnel wall effects were minimal caused by the effective depth (80 ft) of the tunnel and the geometric aspect ratio, assuming the end plate (which was fixed and nonmetric) was the reflection plane. For the 7 by 10 tests (Ref. 13), the model size relative to

the wind-tunnel cross section was much larger, but quantitative measurements were still obtained on the ejector performance and its influence on the external aerodynamics of the wing. For this case, accurate evaluation of hovering performance was obtained in the wind tunnel with the large side access door open and blowing the ejector exhaust into the shop area.

2.5 Instrumentation and Data Acquisition

During the foregoing considerations it must be assumed that model instrumentation and data acquiring and processing have been assigned significant roles in the planning. The continuing development of microprocessors and more economical computer systems must be considered in choosing the data-acquisition objective. For example, it is becoming more feasible to obtain a significant amount of pressure data along with the overall force and moment data and a few directly measured component loads. Nevertheless, as indicated by the possible measurement needs for a V/STOL investigation listed in Fig. 13, the advantage of using large-scale solely for the purpose of storing on-board data-acquisition equipment may still offset possible higher model construction costs for the large models. To obtain all the items that can be evaluated on board one large-scale model, it is possible that two-small scale models would have to be built or that at least a force and a pressure model would be built. It is, therefore, essential in planning to evaluate the state of technology of such items as electronic Scanivalves, straingage or capacitance balances or both, or flow-survey equipment.

Most established wind-tunnel facilities are continually evaluating and updating their data acquisition equipment and, during discussions with the wind-tunnel staff the potential limits on instrumentation should be thoroughly discussed. Since current V/STOL testing taxes the most up-to-date computer system, it has been my experience that a program can be enhanced by the experimenter using an auxiliary small computer for some of the measurements that can be correlated using a time-code with the data reduction supplied by the wind tunnel. For rotary-wing testing, dynamic analysis hardware and software are now available at most of the larger wind tunnels. At the NASA 40 by 80, this system is on-line and is an essential part for a safe and successful test procedure.

2.6 Test Program

Having obtained the above information and made the decisions and commitments, a written test plan should be produced and distributed to interested parties to ensure that agreements were as perceived. Except for smaller programs, which are funded and activated in-house, this is good practice for any experimental effort, but it is essential for V/STOL testing to the extent that all those designated in Fig. 14 be informed. The particular examples shown in Fig. 14 were large-scale test programs, but they are still representative in terms of the significance of planning and coordinating most V/STOL wind-tunnel test programs. They are presented in the order of increasing program costs with the numbers listed corrected for 1983 cost-of-living levels with respect to the level existing at the original test dates. The following is a brief description of each as reprinted from Ref. 4.

The test results for the project of Fig. 14(a) are reported in Refs. 14 and 15. This was an internally managed, basic-research, project with the objective of studying stability and control, high-angle-of-attack characteristics through stall, and acoustics. Project management came from Ames Low Speed Aircraft Research Branch (FHA) with both an engine and an airframe manufacturer acting as consultants. Final reporting was done by Ames.

Test results for this project shown in Fig.14(b) are reported in Refs. 16-18. This was a U.S. Navy-NASA funded program, managed by NASA, with the objective of obtaining static (in and out of ground effect) and wind-tunnel data for loads, stability and control, and performance. The model was heavily instrumented to document propulsion and external-surface pressures. The test management came from the Ames Aircraft Project Office, with the FHA serving as advisors. The airframe contractor supported the tests with design, test support, data analysis, and reporting.

Test results for the project of Fig. 14(c) are reported in Ref. 19. This was U.S. Navy funded with test management coming jointly from the FHA, the contractor, and the Navy. The model was equipped primarily for full-scale stability, control, and performance checks with the instrumentation required to document power settings together with a few loads. The cost of the model was an order of magnitude higher than those in the foregoing projects because the model combined a fuselage flight structure with the Rolls Royce F402-R-402 engine and a boiler plate wing-flap system. In addition, since the tests were part of an aircraft development program on a tight schedule, it was highly "visible," and a large number of contractor personnel were required to support the operation of the tests and correlate test results on a daily basis.

Each of these projects has proved to be productive, with the first program being the forerunner of the NASA Quiet Shorthaul Research Aircraft (QSRA); the last program is currently near the production stage. All projects included considerable wind-off testing, as well as wind-tunnel work, and measurements obtained were in the following areas of study.

1. Stability and control
2. Aerodynamic performance
3. Propulsion performance, inlet and nozzle
4. Loads on flaps and control surfaces
5. Surface-pressure measurements on all components
6. Boundary-layer surveys
7. Acoustic studies, near- and far-field
8. Wake surveys, downwash, sidewash
9. Static pressures on tunnel walls to evaluate wall effects
10. Flow visualization
11. Structural static and dynamic loading
12. Aircraft systems check

All of these topics plus those pertinent to rotating-wing systems continue to be subjects of V/STOL wind-tunnel testing, and the remainder of this lecture will address details to be considered in their measurement.

3. WIND TUNNELS

This section presents a short survey of available wind-tunnel test facilities that have, in general, large test sections, are subsonic, atmospheric, and have sufficient support equipment and personnel for testing a complete, powered V/STOL aircraft model through transition speeds. The section is not intended to be a complete survey but rather one that indicates types of wind tunnels and equipment that are available. For this reason, only one large industrial tunnel is mentioned; only the high-speed and pressurized wind tunnels at Ames are listed, though they are not described in detail.

For evaluating the capability of a wind tunnel for V/STOL testing in which flow separation may be occurring at anytime during normal flight operation, it could be assumed that the flow quality in the test section may have a large effect on the power-induced aerodynamics. Because of this, at most of the large wind tunnels, considerable effort has been made to evaluate and improve these characteristics. The significance of flow qualities is discussed in Refs. 20-22 but, for V/STOL, they should include turbulence as well as uniformity of test-section dynamic pressure. Unfortunately, except for the DNW and Langley 4- by 7-m tunnels, complete documentation of these characteristics was not available at this time.

3.1 DNW Wind Tunnel

The DNW facility is probably one of the most recently developed. A general description appears in Ref. 23, and a compilation of calibration data is included in Ref. 24. As indicated in Fig. 15, the wind tunnel is a closed-return design and has interchangeable test sections. The latter include 6 x 6 m, 8 x 6 m, and 9.5 x 9.5 m sections as well as an open section for acoustic testing for which longitudinal slots are provided in the walls permitting an open-to-close area ratio variation up to 12%. Flow qualities measured to date are excellent with a deviation of static and dynamic pressure across the test section of less than 0.3% flow angularity $\pm 0.1^{\circ}$, and a turbulence level of 0.1%.

The facility has hardware for either floor or sting mounting. The sting has sufficient degrees of freedom to allow strictly vertical movement without pitch change or pitch and yaw without vertical or lateral displacement. The hydraulic actuation allows a downward velocity of 5 m/sec at 0.5 g for possible use in flare simulation. As with most modern sting arrangements, a high-pressure air-supply line is included to supply compressed air to the model. Floor mounting to the external balance is possible for either strut-supported or semispan models. For gound-effect tests, a 6.3 by 7.6 m (width to length) moving belt can be installed in the two large test sections with a belt speed of 5-60 m/sec. The open-throat feature has been designed for use in acoustics studies. An acoustic evaluation of the facility is reported in Ref. 25.

3.2 8-m ONERA Transonic Wind Tunnel

The ONERA facility has been operating since the 1950s in Modane, France (Ref. 26). The Mach number range is from 0.03 to 1.02, which might enhance its utility for V/STOL testing by making it possible to test with the same model installation from low transition airspeeds to transonic speeds. Although, as discussed in Sec. 5.3, it may not be practical or economical to do this. The facility has a round test section but is equipped with a blown ground board for handling strut- as well as sting-mounted models. An important feature affecting test operations is the ability to exchange test sections, with options such as those shown in Fig. 16(b). For complicated powered models with a network of instrumentation needed, this makes it theoretically possible to make all the pretest checks while another project is occupying the tunnel.

3.3 Langley V/STOL, 4- by 7-m Wind Tunnel

The circuit of the Langley V/STOL facility is shown in Fig. 17. The test section is 4.42 m (14.5 ft) high by 6.63 m (21.75 ft) wide and 15.2 m (50 ft) long. The maximum speed is 103 m/sec (200 knots) and it can be operated in a variety of configurations — closed, slotted, partially open, and open, the latter being open on three sides. Studies have been conducted on methods of improving the flow quality in the test section (Ref. 27). Nevertheless, the wind tunnel has continued to be an essential tool in NASA's low-speed experimental aerodynamics studies and has most of the hardware required for supporting models either by a sting or by using a floor-mounted strut. A moving-belt ground plane is also available. The effort to improve the flow quality and productivity will take a significant step when the wind tunnel undergoes major modifications in late 1984.

3.4 Boeing V/STOL Wind Tunnel

The Boeing tunnel (Fig. 18) is a typical industry-managed facility which is kept uo-to-date as required for company developmental testing, as well as for industry-wide and government-supported programs. There is an option of a 6.6- by 6.6-m (20- by 20-ft) or an open-throat test section, as shown in Fig. 19, with the test section open on both sides. The particular model installation shown is for a small-scale aero-acoustic test for which the model design is discussed in Sec. 4.1.3. This wind tunnel also has the options for either strut- or sting-supported tests. At present, the tunnel is capable of maximum speeds of 250 and 100 knots for the closed and open test sections, respectively.

3.5 Ames 40- by 80-ft/80- by 120-ft System

The Ames 40- by 80-ft has been in operation for about 40 yr, but a recent project (described in Ref. 29) has extended the speed range and added a new test section installed in another "leg" as shown in Fig. 20. To do this, a new drive system has been installed, and vanes are being designed to divert the 80 by 120 test section inlet flow into the fans through the new inlet. It is too early to detail all features of operating in the 80 by 120 test section but the 40 by 80, as it was originally conceived, has proved an invaluable tool for investigating V/STOL aerodynamics, as well as flight-like aircraft systems. With reference to the 40 by 80 test section shown in the elevation view (Ref. 30) of Fig. 21 (updated to show recent changes), the large (and sometimes very heavy) models or aircraft are moved into the outer "high bay" ground level or "2 ft level" and, when readied, hoisted up over the clamshell doors onto the support system. A three-support model installation (the full-scale model of the Grumman tilt-nacelle configuration G698) is shown in Fig. 22. A sketch of the 80 by 120 test section is shown in Fig. 23, viewed from outside the test section.

The size of such a test section as the 40 by 80 has allowed special studies and tests on aircraft components; for example, the acoustic investigation with an installation shown in Fig. 24(a) (see Sec. 6.2.2) and the small-scale hover test in Fig. 24(b). In the latter case a "flying" ground plane was used to incorporate pitch and roll effects into the basic ground-effect study. The data-acquisition support hardware and power systems have been gradually updated through the years, and current data systems include an on-board system that can be made compatible with flight-test installations. Most large- and full-scale models can only be practically supported from below, but for moderately sized models, sting-support hardware has recently been made available. Since aircraft engines at this scale are commonly run in the test section, available support systems include those for fuel, CO_2 and engine servicing equipment, and the power systems usually available, such as air supply and variable frequency power. The facility has a group of qualified aircraft mechanics.

3.6 Langley 30- by 60-ft Wind Tunnel

The Langley 30 by 60 is a classic large-scale installation, and has been in operation since the 1930s. The circuit is shown in Fig. 25. As shown in Fig. 26, it is an open-throat tunnel with the model located just in front of the fans. It has been used for the dynamic stability and control studies described in Refs. 31 and 32 and discussed in Sec. 4.4.1. The wind tunnel has been utilized quite regularly in aviation development as was the case for the installation in Fig. 26. Unfortunately, because of the porximity of the test section to the drive fans, valid acoustic testing has been difficult.

3.7 NRC 9-m V/STOL Wind Tunnel

Except for DNW, the NRC 9-m wind tunnel (Ref. 33) is one of the newest low-speed tunnels, having been in service since 1970. Its development included testing of a 1/10-scale model of the wind tunnel and, although quantitative values of flow turbulence are not available for publication, there is a set of screens immediately upstream of the test section. Most of the V/STOL testing experience to date has incorporated a floor-mounted strut system such as the installation shown in Fig. 27, which is connected to the balance system below the floor. One particular asset for air-driven V/STOL testing is the compressed air supply. It has nearly full use of the NRC Blowdown Wind Tunnel supply which produces dry filtered air at 2050 kPa (300 lb/in.^{2}). At the wind tunnel, this means 1,700 kPa (250 lb/in.^{2}) for 30 kg/sec (45 lb/sec). Unfortunately, heating capability is limited.

3.8 Other Wind-Tunnel Test Facilities

The foregoing brief survey has identified some of the larger wind tunnels that are atmospheric and have complete facilities for both fixed and rotary-wing investigations. Not described were the United Kingdom large subsonic tunnels, the Lockheed tunnel, the high-speed tunnels such as the Ames Unitary System (Fig. 28), and the 12-ft pressure tunnel. The 11-ft test section of the Unitary System is capable of holding a continuous speed down to $M = 0.4$ so that a program can cover subsonic airspeeds for models designed for transonic and supersonic testing. The CMAPS program, at Ames (see Sec. 5.2.4) is designed to make such testing evantually practical by accurately simulating inlet and exit flows. In addition, ther are several 7 by 10 wind tunnels in academia, government, and industry which can be useful for small-scale or component testing.

One of the most economical systems of wind-tunnel testing, particularly as it is applied to V/STOL testing, is the one described by Knott (Ref. 34) and operated by British Aircraft Corporation (BAC), Military Aircraft Division (Fig. 19). The test section is 5.5 m (18 ft) wide and 5.0 m (16.5 ft) high, but the system operates over a narrow speed range of 11 to 21 m/sec (35 to 70 ft/sec). This requires an installed power of only 200 kW (250 hp). There is some disadvantage in that the existing installation is the open-throat, no-return type and its test-section flow qualities are, therefore, subject to weather. The design trade-off may, then, be one of flow quality required against the cost of screens and flow straighteners resulting in increased power required. The testing and scaling techniques assume that Mach number simulation is not important. Table 2 shows typical values for the test velocities compared with full-scale values. A major advantage could be lower model costs and lower on-board power requirements. This also could mean a "lower profile" support system required to take the lower model loading.

4. TESTING INSTALLATIONS FOR V/STOL

Since the choice of the proper testing installation depends on many factors — not the least of these is cost — it would be meaningless to suggest any given procedure for choosing the model installations. The following are examples of test programs that in most cases, proceed through a variety of wind-tunnel test setups.

Much information can be obtained from such exploratory tests as that shown in Fig. 30 (Ref. 35), which had the objective of evaluating characteristics in hover and forward flight for a ground-effect vehicle — the "Avro" car. This test, in the Ames 7- by 10-ft tunnel was made after 40 by 80 tests showed the full-scale vehicle had a large aerodynamic center location change as it lifted out of ground effect. The small-scale test was a very low-cost effort to investigate the fundamentals. A sampling of the test results is shown in Fig. 31. Ground effect was measured very close to the ground board. Although not done, the data could have been corrected for the displacement thickness of the boundary layer by the method similar to that suggested later by East (Ref. 36):

$$C_{corr} = C_{meas} \times \frac{\delta^*}{h} \frac{\partial C}{\partial(\partial^*/h)} + \frac{\partial \delta^*}{\partial X} \frac{\partial C}{\partial(\partial\delta^*/\partial X)}$$

where the gradients of C are determined by carrying out additional tests with other boundary-layer thicknesses. No moving belt was needed with BLC being planned for but not used and qualitative correlations were made with the full-scale data.

An example of a more sophisticated (and more costly) test is that of the Grumman 698 tilt-nacelle development. It was decided that a full-scale test was needed to verify control which might be available from the 698 control-vane effectiveness design. A component test installation in the Ames 40 by 80 tunnel was used

(Ref. 37). The nacelle was powered by the Q-fan (Ref. 38), and was mounted on the 40 by 80 wind-tunnel turntable as shown in Fig. 32, which provided the nacelle with a large angle-of-attack range. In this case the inlet and fan itself were the subject of another investigation (Ref. 39), so that two test objectives were met using common hardware.

A third example, that of the development of the XFV15 tilt-rotor aircraft (Refs. 40 and 41), included the series of test installations shown in Fig. 33. Going to a higher disk loading and a more usable drive system meant a series of tests varying from small- and large-scale semispan models to testing the actual aircraft in the Ames 40 by 80 tunnel.

The range in possible types of installations varying in complexity and cost between those of the previous examples is large, and the test objectives are diverse. In the following discussion, experience with test installations varying in type and complexity will be discussed in more detail.

4.1 Partial Installations

Even though for V/STOL investigations it is usually essential to simulate the complete aircraft configuration in the final aerodynamic evaluation of the aircraft, component testing, two-dimensional testing, and quasi-two-dimensional testing can take a major part in the program. Examples of these installations follow.

4.1.1 Component testing

In one of the previous examples (Fig. 32) it was necessary to establish the control effectiveness of the pitch-control vane before going ahead with a full-scale model. In that test, the data of Fig. 34 verified predictions that the fan efflux would provide sufficient control effectiveness through a wide range of nacelle attitudes. The vane loads and fan flows were documented with sufficient on-board information to establish design information for proceeding with the program. Note that in this case, it did not seem necessary to simulate the wing or fuselage interference effects. This would be the subject of the next phase — a full-scale model an order of magnitude more costly than this one.

For a two-engine fighter configuration, overhead inlets have recently been investigated by Smeltzer et al. (Ref. 42) and Durston and Smeltzer (Ref. 43), using a component or partially complete model installation, as shown in Fig. 35. The inlet region of the model was sufficiently instrumented to obtain both external flowfield contours forward of the inlet and inlet distortion and pressure recovery. This was done using five-hole cone probes. The forward part of the model was sufficiently simulated to relate changes in leading-edge configuration to flow at the inlet plane for both subsonic and supersonic speeds. The model had flow through the nacelles, but metering plugs were added to vary flow through the inlet.

Certain basic study projects and key experiments can also be placed in this category. Many researchers have been accumulating wind-tunnel data on the jet-in-cross flow problem, as reported in Refs. 44-46 for the installation of Fig. 36. Initially, this type of experiment was started with the use of a flat plate, as shown in Fig. 37, with a 10-cm (4-in.) jet issuing from the center. Then, using a smaller test section (Ames 7 by 10), the body of revolution and another flat plate were tested. All tests have been closely coordinated in objective and scope, that is, to evaluate the pressure on the surface surrounding the jet exit and to study the flow in the jet itself. From this data base, several jet models of the jet-in-cross flow problem are being evaluated, among them being the diffuse vortex model of Fearn and Weston (Ref. 45). The 5-cm (2-in.) jet model has also been used recently to study the flow characteristics using a three-component LDV technique which is described in Sec. 6.3.2.

4.1.2 Two and Quasi-Two-Dimensional Testing

Before the significance of powered-lift effects on airfoil section characteristics was fully realized, airfoil sectional characteristics were accurately evaluated using test installations of constant chord and spanning the width of the wind-tunnel test section. The height of these tunnels was generally much more than their width to minimize blockage corrections. For high or powered lift airfoils the technique has been successfully applied using precautions for preventing flow separation on the end wall. In one case (Ref. 49) for the installation of Fig. 38, a powered nacelle was added to a two-dimensional high-lift externally blown flap (EBF) installation to evaluate leading-edge stall control and turning effectiveness. As in the case of any airfoil adjoining a flat plate, the adverse pressure gradient on the airfoil is transmitted to the wind tunnel or end-plate walls. A positive way of controlling this is to use local BLC at critical locations on the plate itself.

This was also done to the quasi-two-dimensional model shown in Fig. 39. In this instance, the objective was to study effects of airspeed on a span-wise ejector (Ref. 50) and to derive the two-dimensional section characteristics of such a high-lift device for correlation with large-scale tests on a complete model configuration. It was found that although the two-dimensional effective angle of attack could not be evaluated to much closer than ±2°, the effective aspect ratio was sufficiently large, — approximately 8 (based on the power-off drag polar) — to make the power-on data useful in evaluating the ejector performance as functions of both power and angle of attack. The key to such an installation is the design of the end plate. There are very few published data on large end plates except those by Riley (Ref. 51); more recent studies are being directed at drag reduction of higher aspect ratio wings. For the installation of the high-speed evaluation of wing cruise blowing system by Mahal (Fig. 40; Ref. 52) the angle of attack was evaluated as

$$\alpha = \alpha_{geom} - k\,Cn$$

$$k = 3.54 - 1.26(1 - M^2)^{1/2}$$

This is consistent with all the power-on data obtained, and was used in evaluating the effects of blowing on the drag rise Mach number at a target cruise lift. This installation shown installed in the Boeing wind tunnel (Fig. 40) had an end plate that was contoured to minimize drag at high subsonic speeds. All data were in the form of surface pressures integrated to give lift and pitching movement with momentum rake data being used for drag evaluation.

4.1.3 Semispan Installations

Semispan models have been widely used in the conceptual stage of a high-lift concept. In the 1950s very economical installations, such as the one described by Anscombe and Williams (Ref. 53) and shown in Fig. 41 were developed. The advantages over complete aircraft simulations are lower cost plus larger scale potential for a given test-section size. The main disadvantage is lack of any lateral-directional information and, possibly, questionable pitch control-data. Most installations rely on the use of either a mechanical or electrical balance, located below the floor.

A major choice for such an installation is whether to have the model include a half fuselage that is metric, such as the one in the sketch of Fig. 41; a fuselage that is nonmetric, or attached to the wind tunnel floor; or an end plate that is nonmetric with the wing protruding through it. Except for exploratory tests in which the longitudinal characteristics of a canard/tail-wing configuration are needed and each component must be repositioned, the author is partial to the use of the metric half fuselage. Experience in the Ames 40 by 80 with the semispan installation of Fig. 11 (Ref. 12) has been excellent to the extent that approximate correlations were made with a complete jet flap wing-fuselage model. For the installation of Fig. 11, the root or effective plane of symmetry was raised to be clear of the floor boundary layers. The test reported in Ref. 54 and shown in Fig. 42 incorporated a half fuselage that pitched with the wing but was nonmetric and attached to the floor fairing of the tunnel. The disadvantage of this is sealing problems where the root of the wing had to be nonrestrictive in order to avoid affecting the measurements of the wing characteristics. For high-lift conditions, the pressure difference places an additional force on any seal that is installed.

The semispan installation was also used economically in the development of the XV-15 tilt-rotor model mentioned earlier. Using the installation in Fig. 33(c), both power-off and power-on tests were made as described in Ref. 55 to evaluate rotor aerodynamic performance, rotor dynamics, and hardware of the rotor systems. Even though the root of the wing was rigidly fixed, the wing-rotor dynamic measurements could be used to predict operating limits of the complete aircraft. The model shown was unpowered and could be assembled with spars of three different natural frequencies. During the windmilling tests, the effect of damping of the rotor-pylon-wing twist mode was evaluated with step inputs into the rotor tilt actuation system. The rotor performance was later studied using a dynamometer test installation. All test results were correlated with small-scale measurements and predictions.

4.2 Testing Complete Aircraft Configurations

Since the wind-tunnel time for complete aircraft configurations is a major part of the aerodynamic and dynamic development for any aircraft, conventional or V/STOL, any cost saving in this phase can have a major effect on the overall development costs. Powered V/STOL models themselves are inherently more expensive than unpowered conventially configured models. This is a result of additional costs that are incurred not only because of adding power to the model but also because of the additional effort needed to support the tests. Other costs come from the increased amount of on-board instrumentation for which leads have to be "funneled through" or around model supports. As for moving-base or for free-flight operation, the model must be sufficiently light and designed for adequate remote control. Low model weight and light power units are also required for track-supported models such as used at the Princeton track facility. Examples and problems of each of the above will now be discussed.

4.2.1 Sting Supports

For the rigid mounting category, sting supports, in addition to high-speed requirements, are sometimes desirable for minimizing aerodynamic interference induced by model lift, particularly in ground effect. For some test conditions, strut mounts can induce buoyancy or blockage under the model that may be difficult or impossible to evaluate. For V/STOL configurations, it is important that the sting support be downstream of the area generally occupied by lifting jets and flaps. As can be seen by the model support in Figs. 43 and 44 (Refs. 56 and 43), however, the rear end of the model can be adapted to receive a sting of sufficient size to minimize support flexibility and, at the same time, enter the model with a minimum alteration of the rear contour.

In the case of the CMAPS-powered model shown in Fig. 45 (Ref. 57) for the two-engine supersonic fighter, the pressure and instrumentation leads were routed forward under the fuselage. During these tests an attempt was made to set the narrow segment of sting as short as possible to reduce "bounce" and length of high-pressure leads. Lower surface pressures were calculated at the model plane-of-symmetry; a summary of the results is presented in Fig. 46 (Ref. 58). It is evident that lengthening the sting or moving the adapter 0.30 m (12 in.) farther from the model reduced the influence of the adapter to a very small amount ($\Delta C_p = 0.05$) at the model trailing edge.

For some powered fighter configurations, an off-side or overhead mount could minimize restrictions in direct simulation of the rear of the aircraft such as the mount shown in Fig. 47 for a generic fighter investigation. Instrumentation leads and the air for powering the propulsion jets were routed in through a twin support at the vertical tails, thus leaving the lower-rear of the model free of any induced flow generated by the deflector nozzles. This was mandatory in this case because the objective of the test was to evaluate the effect of nozzle configuration on the aerodynamics of the model over a large Mach number range.

A somewhat larger model built for lower speed with a corresponding lighter construction (lower weight per size) was tested in the Ames 40 by 80 as shown in Fig. 48 (Refs. 60 and 61). This was a sting-supported model to be installed on the 40 by 80 turntable, and the model chord plane was vertical so that rotation of the turntable would change angle of attack through high angles. The configuration was a side-by-side twin-engine configuration so that the sting installation required a widening of the rear fuselage slightly beyond scaled width. For this case, it was judged acceptable since aerodynamic corrections could be made using integrated surface pressure measurements. Also, in this case, it is believed that the thrust of the fans had little interaction with the sting since they were used to pump air through the inlets, and the momentum of the exhaust was exceptionally low. A disadvantage of this installation was the asymmetrical lateral/directional effects on the model induced by the vertical strut.

As the full model size capabilities of the large atmospheric wind tunnels are utilized, the models may become large and heavy enough to preclude sting supports. At this stage available sting hardware may produce mounting that is too flexible to maintain a stable platform for the balance. There is probably some model size-weight level for which strut mounts become mandatory for practical reasons and for which the required sting size becomes too large to allow tailoring the rear of the model to scaled aircraft contours. There appears to be no coherent criteria to help in the strut or sting choice but a thorough study of the interaction of possible oscillating aerodynamic loads and the model-support dynamics is an essential part of this choice.

4.2.2 Strut-Supported Installations

For a configuration in which there is a large amount of power-induced circulation from the wing, the single support mount shown in Fig. 49(a) (Ref. 62), a 1/7-scale test of the H126 jet wing aircraft, was used successfully. For comparison purposes, the aircraft itself is shown in Fig. 49(b) mounted in the Ames 40 by 80. The small-scale test was made in the Ames (Army) 7 by 10 and employed a pitch link activated by a rod running parallel to the main strut. The large fairing enclosed instrumentation and the pitch-link actuator. In most cases, this actuator can be located below the floor to reduce the required fairing size. When the lift jet efflux is in the center of the model or it is thought that strut interference effects would be excessive, the model can be inverted, as shown in Fig. 50 (Ref. 63). As with sting mounts, a disadvantage of the heavier models is that the single-strut installation tends to be more flexible in the yaw-roll modes of oscillation.

An interesting type of hybrid mounting system (Fig. 51) has been used by Boeing Vertol for rotary-wing testing. It incorporates the air-driven "power pod" in supporting a helicopter model. The pod itself has been attached to the sting which is equipped for pitching and yawing the entire system. The "pedestal" or vertical strut supports the model through the balance inside the model. An optional setup uses the same power pod for a floor-mounted installation.

Because of model weight, large- and full-scale models at the large-scale test facilities (40 by 80 and 80 by 120 at Ames and the 30 by 60 at Langley) must use floor-mounted struts, usually, a three-strut system as shown in Figs. 22 and 52, respectively. The struts tend to be stiff in yaw if the main struts are mounted to the outer wing, such as in the case for the AV-8B model of Fig. 53. A compromise was made in the landing-gear-type mount for the STOL transport model shown in Fig. 6(a) (as well as with the 698 model of Fig. 22). For these models there was a special effort to design the model with the struts away from the undersurface of the wing in order to minimize any local effect on wing airflow separation.

Even with the effective thickening of the strut tips due to attachment of leads, there has been a wealth of evidence that for the V/STOL configurations tested to date, strut-interference effects have been extremely small. This confidence has come primarily in the comparisons of full-scale wind-tunnel test data for actual aircraft with their corresponding flight-test results (Refs. 64 and 65). Data representing an assortment of V/STOL aircraft have correlated well in both angle of attack for a given lift and power setting, as well as for stability and control. Some of the data for the smaller aircraft, such as the VZ3 and XV3, correlated well without applying any wall constraints or blockage corrections to the data. Concerted efforts to generalize what strut tares exist, as suggested in Ref. 6, have not been successful for V/STOL models, particularly at the low-speed end of transition with high flap settings and jet deflections.

4.3 Ground-Effect Testing

As shown by the experience with evaluation of the flight versus wind-tunnel data of the Augmentor Wing Research Aircraft at Ames and discussed by Cook and Whittley (Ref. 64) a highly deflected jet impinging on the floor of the wind tunnel must be accurately simulated. It must be prevented from migrating too rapidly forward through the low momentum of the floor boundary layer then blowing back up (which may or may not be the case for the actual aircraft in flight) and over the wing. This can be reasonably well simulated by maintaining a small boundary layer by either or both BLC and moving belt (Ref. 66). An additional method is the moving-model technique such as has been used at the Princeton and other towing facilities (Sec. 4.4.2). In 1977, Campbell et al. (Ref. 67) reviewed the status of the use of wind-tunnel measurements to predict aircraft flight characteristics, including initial experience with the C8A just mentioned. Since that time, similar comparisons have been made using both the Harrier and QSRA, results of which have not been well documented. Most of these comparisons varify the so-called Turner criteria which is shown in Fig. 54 (taken from Refs. 29 and 68) or the equivalent if BLC is used to control the boundary layer on the ground plane. Margason (Ref. 5) has also reviewed the need for a moving belt or BLC and concluded that for low-aspect-ratio wing configurations, particularly those using deflected thrust concentrated in a small area, less control of the wind-tunnel floor boundary layer is required. In any case, some of the flow phenomena restricting the measurement of ground effect of V/STOL configuration in a wind tunnel are the same as those governing model sizing (Sec. 5.1). Turner's belt installation (Ref. 68) was in an enlarged inlet of the Langley 7 by 10 300-mph wind tunnel and, as shown in Fig. 55, is close to the inlet of the test section. The result was as expected. As shown in Fig. 56, with the belt speed synchronous to the tunnel airspeed, the boundary layer was completely eliminated. The early development of the moving belt itself, as indicated by Butler et al. (Ref. 69), was tedius, but through advancements in materials and multiple drive systems, current operation is relatively trouble free. At the present time, most of the moderately sized low-speed tunnels having sting supports are equipped with a moving belt similar to the one in the Boeing Vertol tunnel (Fig. 57) where the essential parts of any belt system are noted. As shown, the suction slot provides BLC forward of the front roller.

A more economical method of accounting for the wind-tunnel boundary-layer growth is the placement of BLC on the floor by itself or combined with a raised ground board forward of the model. A study was completed for NASA in 1974 (Ref. 70) to explore the feasibility of a BLC installation in the Ames 40 by 80 wind tunnel. The objective was to facilitate ground-effect testing, as well as to lower the testing airspeed restriction for propulsive systems with highly deflected jets. The finally recommended design was not used for economy reasons, but the design (Fig. 58) is still considered valid, and basic aerodynamic studies by Hackett et al., which were vital in understanding BLC requirements, continued through the 1970s. Other investigations were summarized in a 1973 lecture by Poisson-Quinton (Ref. 71). In most of the studies, small-scale jet flap tests were made, using both a belt and BLC. Typical wind-tunnel results, though preliminary, were updated by Hackett et al. in Ref. 72, and a sample set of pitching-moment data with tail on is shown in Fig. 59 for the case of 2 chord lengths above the floor. The correlation between fixed-ground plus BLC and the moving belt are

good, even though, at $C_\mu = 3$, the jet wake is probably starting to impinge on the floor. When this happens just behind an unswept wing or two-dimensional jet flap model, the flow pattern, which includes a standing vortex, is established and causes suck down. The control and intensity of this flow pattern is affected by floor BLC (or moving-belt velocity), but may not get established during the landing flare or any other transient situation.

4.4 Moving-Base Testing

If the above mentioned flow patterns are not particularly Reynolds-number sensitive, moving-base techniques may be used to evaluate their effects. V/STOL models configured to simulate the power loading as a complete aircraft configuration and at the same time to have sufficient scale to ensure quantitative test results tend to become heavy. An example of hardware needed to move a heavy model in vertical motion is shown in Fig. 60, which was the result of a design study (Ref. 73) to investigate problems of simulating the transient ground effects in the Ames 40 by 80. The design criteria for a 0.11-scale model of a large STOL transport aircraft included the following test conditions and model parameters:

Dynamic pressure, kPa (lb/ft^2)	1.93 (40.3)
Reynolds number, RN	2.24 $(10)^6$
Model weight, KN (lb)	3.23 (727)
Model span, m (ft)	3.7 (12.1)
Sink rate, m/sec (ft/sec)	5.2 (17)
Rotation rate (for flate) deg/sec	67

Scaling full-scale flare and touchdown maneuvers brought large accelerations; the result is the design of Fig. 60 and prohibitive costs. Even though a trade-off between facility cost and model scale may reduce the size of the support somewhat, studies of some of the questions on transient ground effects and aerodynamic damping using scaled experiments may still have to rely on the use of track facilities and free-flight techniques. The following is a brief discussion of two such facilities.

4.4.1 Free-Flight Methods

Although the term free-flight testing is also applied to high-speed or ballistic testing, or the spin-tunnel testing for V/STOL evaluation, it has usually become synonymous with the wind-tunnel free-flight methods such as used in the Langley 30 by 60. With use of this technique, a qualitative evaluation of flight characteristics of a wide range of aircraft concepts has been made in and out of ground effect. The well-known technique (Fig. 61) incorporates Froude-scaled replicas of the aircraft. Reference 74 includes a concise description of significant factors of the technique, and equations of motion for the models are listed in Ref. 75. For most current aircraft designs, the geometric scale tends to run from 1/10 to 1/6, with lengths 2.1 m (7 ft), wingspans of 1.52 to 1.83 m (5 to 6 ft), and weights of 224 to 267 N (50 to 70 lb). With this scaling, the model angular motions are up to 3 times as fast as those at full scale. This brings the requirement for multioperators. Since the operators must attempt to keep the aircraft in one position or on a predetermined flightpath and, as mentioned, the time-constants are 1/3 full scale, light, quick response actuators have been developed which provide the pilot with tight control. The model is instrumented to measure linear and angular acceleration along with control-surface positions which are transmitted throughout the flight to strip charts. The flight cable also supplies the high-pressure air to the model motors. Motion pictures document the flightpath and representations of desired automatic stability and control augmentation systems are input into the control systems.

Although these techniques have gradually been improved through the years, Paulson (Ref. 76) still gives one of the most detailed descriptions of the technique and its problems for use with the B-58. In a more recent application, the free-flight technique was used to evaluate the high-angle-of-attack characteristics of a forward-swept wing fighter configuration (Ref. 31). The program included the use of two models, one a 0.16-scale model of the complete aircraft and a 0.16-scale flat plate model. The former was both fixed-support tested and tested in free flight. The project was coupled with tests of both models on a free-to-roll apparatus in order to evaluate any unclamped roll oscillations at high angles of attack. The model is shown in Fig. 62 being tested in the free-flight mode. Damping in roll evaluated from the free-flight tests was found to agree quantitatively with the flat-plate measurements for moderate angles of attack.

4.4.2 Moving-Base Track

A major difference between the free-flight facilities and the moving-base track is the latter's capability of restraining certain undersired degrees of freedom of the model motion. Therefore, it pre-programs a flightpath such as a landing flare or a roll oscillation. In the case of the Princeton Track (PDMT), Froude-scaled models are moved along a pre-programmed route that is 246 m (750 ft) long (Ref. 77). The track is enclosed in a building 9.8 m (30 ft) wide and 9.8 m (30 ft) high and, during operation, the building is tightly sealed to ensure still air along the flightpath. The facility has been equipped with a model support system (Fig. 63) that allows small amounts of model translational motion freedom, as well as angular motion about a ball-bearing gimbal system. Any motion with respect to the carriage is measured and used as an error signal in a closed-loop servomechanism which can position the carriage with respect to the model. If everything is working properly, there is, essentially, a free-flying model about a mean free flightpath with which to reference the natural dynamics of the model. Note also that the facility can be used for steady-state (Putnam refers to it as static) testing in which the model moves along the track at a constant vertical position. A version of the subsonic tilt nacelle (Grumman 698) V/STOL aircraft was tested as reported in Ref. 78. The principal objective of the tests was to evaluate transient ground effects. Although the results have not been completely analyzed, experience indicates that with this method of testing, the data should represent those of steady state. For another configuration, a comparison of lift and drag data is reprinted from Ref. 77 in Fig. 64 (coefficients are based on slipstream dynamic pressure). The data show good agreement with wind-tunnel test results.

5. MODEL DEVELOPMENT

The V/STOL wind-tunnel model continues to be one of the most expensive parts of any wind-tunnel program; it will be even more so if we are to take complete advantage of recent advancements in model fabrication techniques and instrumentation. The unpowered high-speed models or those adaptable to pressure tunnels are expensive to contour and finish, particularly if equipped with surface-pressure taps; the high cost is a result of the precision required and large design dynamic pressure. Adding power can double or triple any model costs because of (1) the cost of the engine simulator, (2) the power source (electric, compressed air, etc.) hookup, and control, (3) the added instrumentation needed to evaluate power setting, and (4) the additional effort required for data reduction. Once the above complications are added, there seems to be little direct correlation with the size and cost of the model itself so that, in general, within the restrictions of given available wind-tunnel sizes, scale effects continue to dictate as large a model as possible. Except for possible limitations owing to the available propulsion simulators, the initial approach in model planning is to evaluate the magnitude of wind-tunnel wall constraints. To put all of this together requires proper use of material and construction techniques in order to minimize flexibility, change time, or shop costs. The above considerations will be discussed in more detail.

5.1 Model Sizing

Figure 10 was proposed as a correlation of experience in comparing full-scale wind-tunnel test results with those of actual flight tests using, in some cases, the same airframe. Many investigations have, subsequently, evaluated model size limits and related these limits to the magnitude of wall-constraint corrections. Approaches to wall-constraint correction might be organized into application to type of lifting systems as follows:

1. Power-off or low thrust deflection: use classical corrections from Pope (Ref. 6)
2. Power-on with distributed blowing and limited thrust deflection: use Pope based on C_{L_A}
3. Power-on concentrated or focused thrust deflection: Heyson (see Ref. 79 for summary)
4. High angle of attack, Maskell (Ref. 80) with considerations by Peitzman (Ref. 81) and Stoll (Ref. 60)
5. Blockage for all cases (Ref. 82)
6. Corrections using wall pressure signatures (Ref. 83)

The last two items have shown promise for reliable evaluation of wall-constraint effects combining simple modeling of the lifting system with wall surface-pressure measurements in the wind-tunnel test section. These corrections increase rapidly with relative model size to wind-tunnel cross-sectional area and will be enhanced by the rapidly developing computational methods, such as was done recently by Snyder and Ericksen at Ames (Ref. 84). In the latter case, PAN-AIR (a high-level paneling code), was used to evaluate wall corrections with emphasis on a bump under the model. The basic problem and flow modeling are shown in Fig. 65. Lower-level paneling codes and vortex-lattice simulations of walls and lifting systems are getting more attention for treatment of the wall-correction problem and are being integrated with the data acquisition software of some wind tunnel facilities.

The question now is at what point do these corrections become meaningless or questionable. The physical constraint for highly deflected jets is classically illustrated in the sketches of Fig. 66, which are reprinted from Ref. 5, and are taken from the study done by Tyler and Williamson (Ref. 85). Also included is an example of one jet height and several velocity ratios which were studied for several relative test section sizes. The general flow pattern at the limit of testing consists of a vortex surrounding the point of jet impingement on the wind-tunnel floor. In this case (Fig. 66), for two laterally spread jets, the jet exhaust impinged on the floor at

$$V_e' = 1.31\ D_e/h$$

For the lift-fan data of Hoad and Gentry (Ref. 86), Margason (Ref. 5) runs through an example to keep $\Delta\alpha$ at the tail to 5°, and using Heyson's corrections, $V_{e_{min}} = 0.125$. Testing below this velocity would probably cause a vortex formation. There is a suggestion in Ref. 87 that testing should be limited when the wake impinges 2.5 wing spans downstream from the model. This is consistent with Turner's criteria of Fig. 54 for the moving-belt ground plane.

Carbonaro (Ref. 88) considers limits using Heysons criteria of testing for acceptable amounts of correction. A set of limits of wall corrections was assumed, such as $\Delta i_t = \pm 5°, \pm 2°$, and $\pm 1/2°$ for maximum acceptable, moderate, and no corrections, respectively, as listed in Table 3. Values of maximum test lift coefficient are related to ratio of wing span to tunnel width for several semispan and complete lifting systems. In this and previous reviews, Carbonaro concluded that the flow breakdown limit applies mainly to models that are small with respect to the test section; that is, for span-to-width ratios below about 1/4. Typical lift versus test-section width plots are reprinted in Fig. 67. For larger model dimensions relative to test-section size, the wall corrections become too large before flow breakdown occurs.

In the author's opinion, many of these limits can be "pushed" and some valuable information still obtained on power-induced effects for such items as aircraft stability and control, as well as flap and control loadings. Of equal significance is the fact that Heysons early work using a linear wake trajectory has been replaced by a free or "relaxed wake" which tends to move the predicted point of impingement on the wind-tunnel floor downstream. As previously mentioned, low-level CFD methods simulating the complete lifting system as well as the floor are being considered for evaluating both sizing criteria and wind-tunnel wall corrections, including support influence.

The general case of blockage and wall-constraint effects has been studied for some time by Hackett. An updating of this work is published in Ref. 82. The monitoring of wind-tunnel wall pressures and relating the results to an equivalent distribution of sources and sinks continues to be a promising method of evaluating the effective blockage of most conceivable V/STOL aircraft configurations. If properly instrumented, an angle-of-attack correction can also be derived, as illustrated in the block diagrams of Fig. 68(a). The key

is the comparison of the measured pressure imprint on walls (Fig. 68(b)) with results of theoretical modeling of the lifting system.

Investigations into methods of extending these limits have included changes in wind-tunnel design and methods of mounting the models. Off-center mounting, such as moving the model higher in the test section to effectively increase D_e/h, may help in some cases, but as shown by the University of Washington studies (Refs. 89 and 90) it tended to increase the magnitude of the wall-constraint corrections. Adding slots to both the floor and ceiling could be effective in delaying the formation of the floor vortex. Several moderately sized wind tunnels are equipped with hardware needed for this. The systems and correction factors may be similar to those being posed for transonic test sections (Ref. 91). Unfortunately, the amount of suction required through the slots and the system for distributing this suction is still being debated, particularly for the case of high-velocity jet impingement. Along with this debate go proposals of so-called adaptable walls. Sears' concept (Ref. 92), would require linking the wall-constraint porosity and shape to a mathematical model of the wake in order to eliminate any possibility of the wake being ingested by the lifting system (Fig. 69). Small-scale experiments on this concept are now under way, but it seems unlikely that it could be adapted to any of the existing large wind-tunnel facilities.

As the size of the lifting system increases with respect to the tunnel test section, the increase in blockage and, hence, free-stream velocity correction, results from the combined effects of model bulk, deflected jets, or separation wakes. For high-angle-of-attack tests, a model sized for conventional angle-of-attack ranges can have sufficient blockage at angles of attack above 45° to make test results meaningless. For the investigation of Refs. 60 and 61, a correction was used which was based on flat-plate drag data such as those shown in the plot of Fig. 70(a). The gross drag on the model and supports was measured by the tunnel scale system. From this, model-induced drag, less gross thrust and inlet momentum drag, was subtracted and related to a Δq corection in Fig. 70(b). The blockage correction was assumed to act uniformly across the test section. As shown in Fig. 70(b), the resulting Δq correction for the model with $S/C = 3.5\%$ was 11% at 90°. For models having much larger values of S/C, the flow uniformity assumption would be in question.

5.2 Power Simulation

In evaluating V/STOL concepts in the wind tunnel using scaled models, it is becoming evident that the full-scale jet properties must be evaluated in greater detail. Early experimenalists studied engine-airframe aerodynamic interactions using jets of air the quality of which was seldom documented. As a result, there were differences between experimental results which could not always be explained by such things as variances in velocity ratio and placement of the jets.

Ames Research Center has undertaken a major experimental program to evaluate the principal scale effects involved in jet simulation. The initial phase, reported on in Ref. 93, included the full-scale test portion of a full-scale to small-scale comparison program. Measurements of the effects of using actual turbojet/turbofan engines will be evaluated at small scale by attempting to simulate the geometry and jet characteristics of the engine exhaust and evaluating any full-scale differences in suck down and ground effect. The results, using a General Electric YJ-97-GE-100 turbojet engine, are summarized in Fig. 71. Although small-scale experimental results are not yet available for comparison with existing large-scale data, it is evident that the measured suck down is considerably more than the predictions using empirical methods (Ref. 94) which were based on small-scale generic investigations. This program will continue with the small-scale phase and then be extended to co-flowing jets, but until we have answers on the significance of modeling all jet characteristics, including the possible need to simulate jet turbulence, the current objectives should be to model the real jet properties of jet cross-section and velocity profile for a given pressure ratio.

The need to do the latter is demonstrated in the experiments of Kuhlman and Ousterhout (Ref. 95) and Kuhlman and Warcup (Ref. 96). A plug was inserted in a nozzle to change the jet qualities, particularly the total pressure variation across the jet. A typical result is shown in Fig. 72. Inserting the plug near the jet exit added a loss in momentum to the center of the jet and contributed to a more rapid velocity decay and change in jet trajectory in the cross flow.

The foregoing results indicate that simulating jet velocity profile across the jet is mandatory and, possibly, the simulating of jet turbulence could be significant for evaluating jet-airframe interference effects. As the requirement for more quantitative test results increases there is a need for a more careful choice of the propulsion simulator to be incorporated in the model design. In planning the test program, this choice is integral to model size consideration because of the availability of off-the-shelf simulators and the large cost of simulator units already developed.

5.2.1 Simulator Classification

Classification of aircraft engines, and hence engine simulation types, was well organized by Wulf and Melzer (Ref. 97), as shown in Fig. 73.

The choice of simulation is between "self-manufactured motionless systems" and "expensive, purchased rotating systems," with rotary-wing model power and turbofan engines falling in this latter class. Although not listed, hydraulic-powered motors should not be overlooked for driving rotary-wing models or for installations in which a return lead can be installed. Table 4 bridges the two branches for air-driven models classified according to nacelle type. To extend the application to full or large scale, I added the line item, gas-turbine engines. The following three sections cover the fixed blown simulators which include the full, blown jet, and ejector, as well as the turbine powered simulator and gas turbine engines. Electrical power is considered beyond the scope of this lecture though it is a significant factor in model costs. Its application is typically a mechanical problem and one of tying into either an on-board model motor or to a wind-tunnel auxiliary power facility, such as the one available at the Vertol tunnel (Fig. 51) or at the Ames 40 by 80 (Fig. 9).

5.2.2 Fixed Blown Simulators

Fixed blown simulators probably have been and will continue to be used because of their economy, particularly for powering partially complete models. Most initial studies in jet/airframe interference effects have incorporated this type of power for jets, such as the work by Vogler (Ref. 66) and, more recently, in the jet-in-cross-flow studies of Refs. 44 to 48. The simulation of a uniform jet and, at the same time, getting it within the contours of a small model of a complete aircraft configuration, is a difficult task, particularly if the entire assembly must be metric (total forces measured by the balance). Effective designs of the fixed blown simulator were used in the early studies of the Hawker P-1127 using a 1/10-scale model; an illustration of the model is reprinted in Fig. 74 (Ref. 63). In the most recent development of the AV-8B, a 0.15-scale model was powered by the airfeed plenum shown in Fig. 75.

In any of these, and also in similar designs, the quality of the jet is a function of the screen or colander design combined with the size of the settling chamber. A very uniform jet velocity was obtained in the AV-8B model just mentioned. A very compact installation, it still had a settling chamber up stream of the conical screen (Fig. 75). In these installations the desired contraction from screen into the nozzle entrance was difficult to package. For the basic jet-in-cross-flow studies of Aoyagi and Snyder (Ref. 46) and Fearn and Westen (Ref. 47), a very uniform jet velocity profile was obtained by the relatively bulky design shown in Fig. 76. The need for some contraction ratio is always a major problem in designing fixed blown propulsion simulators for complete aircraft models because of limited available space inside the model.

For simulating (approximately) engine inlet velocity, as well as in providing exhaust flow with a minimum of high pressure flow, the ejector should be considered. The application of the ejector was aided by the work published in Ref. 98. The ejector used was fed by air with pressures up to 2.41 MN/m^2 (350 psig) through a large number of primary nozzles in order to maintain uniform flow across the ejector. Ejector performance for one design is presented in Fig. 77. Even though an overall pressure ratio of 1.5 could be obtained, the ratio of ejector inlet flow (secondary flow) to total exit flow (primary plus secondary) was less than 0.5, meaning a subscale inlet area. Jet-pump theory indicates that this ratio would increase rapidly as less exit pressure is required. The effort did show that effective gross thrust for any given ejector configuration could be set to a known value and maintained, providing a complete calibration was made for each exit nozzle or deflector-inlet combination. The ejector is adaptable to packaging into nacelle configurations, as shown in Figs. 78(a) and 78(b) for a turbojet or turbofan, respectively (Refs. 97 and 99). Subsequent development such as the effort by General Dynamics (Ref. 100) has refined the use of the ejector for simulating high bypass ratio engines. (See also Ref. 99 for application to an investigation of the EBF – externally blown flap.) The simulator used here, and shown in Fig. 78(b), simulated the correct exit thrust split but the incorrect inlet flow simulation, though probably close enough to have had little effect on measurements of EBF performance.

5.2.3 Turbine Powered Simulators: Low Pressure Ratio

The tip-drive fans (Fig. 79) are roughly one tenth the cost of the center turbine driven fans but still have a big advantage over the ejectors in being able to move the bypass flow at 5 to 6 times the flow rate of the drive air. As for U.S. designs, a major workhorse has been the 5.5 in. (14 cm) fan shown (Fig. 80) disassembled and installed in an early Rockwell lifting-nacelle configuration (Ref. 101). The fan was also used to simulate the fan flow in the built up nacelle (Fig. 81 from Ref. 102). The 5.5-in. fan was combined with a direct blown simulation of an engine core in a 0.094-scale model of a V/STOL research airplane to be powered by Allison PD 370-16 engines. For this test, the fan turned out to be a reliable performer. One of the largest of the tip-driven type was Tech Developments 12-in. fan (Ref. 103), which was incorporated in the high-angle-of-attack model tested in the Ames 40 by 80 tunnel (Ref. 60) and in ongoing inlet work at NASA Lewis. In both of these cases, it has been used only to suck the inlets rather than provide a propulsive jet since, at this stage of its development, it has a large radial variation in total pressure. Initial calibrations established, however, that it met the design objectives of an effective pressure ratio of 1.4. Air supply required for a full total thrust of 800 lb is 6.5 lb/sec heated to 250°F. Again, testing experience has shown this fan to be reliable.

In the final stages of aircraft aerodynamic development, the turbofan or central powered simulator has had a strong role. Here, the engine bypass and pressure ratios are both closely simulated for given thrust loadings, T/A_L. As a result, for a given nacelle configuration, scaled to the same A_L/S as the aircraft, testing can be accomplished at high subsonic Mach numbers for effective evaluation of cruise drag. The TF 34 simulators are also being used in the small-scale tests of the Grumman 698 (subsonic tactical aircraft) model shown in Fig. 82 mounted for hover testing in the Ames 40 by 80. Results have not been published for these tests, but long-range plans involve comparison with full-scale static and wind-tunnel tests, with documentation of the jet efflux coming from both large- and small-scale models.

5.2.4 Compact Multimission Aircraft Propulsion Simulator

The ejectors and rotating simulators just discussed can be applied only to simulated turbofan engines having subcritical pressure ratios. For power-on testing of high-performance aircraft, techniques used in the past have required direct feed of the air and, if the inlet were to be simulated at the same time, a bulky suction lead would have to be routed outside the wind tunnel. The continuing development and application of the compact multimission aircraft propulsion simulator, CMAPS (Fig. 83), has had the objective of simulating both propulsive jet and inlet flow at total pressure ratios corresponding to those of current high-performance engines. The simulator (Fig. 84) is a miniature four-stage turbocompressor driven by high-pressure air expanded through a single-stage turbine. It has the capability of changing the engine pressure ratio at a constant compressor airflow by changing the fraction of turbine discharge air of the exhaust nozzle. The hardware development started by McDonnell Aircraft Company under the auspices of the Air Force Aero Propulsion Laboratory; a complete history of its development is provided in Ref. 104.

Ames Research Center is funding a major program to develop the technology for the application of the CMAPS to small-scale wind tunnel models. The primary objective in this program is to measure the aerodynamic interaction effects that may result from geometrically close-coupled propulsion/airframe components. A second objective is the development of installation and test techniques for propulsion-equipped wind-tunnel models. A third objective is the expansion of the high-speed V/STOL aircraft aerodynamic data base. The initial

aircraft configuration chosen was that of a two-engine, close-coupled, canard-controlled aircraft similar to the General Dynamics design (GD 205) resulting from the study of Ref. 2. The model is shown installed in the Ames 11-ft transonic tunnel in Fig. 45, and the basic model design features are described by Bailey et al. in Ref. 105.

As the model was developed, the problem of isolating the aerodynamic forces acting on the airframe from the propulsion forces was addressed, as shown in Fig. 85. As it turned out, a single internal balance was used which supported all external surfaces except the boattail. The boattail forces were measured using surface-pressure instrumentation. In this manner, the use of seals was kept to a minimum, with one at each inlet and exit of the simulator and at the intersection of the support and lower fuselage.

A major part of the program has been the development of the calibration tank (Ref. 106) along with the control system itself, and the instrumentation needed to monitor inlet flow (Ref. 107). The general purpose of this facility (Fig. 86) is to obtain pretest relationships between the inlet and exit flow rates and pressure ratios as functions of the CMAPS control air parameters. As may be seen in Fig. 84, it will meter inlet air supply and exhaust extractors. All the required pressure valve controls and pressure instrumentation will be linked to a digital control console adjacent to the calibration tank.

5.2.5 Aircraft Engines

For large subscale or full-scale V/STOL testing, gas turbine engines are needed. It is at this scale that the larger size simulators, such as the 30-cm (12 in.) tip-driven fan, either have limitations in fan pressure ratio or require an excessive amount of compressed air for continuous operation. For direct blowing, most wind-tunnel facilities do not have sufficient compressed air capacity in either amount, pressure ratio, or heat. For large subscale models, the gas turbine engines developed for business jet aircraft adapt well to scales from 0.3 (for light transport aircraft) to 0.7 for tactical fighter designs. For larger models, there is a jump in thrust to the 10,000-lb class engines. Relative geometric profiles for some of the smaller engines are shown in Fig. 87 (Ref. 4). Ames Research Center has used these engines in several large-scale research investigations in the 40 by 80 tunnel. The engines have seldom been flightworthy, but have been maintained sufficiently to run at or near maximum thrust in most cases. An installation of the JT15D engine (as bypass ratio 3) used in a large-scale upper-surface-blowing investigation is shown in Fig. 88 installed in a boiler-plate nacelle without some of the nozzle fairings installed. One disadvantage of using this size of engine is that the fuel control and starter are usually located at the bottom of the engine, making it sometimes difficult to exactly scale the external nacelle contours of an aircraft configuration. However, this gave few problems in simulating the significant USB geometrical parameters needed for the model of Fig. 89 (Ref. 15).

Maximum rated performance is shown in Fig. 90 (Ref. 4) for an assortment of engines and tip-driven lift fans (LF 336 and LF 376). The augmented wing compressor and the Viper compressor are gas-turbine driven pumps which might be too large to be housed in a fuselage of a high-performance fighter model, but they provide cool air at 30 to 50 lbm/sec at pressure ratios up to 3.5. The J97 General Electric engine has been used in the basic research models with one shown in Fig. 8 (Ref. 108) and has a moderate combination of thrust-to-pressure ratio. NASA "inherited" all of these engines from a military program; they were in good enough condition to serve as reliable power sources. As can be seen from Fig. 90, there are no engines immediately available in the 10,000-lb class with sufficient pressure ratio to simulate some of the larger power plants now being planned with pressure ratios of 3 to 3.5. This is forcing the model size to nearly full scale for testing V/STOL supersonic tactical aircraft configurations in order to duplicate pressure ratio.

5.3 Model Planning

The foregoing discussions have attempted to treat model sizing and propulsion simulators separately. This was done primarily to allow emphasis on significant factors for each topic such as scale effects or details of the CMAPS. As was the case for using available engines (previous section), in actual model development, an experimentalist may have to take whatever power simulation is available. Providing it gives him the necessary parameters such as NPR or thrust, with the support equipment in the wind tunnel that is available to him, he will design his model around that particular simulator. The following are a few examples of V/STOL wind-tunnel model design and construction.

An 11% scale model of the Grumman 698 tilt nacelle aircraft is currently undergoing wind-tunnel tests in several U.S. facilities. This high-speed steel and aluminum model was designed and built simultaneously with the hover and wind-tunnel testing of the full-scale boiler-plated model. From previous development of conventional military aircraft using the TF34 simulator, sufficient experience with the unit indicated that it could be a reliable power plant for a V/STOL model. The model was constructed with provisions for both three internal balances and 200 surface-pressure taps, which resulted in the tubing network (Fig. 91) leading to the on-board Scanivalves. The nacelles, shown partly disassembled in Fig. 92, were designed to house the TF34 simulator, supply the required amount of drive air, and attach to the model through a floating or metric frame so that the propulsive forces and moments could be measured independently of those acting on the wing fuselage. In the process, a coil (Fig. 93) for the fan drive air was developed to minimize force and moment tares from the air. This was done before the air entered the model since there was not enough room inside the model to house isolation systems such as flow-through balances (see Sec. 6.1). As might be expected from the complexity of the model, there were several problems that had to be addressed, not the least of which was the excessive time needed to assemble the model on the sting. Tests using the model have been considered successes since reliable data were finally obtained and are now being analyzed. The final cost of this model corrected for 1984 dollars was probably over $800,000, and this did not include the cost of the TF34 simulators (approximately $100,000 per unit).

The prime question is could the above model have been designed in such a manner that the cost would have been lower. The answer is that it probably could not have been, although there were alternative designs which might have included two complete models, one being a force model with no surface-pressure instrumentation and the other strictly a pressure model. This is commonly done for high-speed conventional models, such as that shown in Fig. 94, which shows the model plus some of its components needed for alternative configurations and model changes. However, the principal cost of such models comes from the close tolerances required to

maintain scaled contours and model components that are interchangeable. Rapid advances in computer aided design and manufacture (CAD-CAM) techniques where applied to these complicated wind-tunnel models is reducing some of the time for construction, but there will always be a need for a certain amount of hand fitting, which runs up costs. Another option for the tilt-nacelle model, could have been the use of an unpowered or transition test that if the proper propulsion simulator had been available, could have been of larger scale but sized (about 0.2 scale) to the limits of testing in a moderately sized subsonic tunnel, such as the Langley V/STOL tunnel. The actual contouring tolerances could have been relaxed and wood-plus-foam-fiberglass materials considered. Even so, if the on-board pressure instrumentation were needed in both high- and low-speed models, the total costs of both models would be the same or more than the one that was built.

For large-scaled V/STOL models designed for testing in the NASA large-scale wind tunnels, the options in model design and construction are more numerous. Levels of sophistication and particular examples are shown in Table 6 defining several levels of costs. Level 1 would include the component tests such as the Q-fan (Fig. 32) or the high-angle-of-attack studies using the 0.4-scale model of Fig. 48. Level 2 would include large but probably subscale models of mostly boiler-plate construction and probably powered by the smaller gas turbine or turbofan engines mentioned in the previous section. Level 3 would include full-scale, mostly boiler-plate models using the same or similar power plants as planned for the aircraft, such as the AV-8B flight-like model of Fig. 5. Since this type of model is full scale, it could incorporate flight-weight components where appropriate. Level 4 would be wind-tunnel tests of the actual aircraft remotely controlled as required and adapted to the wind-tunnel support struts, using either the landing gear attachment points or reinforced wing-mounting arrangements. The increasing cost with level applies principally to tactical V/STOL aircraft for level 3 and below since the actual aircraft might be wind-tunnel tested cheaper than the total costs of building and testing a large but subscale fully powered model.

The term boiler plating might wrongfully have the connotation of making something overly heavy and strong with little regard for model weight and some of the aircraft details to be modeled. This is generally not the case at all though some models turn out heavy. What does reduce construction costs is to stay away from complex surface curvatures by using straight-line elements and rolling or multiple bending of the skin. Care must be taken in the planning of the model so that short straight-line elements simulate the scaled, gradually changing, surface contours. Stamped or machined elements are used for sharp curves such as leading edges or inlets. An example was the USB STOL model (Fig. 89) which incorporated the Pratt and Whitney JT15D powered nacelle of Fig. 88. For this model, the wing leading edges and flap skin were formed using multiple bends along straight-line wing elements and the inlets were spun-formed for blending with the skin of the nacelle. Most of the rest of the model was boiler plated, using welded steel construction, as shown in Fig. 95(a) for the two-engine fighter model (Fig. 8, Ref. 108). Where the surfaces are not exposed to hot flow, a rigid and complex surface is obtained by polyurethane foam, which is applied in liquid form between plywood ribs, allowed to expand, and then cured. This is then shaped and covered with several layers of fiberglass and filled. Going one step further, this technique can be incorporated with aircraft parts such as was done for the full-scale AV-8B model shown in Fig. 96 (Ref. 19).

6. TEST OPERATIONS

Planning and carrying out the actual wind-tunnel testing operation must depend not only on the capability and test limitations of the model but must also rely on full use of support and equipment available at the wind-tunnel facility. This is particularly true for the powered V/STOL model, testing at all speeds, where such things as time to set power, tunnel venting (where actual engines are used), change time, or time to take a data point can determine the success or failure of the test operation. Examples of the latter are factors considered in Ref. 4 and reprinted in Fig. 97. The actual data were obtained from experiences with gas-turbine powered models in the Ames 40 by 80, but they are significant factors to be dealt with for any powered-lift testing, particularly, downtime for configurational changes and time per data point. Many other factors influence facility use time. The ones chosen for the following brief discussion are instrumentation and data acquisition, acoustics studies, and flow surveying.

6.1 Instrumentation and Data Acquisition

It will be assumed that the experimentalist has available to him the most up-to-date instrumentation with potential for on-board use such as Scanivalves (if possible to install on the model) or a reliable flow-through balance similar to the one shown in Fig. 98, which was used in the investigation of Ref. 109. For power coming from cool compressed air, this design integrated the force isolation scheme for the drive air with the balance itself. In this case, opposing bellows and seals were used with a metric mass-flow distributor routing the air to various blowing systems in the model. When the air must be heated above about 200°C, the flow-through feature might not be practical, a result of thermal sensitivity of the force-measuring part of the balance. In such a case, drive air might have to be "jumped" through an isolation coil similar to that shown in Fig. 93.

As for Scanivalves, at the date of this lecture, many test facilities are converting to the electronic type which takes advantage of low-cost silicon pressure transducers whose inherent errors (such as thermal zero shift and output drift with time) are corrected by the periodic on-line calibrations. The advantage of this system, particularly for a powered model testing under fluctuating load, is that all pressures can be sampled almost simultaneously within the channel capacity of the data-acquisition system. At first glance, some of the possible installations seem geometrically smaller than the smallest of the mechanically driven ones (although this may not generally be the case). A possible disadvantage for low-speed V/STOL use is a measurement error resulting from the requirement to use a ± 5-lb/in.^{2} transducer for a ± 1-lb/in.^{2} measurement range. A unit of this range, however, will be available shortly. Other uncertainties are possible adverse effects caused by temperature and by high-frequency vibration of the mount.

For large-scale testing, an on-board data-acquisition system using pulse-code and modulation (PCM) similar to that used in flight testing, has been used for several years with the remote digitizer multiplexer unit (RMDU) which is evolving into the remote millivolt multiplexer and amplifier module (RAMM) (Ref. 110). This allows all conditioned analog signals except those from thermocouples to be digitized and multiplexed so that they can be transmitted to the data acquisition through a minimum of leads. The compatibility of electronic scanners with this system is under evaluation.

The wind-tunnel data-acquisition system that is finding acceptance at Ames Research Center with similar systems in industry was detailed by Cambra and Tolari in the mid-1970s (Refs. 111 and 112). The version finally adapted for the Ames Large Scale Test Facilities (40 by 80) is shown in Fig. 99. It is sufficiently flexible to be applied to both dynamic and steady-state testing. Also shown are the other operating systems, including the inputs from the mechanical (below the floor) wind-tunnel balance (Toledo system) which are transmitted to the data gathering processor (DGP) through the control processor. The real-time executive processor (REP) processes information from the DGP and rapidly returns the result to the displays in the control room. For normal V/STOL testing, real-time updating of the displays, which might include aerodynamic and propulsion parameters, every 1 sec has been found satisfactory. The existing choice in software provides a large range in time for data sampling during the recording process. For dynamic tests such as rotary-wing investigations, the dynamic analysis system (DAS) is available to be used either separately or combined with the DGP.

6.2 Special Requirements for Acoustic Studies

The strength of all possible noise sources on an aircraft should be determined during the final development of the aircraft in order to obtain the acoustic loading and to ensure a safe working environment for both the crew of the aircraft and ground-support personnel. For the USB tests of Schoenster et al. (Ref. 113) there were small but noticeable differences in surface acoustic loads owing to airspeed even though the airspeed tested (in the Langley 30 by 60) was only 16 m/sec. The investigation of the 727/JT8D flight noise (Ref. 114) compared model, full-scale wind-tunnel data, static-test data, and level flyover data for the 727 airplane. The JT8D installation shown in Fig. 100 was used with microphones on a traversing beam 3 m to the right of the engine centerline (looking aft) but still in the near-field. In this way, the angle relative to the noise source could be changed. When the measurements were extrapolated to the far-field, they compared well with the aircraft forward-speed effects, as shown in Fig. 101. The investigation has been one of several which pointed out the need for and value of continued acoustic study in the wind tunnel.

6.2.1 Method

Problems with and techniques for measuring strengths of noise caused by jets and inlets in the wind tunnel were evaluated by Soderman and others in the 1970s (Refs. 115-117). Measurements of noise radiation from powered V/STOL models can, generally, be confined to using incomplete or component models of the primary noise systems as was done for the Boeing 727 study just mentioned. In this way, the study of forward-speed effects on the acoustics of an aircraft can be investigated at full-scale with accurate model simulation of the anticipated noise sources. An exception to this was the evaluation of airframe noise (Ref. 118) where the noise radiating from a large-scale semispan model of the complete lifting system was measured in the 40 by 80.

The principal problem areas in measuring noise in a wind tunnel are source-noise reverberation, background noise owing to the wind-tunnel drive system, and microphone wind noise. To alleviate these, some tunnel facilities are updating the equipment and, in effect, doing the following: (1) acoustically treating the walls, (2) reducing fan-drive noise, and (3) reducing wind noise by refining support struts or eliminating protuberances from the walls. The challenge is one of selecting measuring devices that are directional or discriminate against unwanted sound, and by using special techniques and free-field comparisons to evaluate the reverberant field. An example of the latter is reverberant field simulation in which the reverberant sound field of compact wind-tunnel models is simulated by operating a calibrated loud speaker at the noise source location (Ref. 119). When the reverberant field level is known, the model noise data can be corrected to give approximate free-field noise levels. The technique was verified by wind-tunnel and flight correlations using the actual flyover noise, such as the XV-5 comparison of Fig. 102 (Ref. 120). Unfortunately, where the noise source is large and distributed relative to the size of the tunnel test section, such as for spanwise distributed blowing models, the technique cannot be applied, and reverberation corrections must come from operating both in the wind tunnel (at $V_\infty = 0$) and in the free field.

6.2.2 Forward Velocity Effects on Advanced Inlet Suppression of Fan Noise

The inlet-fan acoustic studies of Falarski and Moore (Ref. 121) and of Moore (Ref. 122) are other examples in which the wind tunnel was effective in evaluating forward-speed effects on acoustic sources. Flight effects on fan noise have been observed by investigators who have compared turbofan flyover noise with static noise, but the details are obscured by the mixture of aircraft-noise and other engine noise sources. Therefore, in order to understand fan noise, the actual flight conditions must be simulated. To suppress compressor noise, advanced inlet designs were devised. One design, the hybrid inlet, had a smaller than normal throat area and acoustic treatment in the diffuser. The other, the deflector inlet, had an extended low inlet lip with acoustic treatment to deflect fan noise up as well as forward. The performance and acoustics of both of these inlets were to be compared with those of a standard inlet with no diffusion. The objectives of the program were to determine the low-speed flight effects as simulated by the 40 by 80 on the forward radiated fan noise and on the acoustic suppression characteristics of the inlets.

The series of test inlets was designed around the requirements of the JT15D, with the resulting basic nacelle shown in Fig. 103. The turbine and the fan exhaust ducts, as well as the skin of the nacelle, were acoustically treated. The simulated flight tests in the Ames 40 by 80 used the test installation shown in Fig. 24(a), which is shown with microphone stands installed and with a circular traversing stand mounted in front of the model. The entire fan-strut assembly was mounted on the turntable of the wind tunnel for angle-of-attack adjustment. In both installations, a foam mat was installed which removed reverberant reflections from the noise data at all frequencies above 500 Hz. As a result, the fan-nacelle installation, using the JT15D as mounted was about 1/4-scale of moderately sized current, commercial turbofan aircraft's engines. To enhance simulation of the larger engine, the core IGV (inlet guide vanes) had been modified. The traversing microphone was kept aligned with the free stream by using a vane-type pivoted mount. The standard 0.25-in. microphone was used with a faired nose cone attached to reduce wind noise. Noise inside the inlet was measured using Kulite pressure transducers (outside tests only) mounted flush to the local surface.

Care with the details just mentioned, as well as with many other factors that influenced the data, eventually produced some interesting results, the foremost being that the hybrid inlet suppressed the high-tip-speed fan noise as much as 18 PNdB on a 61-m (200-ft) side line which was scaled to CF6 size engines. In

addition, it was found that no significant changes in fan-noise suppression for either inlet occurred for forward-velocity changes above 21 m/sec (68 ft/sec) or for angle-of-attack changes up to 15°.

This is another clear instance of wind-tunnel acoustic studies helping in the evaluation of flyover noise. In another sense, it verified some of the noise evaluation techniques prevailing today and which are applicable to acoustic studies of V/STOL aircraft.

6.3 Flow Surveying

For V/STOL wind-tunnel testing operations, flow visualization, if not flow-field surveys, can be a major part of the test program. The traditional method of using surface tufts, tuft or smoke probes, and directional flow surveying are necessary tools in understanding the complicated flow patterns which surround a powered-lifting system, and how they influence the aerodynamic parameters of the aircraft. For example, in the study and modeling of lifting jets, the flow visualization tests of Margason (Ref. 123) have been considered by some to be sufficiently quantitative to define the path of the jet-in-cross flow.

6.3.1 Surface Effects Study

No subsonic test of a lifting system is complete without the model being covered with tufts, oil, or kerosene. Studies such as that shown in Fig. 104 are instrumental in evaluating flap performance (and, in this case, model installation effects). For a review of some of these techniques used near the model surface the reader is referred to Werle (Ref. 124) (a general treatment of all flow-visualization technique) and Merzkirch (Crowder) (Ref. 125), who has specialized in the use of fluorescent minitufts for nonintrusive surface-flow visualization.

In addition to qualitative information that flow visualization has always provided, more quantitative information is now being obtained, from the imaging and numerical processing of flow-visualization pictures (Ref. 126). For two-dimensional flow, flow separation is becoming well understood, but in three dimensions the problem still needs considerable research. For interpreting flow-visualization data in three dimensions, the current trend is to use topological concepts with skin-friction lines. Although these concepts have been with us for some time, Hunt et al. (Ref. 127) initiated more interest in the subject. Recently, Kao and Burstadt (Ref. 128) applied the method to analysis of visualization data for deflected thrust V/STOL nozzles, and others have applied it to flow separation at high speed. More application to analysis of flow patterns on V/STOL aircraft in hover and transition should be continued in view of the economy of obtaining this type of data.

6.3.2 Flow-Field Measuring

Methods incorporating pressure probes, LDV, IR imaging, Schleiren, shadowgraphing, and hot-wire surveying are becoming well established. The use of smoke is becoming more common for evaluating flow fields, and, its use and limitations are thoroughly discussed by Werle (Ref. 124) and Mueller (Ref. 129). Where a quick approximate answer is required, the classical tuft grid should not be forgotten. The results of Naeseth (Ref. 130) were certainly descriptive of the effect of high power induced circulatory lift on the upwash near the engine inlet (Fig. 105). In view of the need of survey equipment and methods that can be used for three-dimensional flow in a hostile environment, such as is the case for V/STOL testing, the first two, pressure probes and LDV, will be discussed. Where there is a need for close study of the flow field involving high-energy jets, particularly at small scale and high speed, a special attempt should be made to utilize the wind-tunnel Schleiren and shadowgraphing equipment.

The use of pressure probes and rakes has been essential throughout the history of experimental aerodynamics. Rake survey equipment, boundary-layer rake probes, and directional pitot tubes have been standard equipment in most wind-tunnel facilities. For evaluating highly deflected flows, the directional pitot tube has continued to be used where more sophisticated methods, such as LDV, are not available. The probes have generally been lacking in three main areas: (1) their possible influence on the flow that is being measured, (2) lack of sensitivity for small-flow velocities, and (3) errors in measurement at high angles with respect to the axis of the probe. The first problem, has been reduced — but will never be eliminated — by the use of very small tubing with off-the-shelf probes of 1/8 D or less now being available. The second difficulty can only be helped with the use of careful calibration and sensitive pressure transducers that are geometrically close to the head of the probe. The third problem has been alleviated recently in two ways. First, the use of the five-hole probe (Fig. 106) (Ref. 47) was enhanced at the high-incidence range by using a potential-flow model to define the form of a calibrating equation. Constants for the equation were then obtained during calibration. Second, the other area has been the development of the seven-hole cone shown in Fig. 106 (Ref. 131), which has been calibrated over a large speed range with good accuracy up to 80° incidence.

Laser Doppler velocimetry (LDV) has been advancing steadily since the early 1970s. At Ames Research Center, Orloff et al. have been extending the measurement capability from the original two-color-two-dimensional backscatter laser velocimeter (2D-LV, 7 by 10 installation) to a 7 by 10 size three-dimensional laser facility and a large scale two-component unit. Because of the capability of obtaining flow velocity and direction measurements with no physical interference with the flow itself, the development of the equipment will continue. In a recent paper, Orloff et al. (Ref. 132) reviewed Ames LVD experience, and plans for and the accuracy of LDV systems are discussed in Ref. 133.

Diagrams of the 7 by 10 three-dimensional laser equipment are presented in Fig. 107. It measures three velocity components by means of three independent dual-scatter channels that operate in the backscatter direction. A combination of mechanical tilt and variable focusing are used to ensure that the focal point of the upper channel remains colocated with the focal point of the lower two-dimensional portion as the lower focal point moves in a cross-flow direction across the test section during a survey. Streamwise and vertical positioning is accomplished by moving the entire package (Fig. 107(a)) on the digitally controlled translation platform of Fig. 107(b). The status of this equipment gives repeatable positioning accuracy to less than 0.5 mm and the probe has a focal volume of 1.5 mm. It is generally operated in a closed-loop mode with the computer performing test-point positioning and path control through communication with five stepping-motor controllers. Rather than use forward scatter, such as the JPL equipment (Ref. 134), to increase

signal-to-noise level for some testing, the signal is enhanced by minimizing the bandwidth, the minimum being controlled by programmable frequency synthesizers. The equipment has been used extensively in the Ames jet-in-cross-flow program, Fig. 108 (Ref. 133), where surveys very close to the flat plate and nozzle have been completed.

The large-scale laser was developed to mount in the large wind tunnels, as shown in Fig. 109 (Ref. 135). It is a single color, dual-beam, scanning, confocal back scatter LDV that directly senses two orthogonal components of velocity; it is shown in operation in Fig. 110. A third component is obtained by further transformation of coupled velocity components. As shown in Figs. 110 and 111, the laser and system optics are mounted and enclosed in a streamline cylindrical shell that is supported along the longitudinal axis. The laser power unit and other components are mounted below the cylinder in a faired structure which also serves as its support. This entire assembly is mounted on a carriage for cross-flow translation. The current options for range are 10 or 20 m. This unit will also be used at the Ames Outside Aerodynamic Research Facility (OARF) to study ground-effect flow fields and ingestion problems being investigated using large-scale models.

7. CONCLUDING REMARKS

Aspects of wind-tunnel testing of V/STOL aircraft configurations have been reviewed. The choice of topics discussed were, generally, based on their significance to the planning stage of a wind-tunnel testing program. Suggestions and comments on techniques to be used during a test program covered a large range in types of testing and possible program costs. Their value would be greatly enhanced as the planning phase of a program matures by obtaining details from the sources listed and, most importantly, thorough consultation with the staffs of the wind tunnels that are being considered.

The material was organized into the given topics as a result of technical consideration with little, though some, discussion treating the economics of testing. Because of ever-increasing cost of wind-tunnel time and model construction, we are always looking for simpler and cheaper ways to construct models and for ways to reduce tunnel use, for example, by faster sampling of the data for each test condition, reduced configurational change time, or reducing the number of data points by improved data analysis methods which incorporate use of advanced prediction methods.

The accelerated use of CFD for isolated multienergy fluid dynamic problems which can apply to powered-lift aircraft concepts combined with a more thorough understanding of scale effects may eventually allow us to feel more confident with hover and transition testing at small scale or models sized for the 7 by 10 size tunnel. This model would then be restricted in on-board instrumentation. Use of the moderately sized wind tunnels, such as the DNW larger test section or the NASA Langley 4 by 7 m requires a model of a complete aircraft configuration which is currently pushing the state of the art in miniaturizing on-board instrumentation and power simulators. In addition, even at this scale for atmospheric wind tunnels there are scale effects, and problems in power simulation which might produce uncertainty in the results. One is therefore led to consider the use of large- or full-scale models powered by gas turbine engines and tested in NASA's large-scale test facilities. In these facilities there is the opportunity to test with both flight-like and flight-weight hardware, and, for some types of tests, the level of total program cost may not be much above small-scale tunnel testing.

Although most of my experience has been with large-scale methods, I will be the first to concede the value of small experiments, not only for exploratory use but sometimes for complete development programs in the design phase. There is ample experience in programs, such as the AV-8B development to show that it is desirable to make good use of small-scale testing in evaluating many of the basic aerodynamic problems and to verify the results using large-scale tunnel tests. During any stage of the aerodynamic development, it is recommended that large-scale testing with flight-like models be phased into the V/STOL wind-tunnel testing program to establish hover and transition characteristics. And, finally (for medium sized aircraft), the aircraft itself should be tested in one of the large-scale wind tunnels, either before or during flight tests, such as was done for the XV-15 tilt rotor or the XFV-5 lift fan aircraft. In this way, aerodynamic predictions, based on small-scale wind-tunnel data enhanced by computational techniques can be continually evaluated.

REFERENCES

1. Hickey, David H., "VSTOL Aerodynamics: A Review of the Technology." AGARD CP-143, V/STOL Aerodynamics, 1974, pp. 1-1 through 1-13.

2. Nelms, W. P., and Durston, D. A., "Preliminary Aerodynamic Characteristics of Several Advanced V/STOL Fighter/Attack Aircraft Concepts." NASA TM-81281, 1980.

3. Roberts, L., Deckert, W., and Hickey, D., "Recent Progress in V/STOL Aircraft Technology. NASA TM-81281, 1981.

4. Koenig, D. G., Aiken, T. N., and Aoyagi, K., "Large Scale V/STOL Testing. AIAA Paper 77-586, 1977.

5. Margason, R. J., "Jet V/STOL Wind Tunnel Simulation and Ground Plane Effects." Paper No. 15, AGARD Conference Proceeding No. 308, Lisbon, Nov. 1981.

6. Pope, A., and Harper, J. J., "Low Speed Wind Tunnel Testing." John Wiley & Sons, Inc., New York, 1966.

7. Pope, A., and Goin, K. L., "High Speed Wind Tunnel Testing." John Wiley & Sons, Inc., New York, 1965.

8. Johnson, D. B., Lacey, T. R., and Vodo, J. J., "Powered Wind Tunnel Testing of the AV-8B: A Straightforward Approach Pays Off." AIAA Paper 79-0333, New Orleans, La., Jan. 1979.

9. Lacey, T. R., and Miller, K., "The AV-8B Wing Aerodynamic Concept and Design." AIAA Paper 77-607, 1977.

10. Clapper, W. S., Mani, R. J., Stringas, E. J., and Banerian, G., "Development of a Technique for Inflight Jet Noise Simulation. Part I." J. Aircraft, Vol. 15, No. 2, Feb. 1978.

11. Pirrello, C. J., Hardin, R. D., Heckart, M. V., and Brown, K. R., "An Inventory of Aeronautical Ground Facilities." Vol. I. Aeronautical Facilities. Vol. II. Airbreathing Engine Test Facilities. NASA CR-1874 and 1875, Nov. 1971.

12. Aiken, T. N., Falarski, M. D., and Koenig, D. G., "Aerodynamic Characteristics of a Large Scale Semispan Model with a Swept-Wing and an Augmented Jet Flap with Hypermixing Nozzles." NASA TM-73236, 1979.

13. Koenig, D. G., Stoll, F., and Aoyagi, K., Application of Thrusting Ejectors to Tactical Aircraft Having Vertical Lift and Short Field Capability." AIAA Paper 81-2629, 1981.

14. Aoyagi, K., Falarski, M. D., and Koenig, D. G., "Wind Tunnel Investigation of a Large-Scale Upper Surface Blown-Flap Transport Model Having Two Engines." NASA TM X-62,296, 1973.

15. Koenig, D. G., and Aoyagi, K., "Maximum Lift of Upper Surface Blowing STOL Aircraft with Swept Wings." AIAA Paper 75-868, Hartford, Conn., 1975.

16. Gambucci, B. J., Aoyagi, K., and Rolls, L. S., "Wind Tunnel Investigation of a Large-Scale Model of a Lift/Cruise Fan V/STOL Aircraft." NASA TM X-73,139, 1976.

17. Gambucci, B. J., Aoyagi, K., and Rolls, L. S., "Wind Tunnel Investigation of a Large-Scale Model of a Lift/Cruise Fan V/STOL Aircraft with Extended Lift/Cruise Nacelles." NASA TM X-73,164, 1976.

18. "Wind Tunnel and Ground Static Investigation of a Large Scale Model of a Lift/Cruise Fan V/STOL Aircraft." NASA CR-137,916, 1976.

19. Hollingsworth, E. G., Aiken, T. N., and Ragget, J., "Validation of AV-8B V/STOL Characteristics of Full-Scale Static and Wind-Tunnel Tests." AIAA Paper 77-597, Moffett Field, Calif., 1977.

20. Steinle, F., and Stanewsky, E., "Wind Tunnel Flow Quality and Data Accuracy Requirements." AGARD-AR=184, Nov. 1982.

21. Mobey, D. G., "Flow Unsteadiness and Model Vibration in Wind Tunnels at Subsonic and Transonic Speeds." C.P. No. 1155, British A.R.C., 1971.

22. Paterson, Robert W., Vogt, Paul G., and Foley, William M., "Design and Development of the United Aircraft Research Laboratories Acoustic Research Tunnel." J. Aircraft, Vol. 10, No. 7, July 1973, pp. 427-433.

23. Seidel, M., and Jaarsma, F., "The German-Dutch Low Speed Wind Tunnel DNW." Aeronaut. J., RAS, Apr. 1978.

24. Duits Nederlands Windtunnel Staff, Noordoostpolder, The Netherlands — Compilation of Calibration Data of the German-Dutch Wind Tunnel. MP-82.01, Mar. 1982.

25. Herkes, W. H., and Strout, F. G., "Acoustic Evaluation of the DNW Free Jet Shear Layer Correction Using a Model Jet." AIAA Paper 83-757, 1983.

26. Christophe, J., "The ONERA Wind Tunnels at Mondane Centre and Le Eouga Centre and Their Utilization in Subsonic Range." Office National d'Etudes et de Recherches Aërospatiales, T.P. n 1983-28. Paper was also presented at the 19th Subsonic Aerodynamic Testing Association, Meeting College Station, Kansas, April 18-20, 1983.

27. Applin, Z. T., "Flow Improvement in the Circuit of the Langley 4- by 7-Meter Tunnel." NASA TM-85662, 1983.

28. "The Boeing V/STOL Wind Tunnel Users Manual." Boeing Vertol Company, Philadelphia, Pa., Oct. 1982.

29. Mort, Kenneth W., Soderman, Paul T., and Eckert, William T., "Improving Large-Scale Testing Capability by Modifying the 40- by 80-Foot Wind Tunnel." AIAA Paper 77-587, 1977.

30. "Guide for Planning Investigations in the Ames 40- by 80-Foot Wind Tunnel Operated by the Large-Scale Aerodynamic Branch." Ames Research Center, Moffett Field, Ca., June 1978.

31. Grafton, S. B., Gilbert, W. P., Croom, M. A., and Murr, D. G., "High-Angle-of-Attack Characteristics of a Forward-Swept Wing Fighter Configuration." AIAA Paper 82-1322, 1982.

32. Phelps, A. E., III, "Summary of Low Speed Aerodynamic Characteristics of Upper-Surface-Blown Jet-Flap Configurations." Paper No. 4, NASA SP-406, 1976.

33. " The 9M V/STOL Wind Tunnel — A Brief Description and Photo Review of Projects." National Research Council of Canada, Ottawa, Canada, July, 1979.

34. Knott, P. G., "V/STOL Aerodynamic Testing Techniques at British Aircraft Corporation." AIAA Paper 77-584, 1977.

35. Grief, R. K., Kelly, M. W., and Tolhurst, W. H., "Wind-Tunnel Tests of a Circular Wing with an Annular Nozzle in Proximity to the Ground." NASA TN D-317, 1960.

26. East, L. F., "The Measurement of Ground Effect Using a Fixed Ground Board in a Wind Tunnel." ARC, R & M 3689, 1972.

37. Betzina, M. D., and Kita, R. D., "Aerodynamics Effects of an Attitude Control Vane on a Tilt Nacelle V/STOL Propulsion System." AIAA Paper 79-1855, 1979.

38. Demers, W. J., Metzger, F. B., Smith, L. M., and Wainauski, H. S., "Testing of the Hamilton Standard Q-Fan Demonstrator (Lycoming T55-L-11A Core Engine." NASA CR-121,265, 1973.

39. Betzina, M. D., and Falarski, M. D., "Aerodynamics of a Tilt-Nacelle V/STOL Propulsion System." NASA TM-78606, 1979.

40. Weiberg, J. A., and Maisel, M. D., "Wind Tunnel Tests of the XV-15 Tilt Rotor Aircraft." NASA TM-81177 (also AVRADCOM TR80-A03, April 1980).

41. Schoers, L. G., "Dynamic Structural Aeroelastic Stability Testing of the XV-15 Tilt Rotor Research Aircraft." NASA TM-84293 (also USAAVRADCOM 82-A-17), 1982.

42. Smeltzer, D., Nelms, W., and Williams, T., "Airframe Effects on a Top-Mounted Inlet System for V/STOL Fighter Aircraft." AIAA Paper 81-2631, 1981.

43. Durston, D. A., and Smeltzer, D. B., "Inlet and Airframe Compatibility for a V/STOL Fighter/Attack Aircraft with Top-Mounted Inlets." NASA TM-84252.

44. Schetz, J. A., and Jakubowski, A. K., "Surface Pressured Induced on a Flat Plate with In-Line and Side-by-Side Dual Jet Configurations." AIAA Paper 83-1849, 1983.

45. Schetz, J. A., Jakubowski, A. K., and Aoyagi, K., "Jet Trajectories and Surface Pressures Induced on a Body of Revolution with Various Dual Jet Configurations." AIAA Paper 83-0080, 1983.

46. Aoyagi, K., and Snyder, P. K., "Experimental Investigation of a Jet Inclined to Subsonic Crossflow." AIAA Paper 81-2610, 1981.

47. Fearn, R. L., and Weston, K. P., "Induced Velocity Field of a Jet in a Cross Flow." NASA TP-1087, 1978.

48. Fearn, R. L., and Weston, R. P., "Velocity Field of a Round Jet in a Cross Flow for Various Jet Injection Angles and Velocity Ratios." NASA TP-1506, 1979.

49. Mavriplis, F., and Gilmore, D., "Investigation of Externally Blown Flap Airfoils with Leading Edge Devices and Slotted Flaps." AGARD V/STOL Aerodynamics, No. 143, Paper No. 7, April 1971.

50. Aiken, Thomas N., "Aerodynamic and Noise Measurements on a Quasi-Two-Dimensional Augmentor Wing Model with Lobe-Type Nozzles." NASA TM X-62,237, 1973.

51. Riley, D. R., "Wind Tunnel Investigation and Analysis of the Effects of End Plates on the Aerodynamic Characteristics of an Upswept Wing." NACA TN-2440, 1951.

52. Mahal, A. S., and Gilchrist, I. J., "Design Integration and Noise Studies for Jet STOL Aircraft — Task VIIB Augmentor Wing Cruise Blowing Valveless System." NASA CR-114,560, Jan. 1973.

53. Anscombe, A., and Williams, J., "Some Comments on High-Lift Testing in Wind Tunnels with Particular Reference to Jet-Blowing Models." AGARD Report 63, Aug. 1956.

54. Schoen, A. H., Kolesar, C. E., and Schaeffer, E. G., "Static, Noise, and Transition Tests of a Combined-Surface-Blowing V/STOL Lift/Propulsion System." NASA CR-151,954, April 1977.

55. "Advancement of Proprotor Technology Task II — Wind Tunnel Test Results." NASA CR-114,363, 1971.

56. Durston, D. A., and Schreiner, J. A., "High-Angle of Attack Aerodynamics of a Strake-Canard-Wing V/STOL Fighter Configuration." AIAA Paper 83-2510, Oct. 1983.

57. Bailey, R. O., Smith, S. C., and Gustie, J. B., "Propulsion Simulation Test Technique for V/STOL Configurations." Society of Automotive Engineers TP-83-1427, Oct. 1983.

58. Mraz, M. R., and Hiley, P. E., "Propulsion Airframe Aerodynamics Interactions of Supersonic V/STOL Configurations, Phase I." McDonnell Douglas MDC A7238, St. Louis, Mo., NASA Contract NAS2-10791, July 1981.

59. Schnell, W. C., Ordonez, G. W, and Smeltzer, D. B., "Axisymmetric and Non-Axisymmetric Exhaust-Jet-Induced Effects on a V/STOL Vehicle Desigh. Part III. Experimental Technique." NASA CR-166,147, 1981.

60. Stoll, F., "Large-Scale Wind Tunnel Tests of a Sting Supported V/STOL Fighter Model at High Angles-of-Attack." AIAA Paper 81-2621, 1981.

61. Stoll, F., Koenig, D. G., "Large-Scale Wind Tunnel Investigation of a Close-Coupled Canard-Delta Wing Fighter Model through High Angles-of-Attack." AIAA Paper 83-2554, 1983.

62. Laub, Georgene H., "Low Speed Wind Tunnel Tests on a One-Seventh Scale Model of the H.126 Jet Flap Aircraft." NASA TM X-62,433, 1975.

63. Trebble, W. J. G., "Technique for the Aerodynamic Testing of V/STOL Models." AGARD, AGARDograph 126, May 1968.

64. Cook, W. L., and Whittley, D. C., "Comparison of Model and Flight Test Data for an Augmented Jet Flap STOL Research Aircraft." NASA TM X-62491, 1975.

65. Hickey, D. H., and Cook, W. L., "Correlation of Wind-Tunnel and Flight-Test Aerodynamic Data for Five V/STOL Aircraft." AGARD, Flight Mechanics Panel Meeting, Oct. 1965.

66. Vogler, R. D., "Ground Effects on Single- and Multiple-Jet VTOL Models at Transition Speeds over Stationary and Moving Ground Planes." NASA TN D-3213, Jan. 1966.

67. Campbell, J. P., Hassell, J. L., and Thomas, J. L., "Recent Research on Powered Lift STOL Ground Effects." AIAA Paper 77-574, 1977.

68. Turner, T. R., "A Moving Belt Ground Plane for Wind Tunnel Ground Simulation and Results for Two Jet-Flap Configurations." NASA TN D-4228, 1967.

69. Butler, S. F. J., Moy, B. A., and Pound, T. N., "A Moving-Belt Rig for Ground Simulation in Low-Speed Wind Tunnels." Aeronautical Research Council, R & M., No. 3451, 1967.

70. Hackett, J. E., Boles, R. A., and Lilley, D. E., "Ground Effect for V/STOL Aircraft Configurations and Its Simulation in the Wind Tunnel." "Pt. I. Introduction and Theoretical Methods." "Pt. II. Experimental Studies." "Pt. III. The Tangentially Blown Ground as an Alternative to a Moving Ground, Application to the Ames 40 by 80." NASA CRs 114,495; 114,496; and 114,497, 1974.

71. Poisson-Quinton, Ph., and Christophe, J., "Special Ground Testing Facilities and Testing Techniques for STOL Aircraft." Von Karman Institute for Fluid Dynamics, Lecture Series 60, STOL Technology, Sept. 1973.

72. Hackett, J. E., Boles, R. A., Lilley, D. E., "Ground Simulation and Tunnel Blockage for a Jet-Flapped, Basic STOL Model Tested to Very High Lift Coefficients." NASA CR-137,857, 1976.

73. Crowder, J. P., Goldhammer, M. I, and Smyth, D. N., "STOL Aircraft Transient Ground Effects. Pt. II. Experimental Techniques Feasibility Study." NASA CR-137,767, 1975.

74. Wolowicz, C. H., Bowman Jr., J. S., and Gilbert, W. P., "Similitude Requirement and Scaling Relationships as Applied to Model Testing." NASA TP-1435, 1979.

75. Gainer, T. G., and Hoffman, S., "Summary of Transformation Equations of Motion Used in Free-Flight and Wind Tunnel Data Reduction and Analysis." NASA SP-3070, 1972.

76. Paulson, John W., "Investigation of the Low-Speed Flight Characteristics of a 1/15 Scale Model of the Convair XV-58 Airplane." NACA RM-SL57K19.

77. Putnam, W. F., and Curtiss, H. C., Jr., "Low Speed Testing-Techniques for V/STOL Aircraft in the Princeton Dynamic Model Track." AIAA Paper 79-0334, 1979.

78. Putnam, W. F., "Tests on a Twin-Turbofan V/STOL Model in Ground Effect in the Dynamic Model Track," Princeton University, Princeton, New Jersey, Final Report for Navy Contract N62269-79-C-0223, Jan. 1983.

79. Heyson, Harry H., "Wind Tunnel Testing of VTOL and STOL Aircraft." NASA TM-7850, 1978.

80. Maskell, E. C., "A Theory of the Blockage Effects on Bluff Bodies and Stalled Wings in a Closed Wind Tunnel." Royal Aeronautical Establishment R&M No. 3400, Nov. 1963.

81. Peitzman, F. W., "Determination of High Attitude Wall Corrections in a Low Speed Wind Tunnel." AIAA Paper 78-810, 1978.

82. Hackett, J. E., "Living with Solid Walled Wind Tunnels." AIAA Paper 82-0583, 1982.

83. Hackett, J. E., Wilsden, D. J., and Lilley, D. E., "Estimation of Tunnel Blockage from Wall Pressure Signatures: A Review and Data Correlation." NASA CR-152,241, 1979.

84. Snyder, L. D., and Erickson, L. L., "PAN-AIR Prediction of NASA Ames 12-Foot Pressure Wind Tunnel Interference on a Fighter Configuration." AIAA Paper 84-0219, 1984.

85. Tyler, R. A., and Williamson, R. G., "Experience with the NRC 10-ft x 20-ft V/STOL Propulsion Tunnel: Some Practical Aspects of V/STOL Engine Model Testing." NAE Quarterly Bulletin, No. 2, 1973, pp. 45-59, 61-75.

86. Hoad, D. R., and Gentry, G. L., Jr., "Longitudinal Aerodynamic Characteristics of a Low-Wing Lift Fan Transport Including Hover Characteristics in and out of Ground Effect." NASA TM X-34020, 1977.

87. "Conference on V/STOL and STOL Aircraft." NASA SP-116, 1966.

88. Carbonaro, M., "Interference Problems in V/STOL Testing at Low Speeds." AGARD-CP-174, No. 40, Oct. 1975.

89. Shindo, S., and Rae, W. H., Jr., "Low Speed Test Limit of V/STOL Models Located Vertically Off-Center." J. Aircraft, Vol. 15, No. 4, April 1978, pp. 253, 254.

90. Shindo, S., and Rae, W. H., Jr., "Recent Research on V/STOL Test Limits at the University of Washington Aeronautical Laboratory." NASA CR-3237, 1980.

91. Steinle, F. W., and Pejack, E. R., "Toward an Improved Transonic Wind-Tunnel Wall Geometry — A Numerical Study." AIAA Paper 80-0442, 1980.

92. Sears, W. R., "Adaptable Wind Tunnel for Testing V/STOL Configurations at High Lift." J. Aircraft, Vol. 20, No. 11, Nov. 1983, pp. 968-974.

93. Christiansen, R. S., "A Large Scale Investigation of V/STOL Ground Effects." AIAA Paper 84-0336, 1984.

94. Henderson, C., and Walters, M., "Development and Validation of the V/STOL Aerodynamics and Stability and Control Manual." AIAA Paper 81-2611, Dec. 1981.

95. Kuhlman, J. M., and Ousterhout, D. S., "Experimental Investigation of Effect of Jet Decay Rate on Jet-Induced Pressures on a Flat Plate." NASA CR-2979, 1978.

96. Kuhlman, J. M., and Warcup, R. W., "Jet Decay Rate Effects on Hover Jet-Induced Loads." J. Aircraft, Vol. 17, No. 8, Aug. 1980, p. 605.

97. Wulf, R., and Melzer, E., "Wind Tunnel Testing with Engine Simulation for V/STOL Airplanes," AGARD, V/STOL Propulsion Systems, No. 135, Paper No. 8, 1973.

98. Margason, Richard J., and Gentry, Carl L., "Static Calibration of an Ejector Unit for Simulation of Jet Engines in Small-Scale Wind Tunnel Modes." NASA TN D-3867, Mar. 1967.

99. Hoad, D. R., "Longitudinal Aerodynamic Characteristics of an Externally Blown Flap Powered Lift Model with Several Propulsive System Simulators." NASA TN D-7670, 1974.

100. Nicoloff, C. B., and Weber, H. A., "Characteristics of an Ejector-Type Engine Simulator for STOL Model Testing." AIAA Paper 72-1038, 1972.

101. Stewart, V. R., "Low Speed Wind Tunnel Tests of Ground Proximity and Deck Edge Effects on a Lift Cruise Fan V/STOL Configuration." NASA CR-152,247.

102. Hunt, D., Clingen, J., Salemann, V., and Omar, E., "Wind Tunnel and Ground Static Tests of a 0.094 Scale Powered Model of a Modified T-39 Lift/Cruise Fan V/STOL Research Airplane." NASA CR-151,923, 1977.

103. "Installation and Operation Manual, Model 1109, 12" Diameter, Tip-Turbine Fan." TM78-114, Tech Development, Inc., Dayton, Ohio, Oct. 1978.

104. Eigenman, M. F., and Bailey, R. O., "Development of the Propulsion Simulator — A Test Tool Applicable to V/STOL Configurations." Society of Automotive Engineers 770984, Nov. 1977.

105. Bailey, R., Mraz, M., and Hiley, P., "The Design of a Wind Tunnel V/STOL Fighter Model Incorporating Turbine Powered Engine Simulators." AIAA Paper 81-2635, 1981.

106. Harper, M., "The Propulsion Simulator Calibration Laboratory at Ames Research Center." AIAA Paper 82-0574, 1982.

107. Smith, S. C., "Determining Compressor Inlet Airflow in the Compact Multimission Aircraft Propulsion Simulators in Wind Tunnel Applications." AIAA Paper 83-1231, 1983.

108. Falarski, M. D., Whitten, P. D., and Harris, P. D., "Aerodynamic Characteristics of a Large Scale Model of a Highly Maneuverable Supersonic V/STOL Fighter: STOL Configuration." AIAA Paper 80-0234, 1980.

109. Dawson, C. R., "Ground Effects and Control Effectiveness Tests of a 0.095 Scale Powered Model of a Modified T-39 Lift/Cruise Fan V/STOL Research Airplane." Boeing Document D 180-20391-1, Boeing Aircraft Company, Seattle, Wash., Feb. 1977.

110. Juanareno, D. B., and Blumenthal, P. Z., "A Remote Millivolt Multiplexer and Amplifier Module for Wind Tunnel Data Acquisition." Pressure Systems Incorporated, Hampton, Va., NASA Lewis Contract, NAS3-22950.

111. Cambra, J. M., and Tolari, G. P., "Real-Time Computer Data System for the 40- by 80-Foot Wind Tunnel Facility at Ames Research Center." NASA TN D-7970, 1975.

112. Cambra, J. M., and Trover, W. F., "The Revolution in Data Gathering Systems." NASA TM X-62,452, 1975.

113. Schoenster, J. A., Willis, C. M., Schroeder, J. C., and Mixson, John S., "Acoustic-Loads Research for Powered-Lift Configurations." NASA SP-406, May 1976, pp. 429-443.

114. Strout, F. G., and Atencio, A., Jr., "Flight Effects on JT8D Engine Jet Noise as Measured in the NASA Ames 40- by 80-Foot Wind Tunnel." AIAA Paper 76-556, 1976.

115. Soderman, P. T., "Instrumentation and Techniques for Acoustic Research in Wind Tunnels." IEEE Publication 75 CHU 993 6 AES, 6th International Congress on Instrumentation in Aerospace Simulation Facilities, Ottawa, Canada, Sept. 22-24, 1975.

116. Falarski, M. D., Koenig, D. G., and Soderman, P. T., "Aspects of Investigating STOL Noise Using Large-Scale Wind-Tunnel Models." Journal of the Canadian Aeronautics and Space Institute, Vol. 19, No. 2, Feb. 1973.

117. Diedrich, J. H., and Luidens, R. W., "Measurement of Model Propulsion System Noise in a Low-Speed Wind Tunnel." AIAA Paper No. 76-91, 1976.

118. Ahtye, W. F., "Wing and Flap Noise Measured by Near- and Far-Field Cross, Correlation Techniques." AIAA Paper 79-0667, 1979.

119. Atencio, A., Jr., and Soderman, P. T., "Comparison of Aircraft Noise Measured in Flight Test and in the NASA Ames 40- by 80-Foot Wind Tunnel." AIAA Paper 73-104.7, 1973.

120. Cook, W. L., and Hickey, D. H., "Correlation of Low Speed Wind Tunnel and Flight Test Data for V/STOL Aircraft." NASA TM X-62,423, 1975.

121. Falarski, M. D., and Moore, M. T., "Acoustic Characteristics of Two Hybrid Inlets of Forward Speed," AIAA Paper 79-0678, 1979.

122. Moore, M. T., "Forward Velocity Effects on Fan Noise and the Suppression Characteristics of Advanced Inlets as Measured in the NASA Ames 40- by 80-Foot Wind Tunnel." NASA CR-152328, 1979.

123. Margason, R. J., "The Path of a Jet Directed at Large Angles to a Subsonic Free Stream." NASA TN D-4919, 1968.

124. Werle, H., "Flow Visualization Techniques for the Study of High Incidence Aerodynamics." AGARD VKI Lecture Series 121, 1982.

125. Merzkirch, W., ed., "Flow Visualization Proceedings of the Second International Symposium on Flow Visualization." Crowder, J. P., "Fluorescent Minitufts of Nonuniform Surfaces Flow Visualization." Proceedings of the Second International Symposium on Flow Visualization, Bochum, West Germany, pp. 663-667, Sept. 1980.

126. Imaichi, K., and Ohmi, K., "Numerical Processing of Flow-Visualization Pictures — Measurement of Two-Dimensional Vortex Flow." J. Fluid Mech., Vol. 129, Apr. 1983, pp. 283-311.

127. Hunt, J. C. R., Abell, C. J., Peterka, J. A., and Woo, H., "Kinematical Studies of the Flows around Free or Surface-Mounted Obstacles: Applying Topology to Flow Visualization." J. Fluid Mech., Vol. 86, May 1978, pp. 179-200.

128. Kao, H. C., and Burstadt, P. L., "Flow Visualization and Interpretation of Visualization Data for Deflected Thrust V/STOL Nozzles." NASA TM-83554, 1984.

129. Mueller, T. J., "Smoke Visualization in Wind Tunnels." Astronaut. Aeronaut., Jan. 1983, pp. 50-62.

130. Naeseth, Roger L., and Hoad, Danny R., "Upwash Angles Near Engine Inlets of an Externally Blown Flap STOL Transport." NASA TN D-8091, 1975.

131. Everett, K. N., Gerner, A. A., and Durston, D. A., "Theory and Calibration of Non-Nulling Seven Hole Cone Probes for Use in Complex Flow Measurement." AIAA Paper 82-0232, 1982.

132. Orloff, K. L., Snyder, P. K., and Reinath, M. S., "Laser Velocimetry in the Low Speed Wind Tunnels at Ames Research Center." NASA TM-85885, 1984.

133. Orloff, K. L., and Snyder, P. K., "Laser Doppler Anemometer Measurements Using Nonorthogonal Velocity Components: Error Estimates." Appl. Opt., Vol. 21, Jan. 1982, pp. 339.

134. Beranl, L. D., and Sarohia, V., "Entrainment and Mixing in Thrust Augmenting Ejectors." AIAA Paper 83-0172, 1983.

135. Reinath, M. S., Orloff, K. L., and Snyder, P. K., "A Laser Velocimeter System for the Ames 40- by 80-Foot and 80- by 120-Foot Wind Tunnels." AIAA Paper 84-0414, Jan. 1984 (also NASA TM-84393, 1984).

TABLE 1.- EVALUATION OF FIXED FRAME FACILITIES (REPRINTED FROM REF. 10)

Facility requirements	Objectives	NASA/ Langley	NASA/ Lewis	NASA/Ames 7' × 10'	NASA/Ames 40' × 80'	GE open throat anechoic wind tunnel
Nozzle weight flow	25 lbm/sec	17 lbm/sec	25 lbm/sec	25 lbm/sec with modification	25 lbm/sec with modification	42 lbm/sec
Nozzle size	4" - 6"	?	4" - 6"	4"	6"	6"
Exhaust gas total temperature range	520°R-2500°R	Burner needs to be provided	Ambient	Ambient	Ambient - 1600°R	Ambient - 3000°R
Nozzle pressure ratio	1.5 - 4.0	?	1.5 - 4.0	1.0 - 2.5	1.0 - 2.5	1.5 - 4.0
Free stream velocity range	0-400 ft/sec	0-400 ft/sec	0-220 ft/sec	0-400 ft/sec	0-325 ft/sec	0-330 ft/sec
Facility wall type	Anechoic	Anechoic	Hardwall	Scottfelt	Partially treated	Anechoic
Performance measurements	Proven nozzle performance system + 1/2% accuracy	Extensive modifications	Will have capability by Dec. 1974	Extensive modifications	Extensive modifications	Feasibility to be studied
Facility availability	1974, 1975, 1976	1974, 1975 1976	1976	1974, 1975, 1976	9 weeks/yr	1975, 1976
Duration of operation	Continuous	Blowdown	Continuous	Continuous	Continuous	Continuous
Capable of performing laser velocimeter measurements	Large window high quality optical glass	Minor modifications	Would require modifications	Yes	Would require modifications	Designed to accept laser velocimeter

TABLE 2.- REDUCED VELOCITY SCALE (FROM REF. 34)

V_o/V_j	0.05	0.075	0.10	0.15	0.20	0.30	0.50
C_μ $(S/A_j = 40)$	20	9	5	2	1.25	0.6	0.2
V_o Full scale, m/sec	20	30	40	60	80	120	200
V_j Full scale, m/sec	400						
V_o Model scale, m/sec	20						
V_j Model scale, m/sec	400	267	200	133	100	67	40
$\left(\frac{V_o \text{ model scale}}{V_o \text{ full scale}}\right)$	1.0	0.67	0.5	0.33	0.25	0.17	0.1

TABLE 3.- ACCEPTABLE LIMITS TO WALL CORRECTIONS (FROM REF. 88)

Parameter	Maximum acceptable corrections	Moderate corrections	No corrections
$\Delta\alpha$	± 5°	± 5°	± 1/2°
q_c/q	1 ± 10%	1 ± 10%	1 ± 5%
Δi_t	± 5°	± 2°	± 1/2°
q_t/q_c	1 ± 10%	1 ± 5%	1 ± 5%
Δi_w	± 2°	± 1/2°	± 1/2°
$d(\Delta i_w)/d(y/b)$	± 5°/semispan	± 1°/semispan	± 1°/semispan
$\Delta q/q_c$	± 10%	± 5%	± 5%

CORRESPONDING LIMITS FOR A JET FLAPPED WING OF ASPECT RATIO 6; B/H = 4/3

	Moderate corrections	Maximum corrections
Normal mounting at the center of a 4:3 test section		
b/B = 1/2	$C_L < 6.3$	$C_L = 14.1$
b/B = 3/4	$C_L < 0.81$	$C_L < 4.14$
Semispan mounting on the floor of a 4:3 test section		
(b/2)/H = 1/3	$C_L < 15$	$C_L < 20.4$
(b/2)/H = 1/2	$C_L < 4.86$	$C_L < 11.0$
(b/2)/H = 2/3	$C_L < 2.4$	$C_L < 5.82$

TABLE 4.- JET THRUST SIMULATION (FROM REF. 5 WITH ADDITIONS)

Nacelle type	Air supply requirement	Principal simulations	Other simulation capabilities	Comment
Flow	None	• Inlet geometry • Inlet V_i/V_∞ at one Mach No.	• Dual flow	• Simple • Good for aerodynamic drag studies
Blown jet	Large	• Exhaust nozzle geometry • Gross thrust	• Dual flow • Hot gas	• Simple operation • Erroneous inlet contribution
Ejector	Moderate	• Inlet geometry/or • Exhaust nozzle geometry/and • Gross thrust	• Dual flow	• Inlet and exhaust flow not simulated simultaneously
Turbine powered	Small	• Inlet geometry or exhaust nozzle geometry • Inlet V_i/V and not gross thrust • Gross thrust and not inlet V_i/V		• Sensitive mechanism • Difficult to simulate inlet and exhaust flow simultaneously
Gas turbine powered	Small	• Inlet and exhaust nozzle geometry • Inlet V_i/V plus gross thrust • Exhaust Mach No. and temperature	• Dual flow	• For subscale use bypass ratio may not always be simulated • For subscale, engine is often over size

TABLE 5.- LEVELS OF SOPHISTICATION: LARGE-SCALE MODELS

Generally Increasing Model Cost >				
Factor	1	2	3	4
Airframe	Approximated configuration	Scaled configuration	Full-scale configuration	
Propulsion	Simulated propulsion	Engine used but small	Including some structure	Aircraft
Controls	Scaled		Same engine	
Dynamics				
Electronics				
Other				
Examples				
Model type	1	2	3	4
Complete configuration	High α (0.4 scale) (VATOL models)	QSRA model	AV-8B 40 by 80	XFV 15 40 by 80
	Q-fan simulation of tilt nacelle	Basic USB/EBF research models	G 698 40 by 80	AV-8B (static)
		M-260		XFV 12A
		97 powered ejector model		Tether and static
Semispan	Aug Wing 40 by 80	Cooling drag	Cooling drag	NA
Components	Thrust reverser	Acoustic test 40 by 80	698 nacelle "D" nozzle	NA

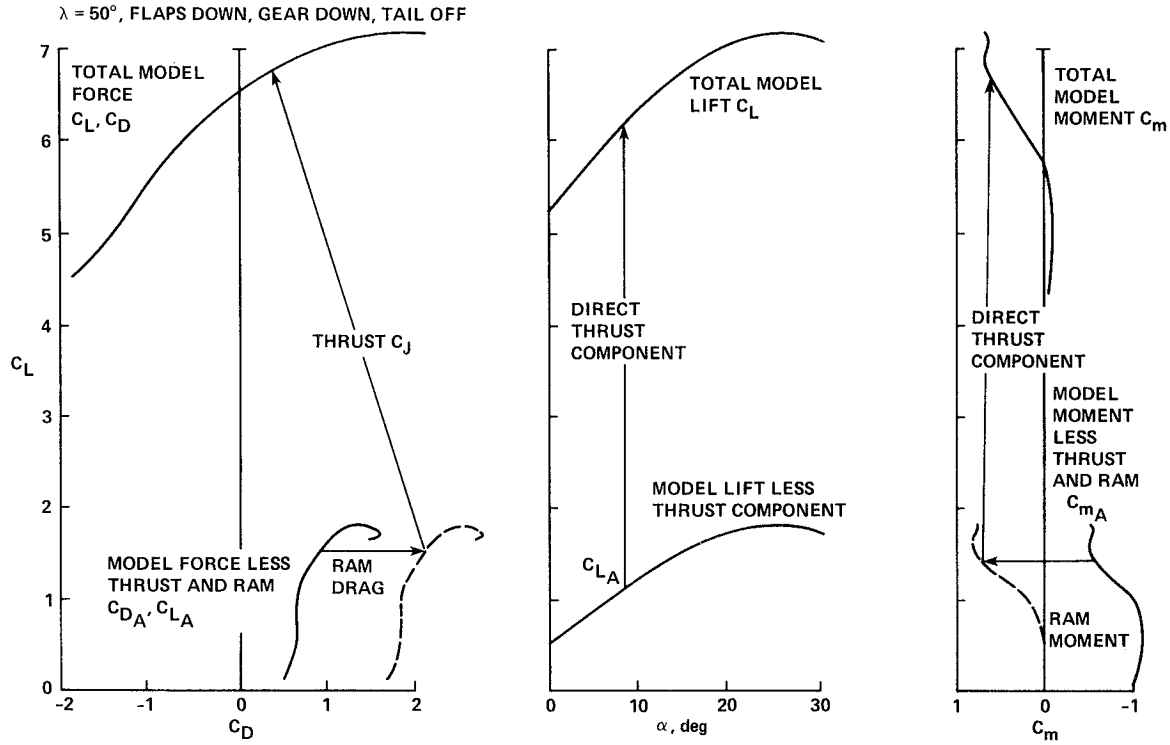

Figure 1. Induced effects for transition flight.

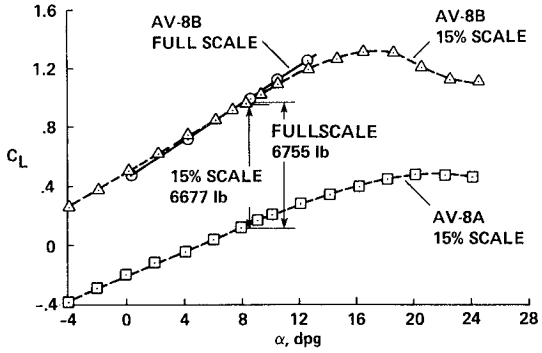

Figure 2. Comparison of large- and small-scale test data for the AV-8B (Ref. 8).

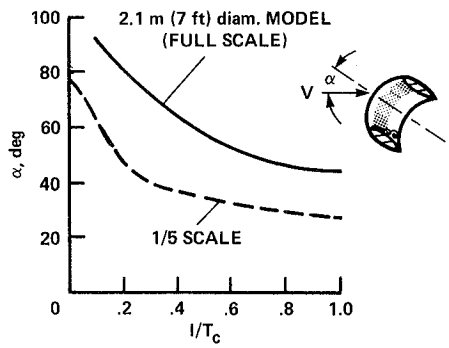

Figure 3. Effect of scale on duct inlet stall boundary (Ref. 4).

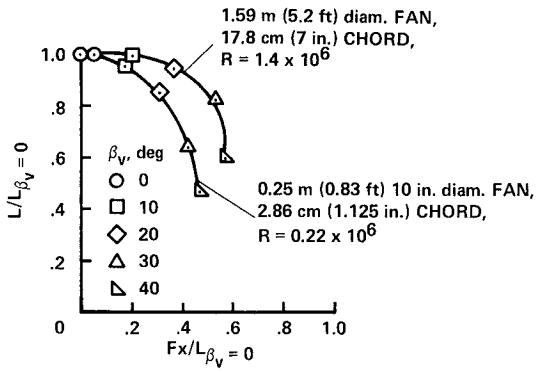

Figure 4. Performance of large- and small-scale exit vanes (Ref. 4).

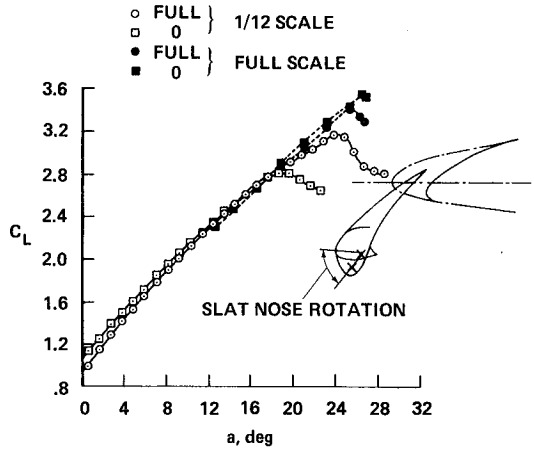

Figure 5. Effect of scale on the lift characteristics of the F111A airplane landing configuration (Ref. 4).

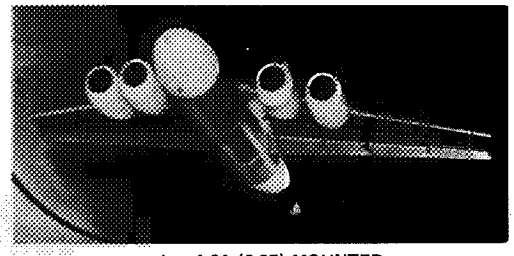

b = 1.91 (6.25) MOUNTED
IN 40 BY 80 INSERT – LANGLEY
V/STOL TUNNEL

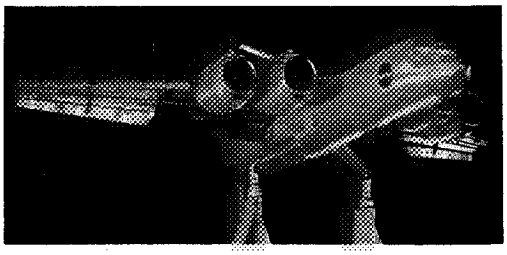

b = 11.62 (38.18) MOUNTED
IN 40 BY 80

Figure 6. Externally blown flap models with the same wing-flap geometry.

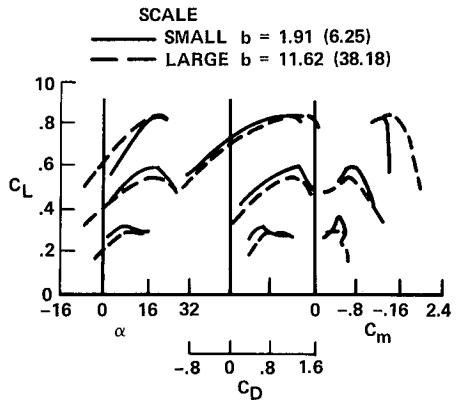

Figure 7. Comparison of wind-tunnel test results on the externally blown flap models of Fig. 6 (Ref. 4).

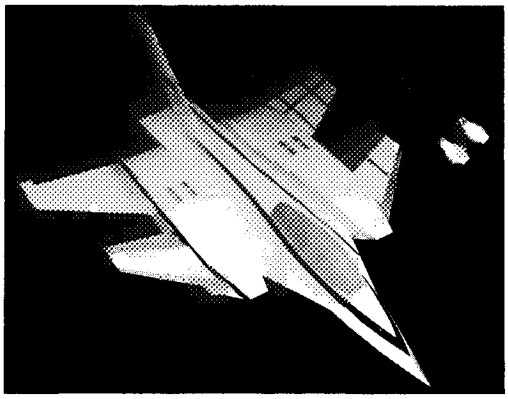

Figure 8. Large-scale J97-powered model of the GD205 two-engine fighter configuration.

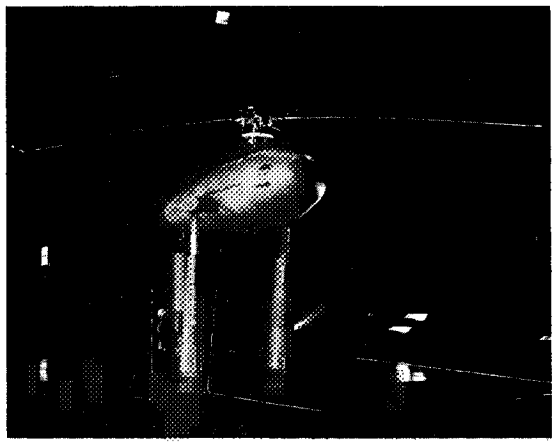

Figure 9. Rotor test rig mounted in the Ames 40 by 80 tunnel.

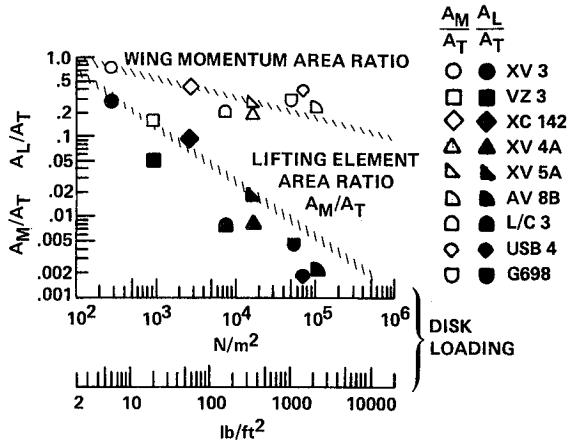

(a) Lift and momentum area sizing.

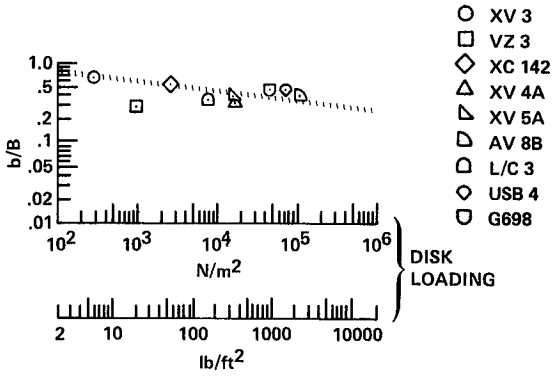

(b) Wing span sizing.

Figure 10. Sizing parameters (Ref. 4).

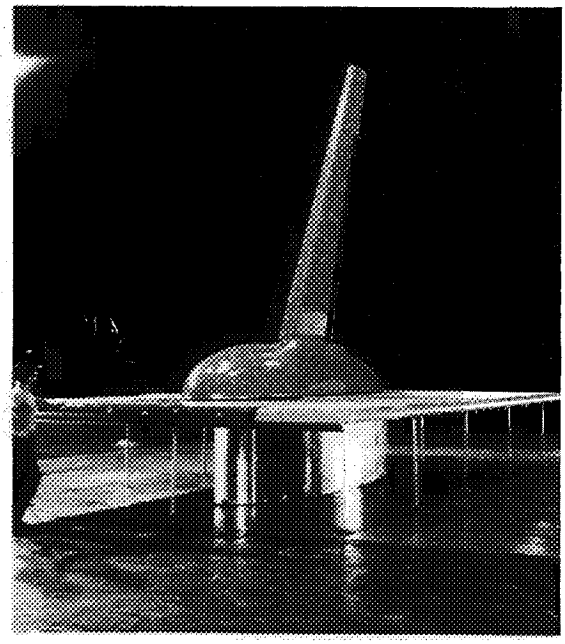

Figure 11. Bell/NASA ejector flap wing semispan model mounted in the Ames 40 by 80 wind tunnel (Ref. 12).

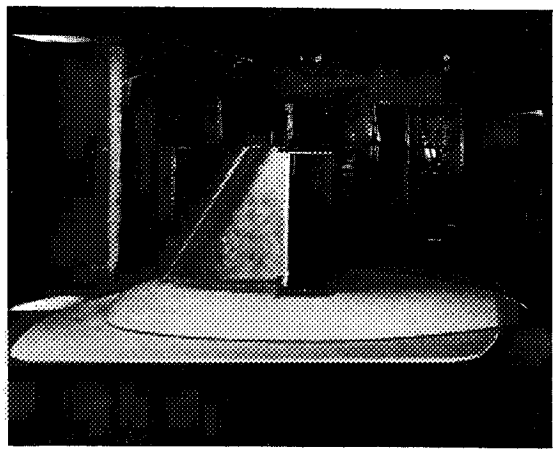

Figure 12. The Air Force ejector mounted in a semispan installation in the Ames 7 by 10 tunnel: $\delta_f = 90^0$ (Ref. 13).

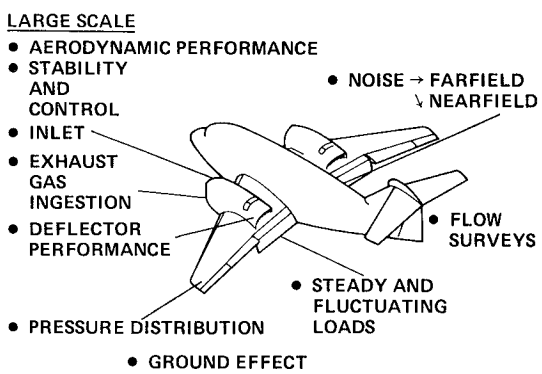

Figure 13. Measurements using large- and small-scale models (Ref. 4).

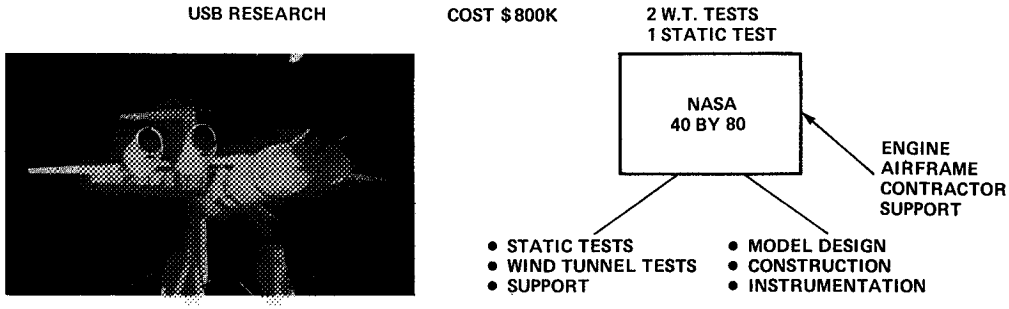

(a) An in-house basic research project.

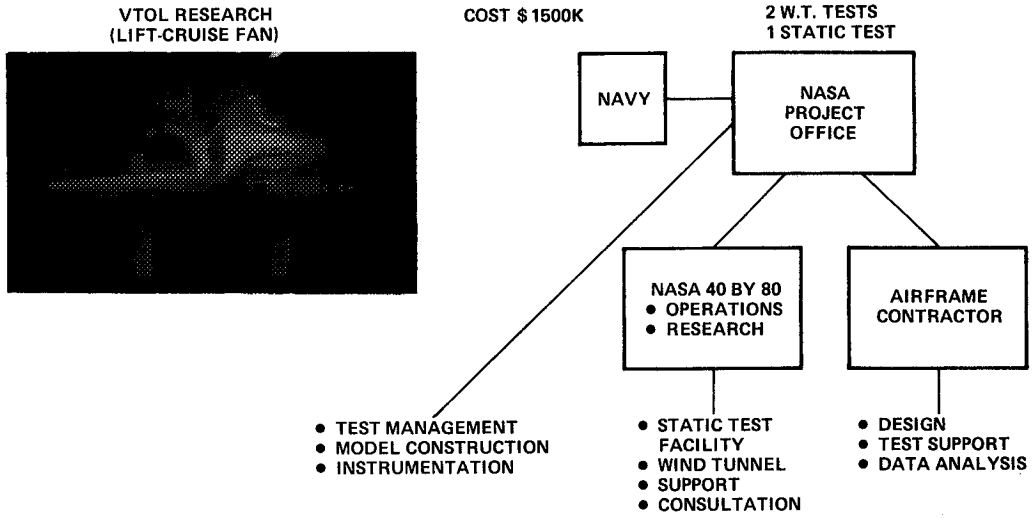

(b) A joint service R. & D. project.

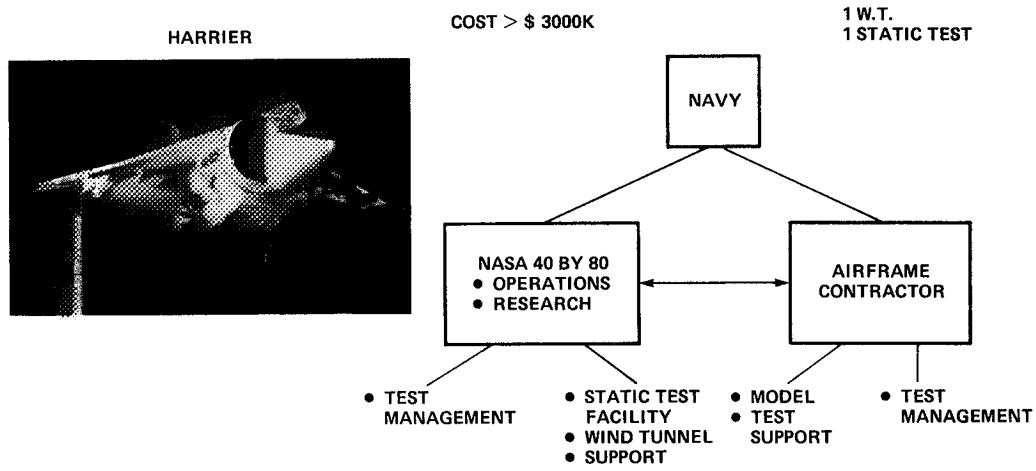

(c) A military development program.

Figure 14. Organization and costs of some large-scale V/STOL wind-tunnel investigations (Ref. 4).

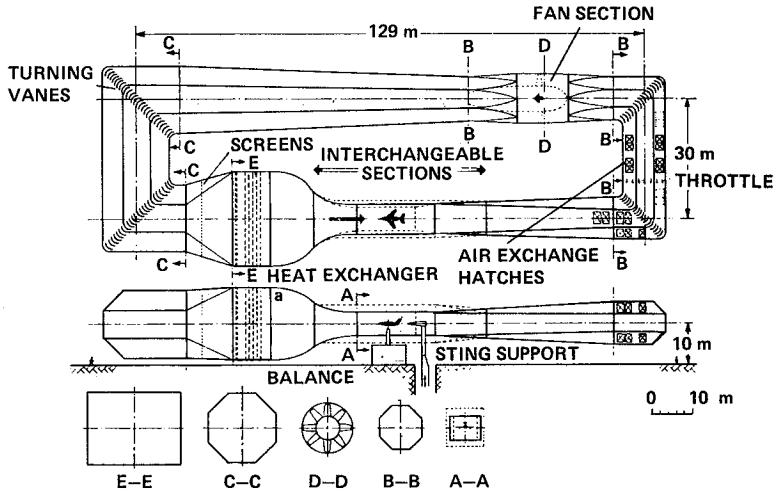

	WORKING SECTION			
CROSS-SECTIONAL SHAPE & SIZE, m × m	9.5 × 9.5	6 × 8	6 × 6	6 × 8
TYPE	CLOSED	CLOSED	CLOSED	OPEN
USABLE LENGTH, m	15	16	9	20
MAX. AIR SPEED, m/sec	62	117	153	80
CONTRACTION RATIO	4.8	9.0	12.0	9.0
MAX. MODEL SPAN, m	≈ 6.5	≈ 5.5	≈ 4.2	≈ 4.0

Figure 15. DNW wind tunnel (Refs. 23, 24).

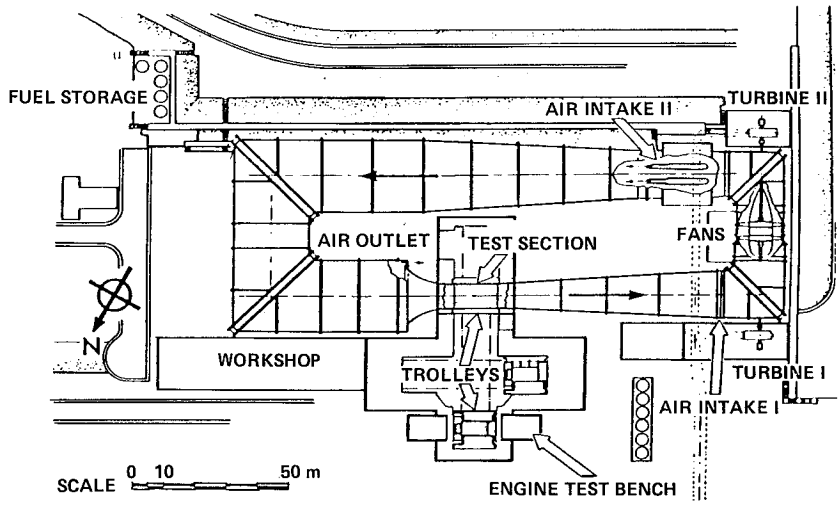

(a) General layout.

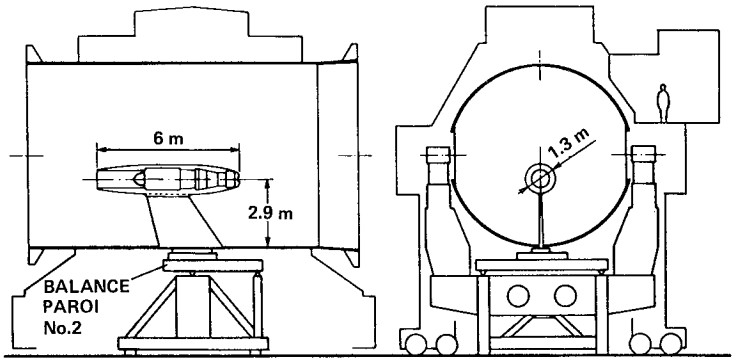

(b) One of the test sections.

Figure 16. ONERA-Modane 8M Facility (Ref. 26).

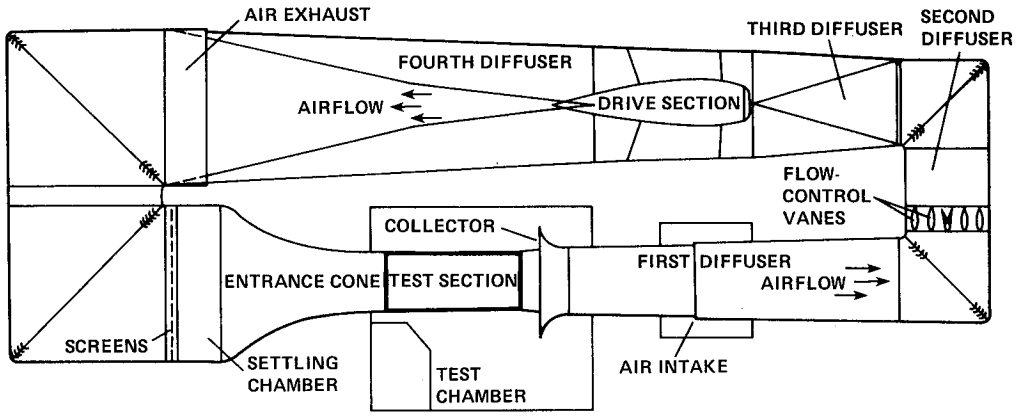

Figure 17. Planview of the Langley 4 by 7 tunnel (Ref. 27).

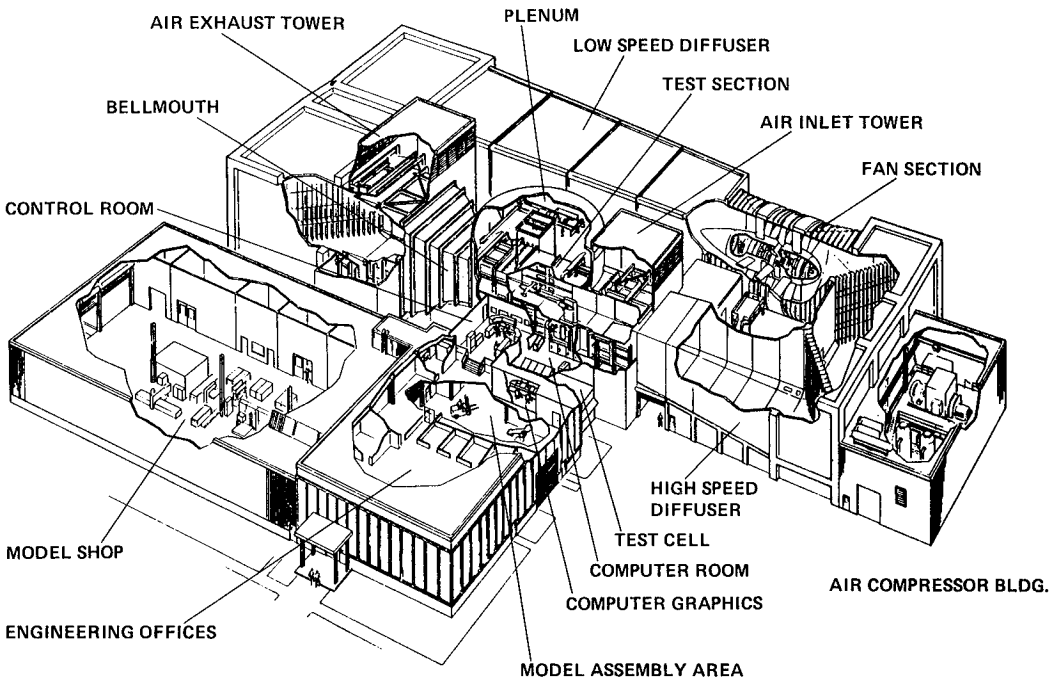

Figure 18. Boeing V/STOL wind tunnel (Ref. 28).

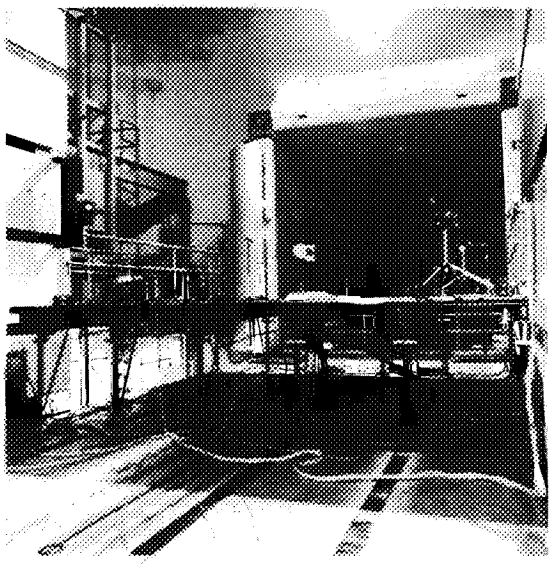

Figure 19. The test section of Boeing V/STOL wind tunnel: open-throat mode.

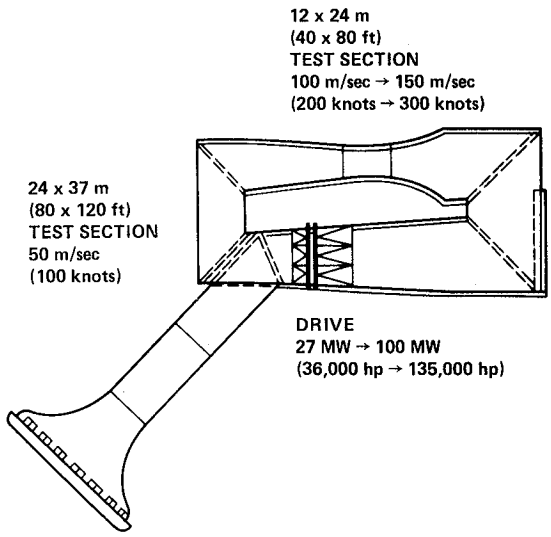

Figure 20. Ames large-scale wind-tunnel system (Ref. 29).

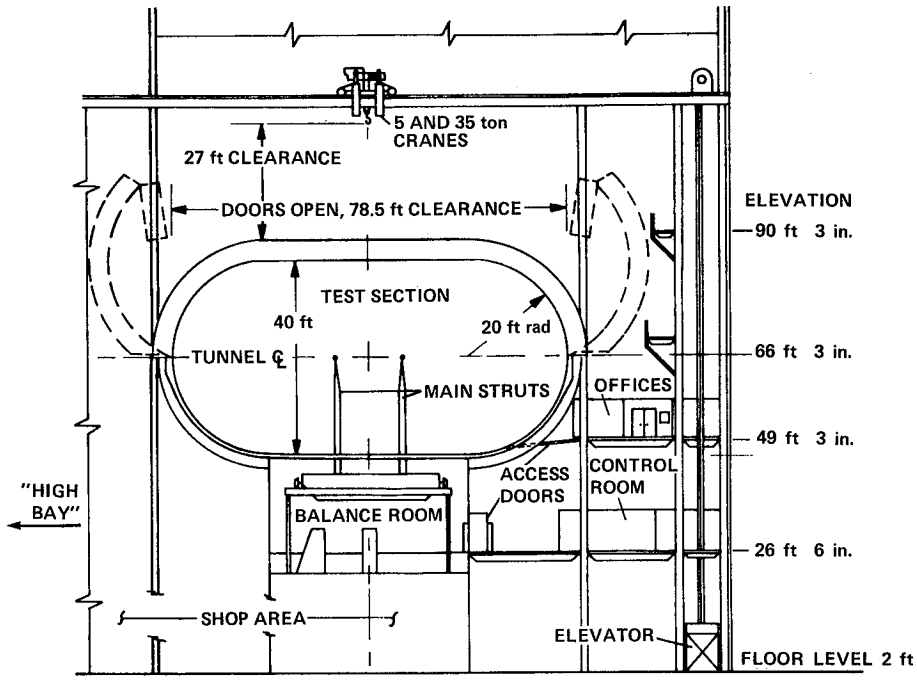

Figure 21. Elevation of Ames 40 by 80 test section.

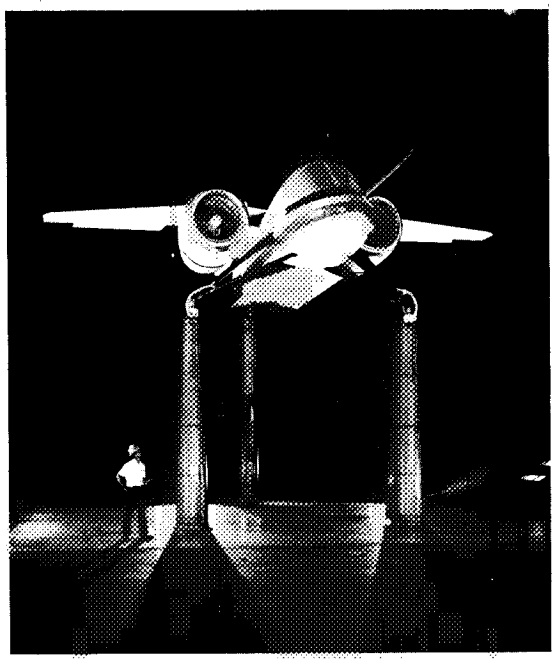

Figure 22. Complete model (G698) installed in the Ames 40 by 80 test section.

Figure 23. Sketch of Ames 80 by 120 test section.

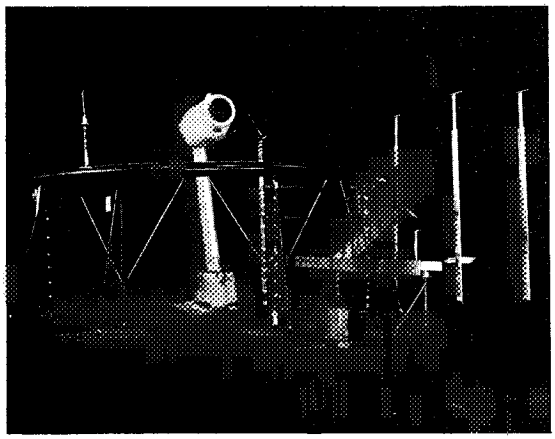

(a) Compressor noise studies: hybrid inlet.

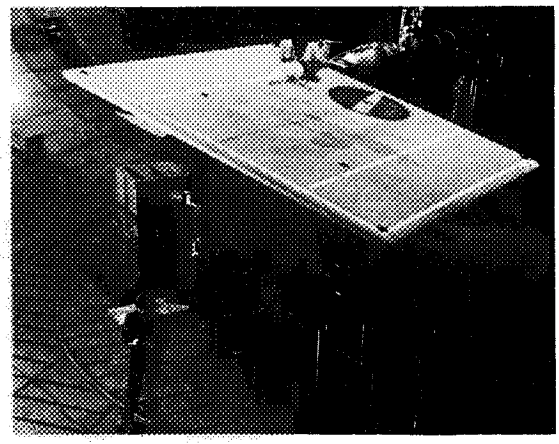

(b) 0.11-scale G698 hover tests.

Figure 24. Special test setups in the Ames 40 by 80 tunnel.

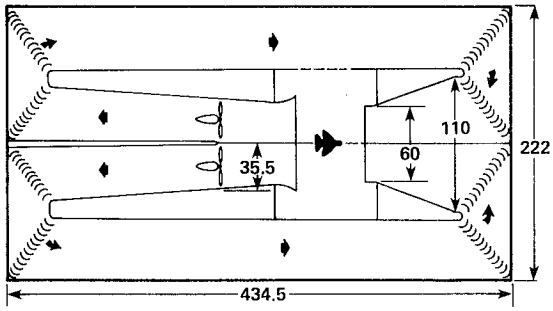

ALL DIMENSIONS IN FEET

Figure 25. Langley 30 by 60 wind tunnel.

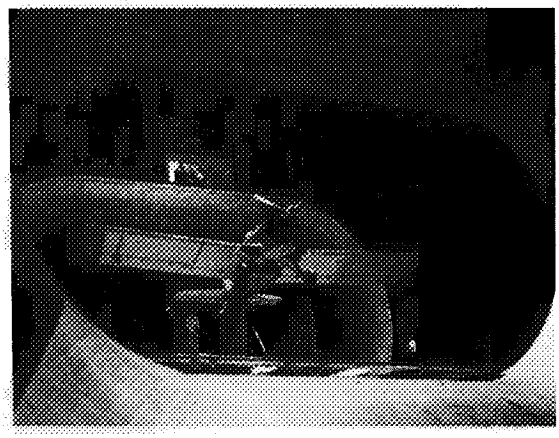

Figure 26. Langley 30 by 60 test section.

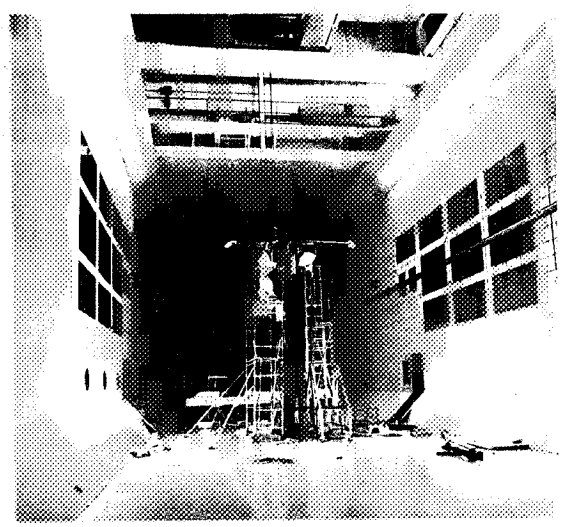

Figure 27. The test section of the NRC 9-m wind tunnel.

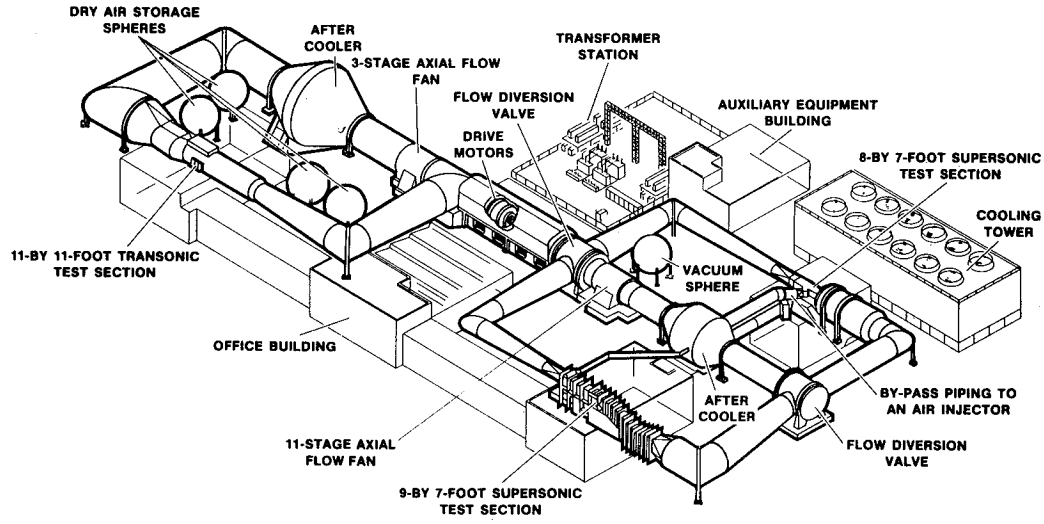

Figure 28. Ames Unitary Wind Tunnel System.

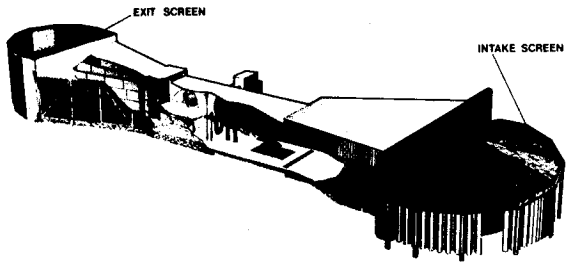

Figure 29. BAC 5.5-m (18 ft) open-throat wind tunnel (Ref. 34).

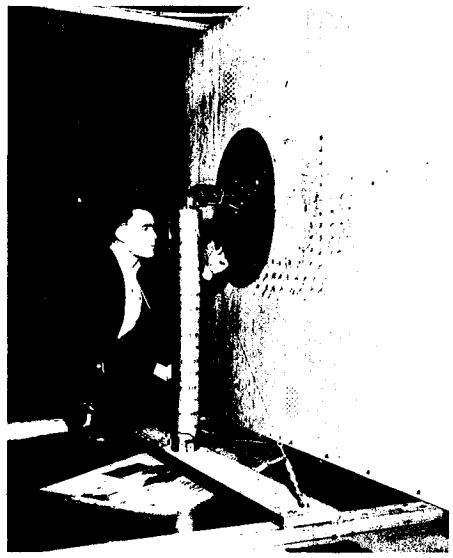

Figure 30. General arrangement of circular wing and ground plane (Ref. 35).

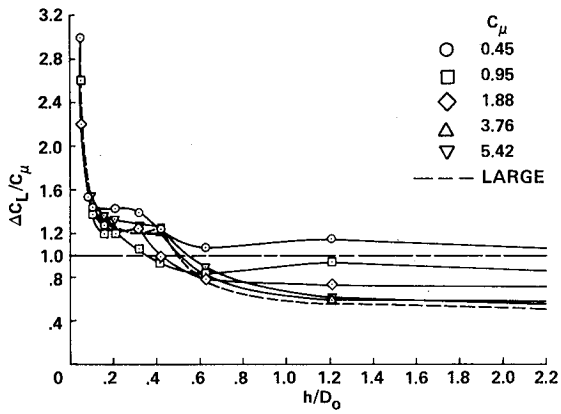

Figure 31. Effect of C_μ on the circular wing vertical thrust variation with altitude: $\alpha = 0^\circ$ (Ref. 35).

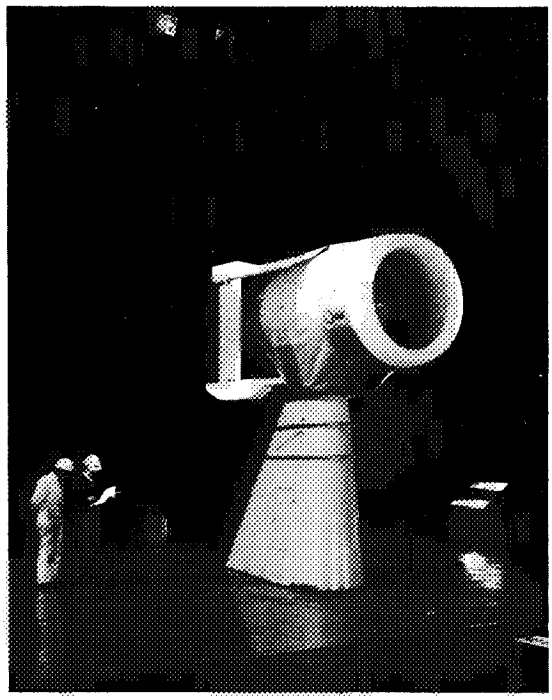

(a) 3/4 front view.

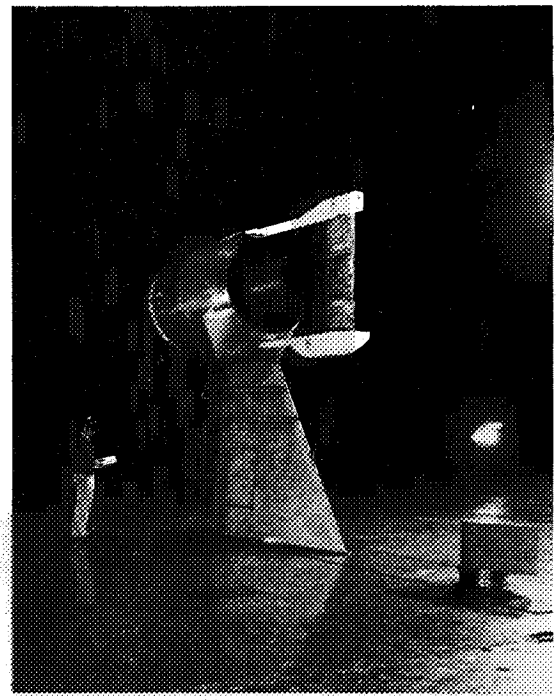

(b) Rear view.

Figure 32. Q fan and a pitch-control vane mounted in the Ames 40 by 80 tunnel (Ref. 37).

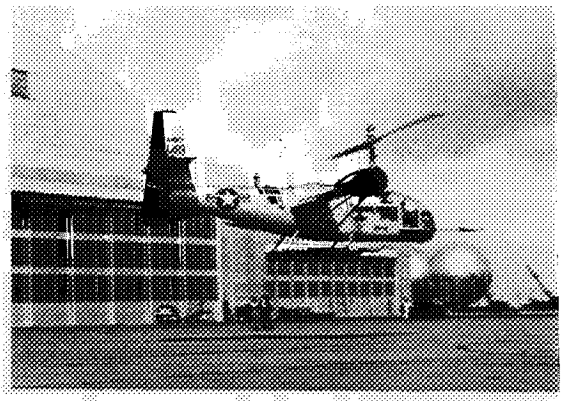

(a) XFV3 flight tests.

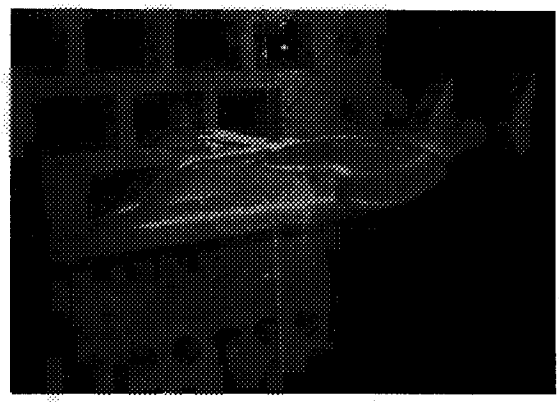

(b) Small-scale tests.

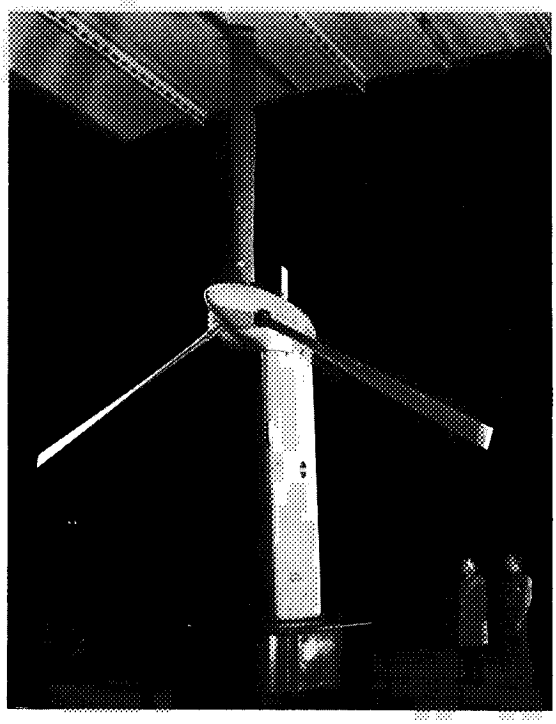

(c) Semispan tests.

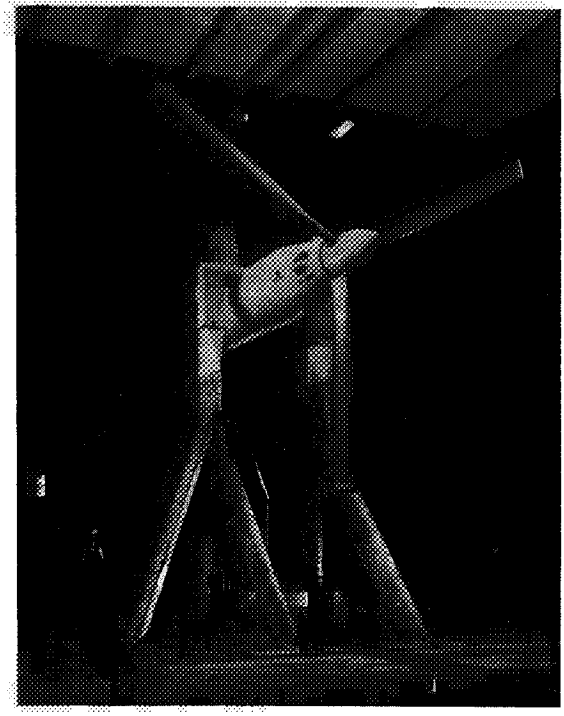

(d) Dynamometer tests.

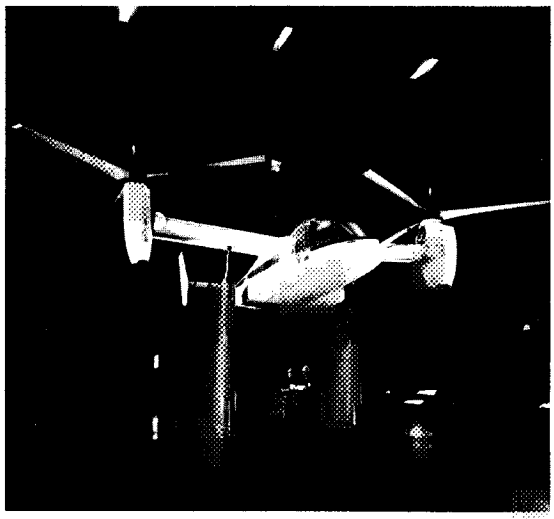

(e) Full-scale wind-tunnel tests.

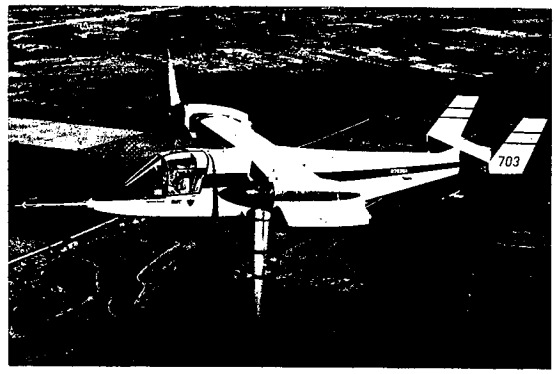

(f) XV15 in flight.

Figure 33. XV-15 development.

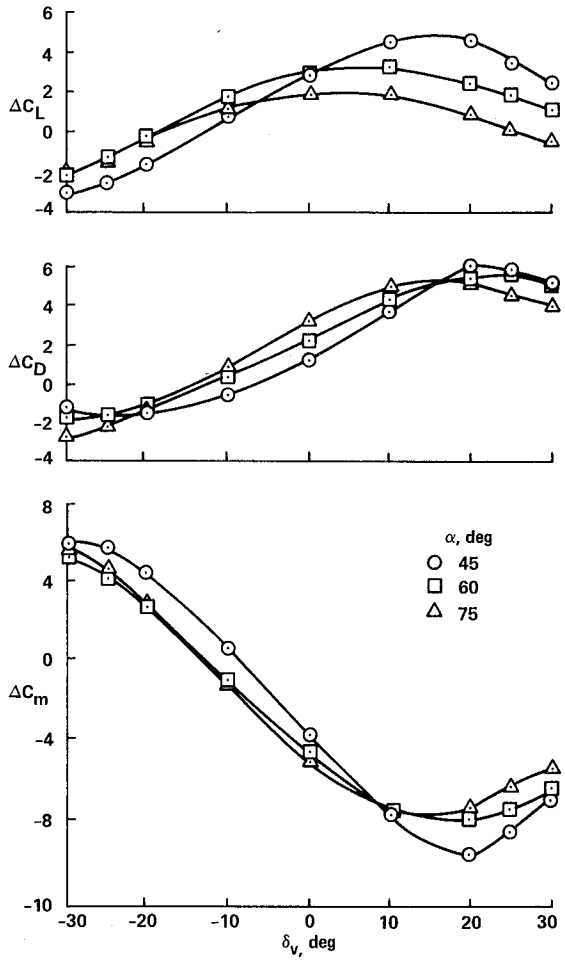

Figure 34. Effectiveness of the pitch-control vane for the subsonic tilt nacelle aircraft: C_J = 10 (Ref. 37).

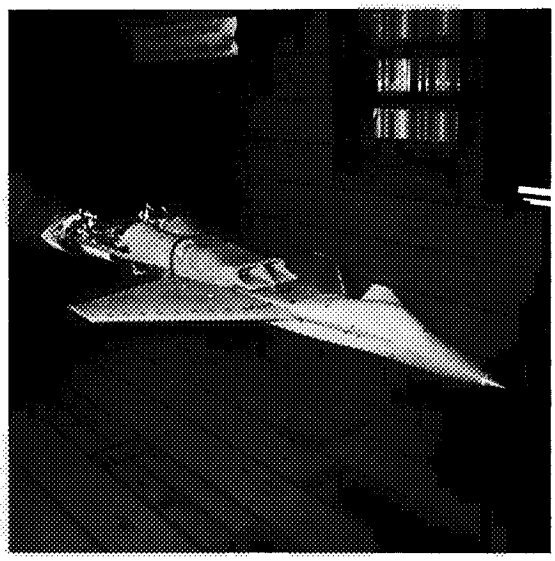

Figure 35. Above the wing inlet study in the Ames 11-ft tunnel (Ref. 42).

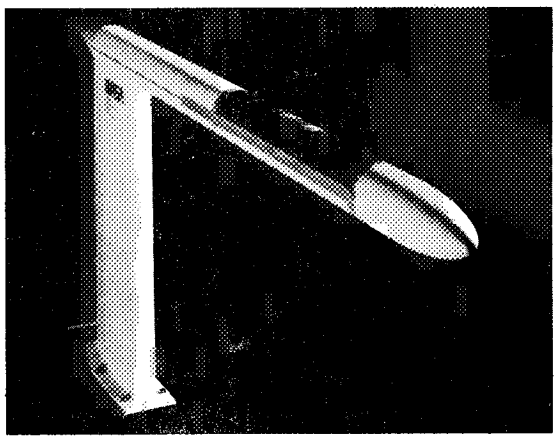

Figure 36. Jet-in-cross-flow body mounted in Ames 7 by 10 wind tunnel (Ref. 46).

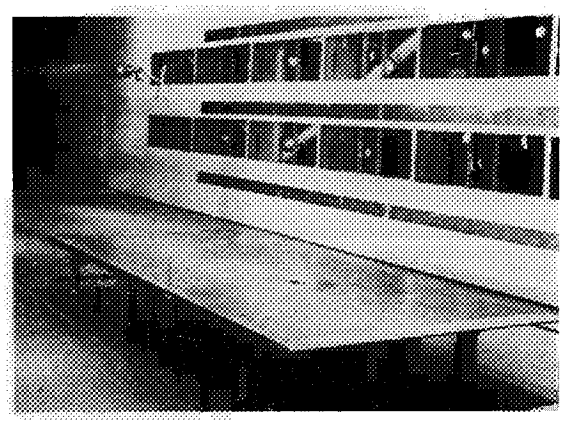

Figure 37. Jet-in-cross-flow installation in the Langley V/STOL wind tunnel (Ref. 47).

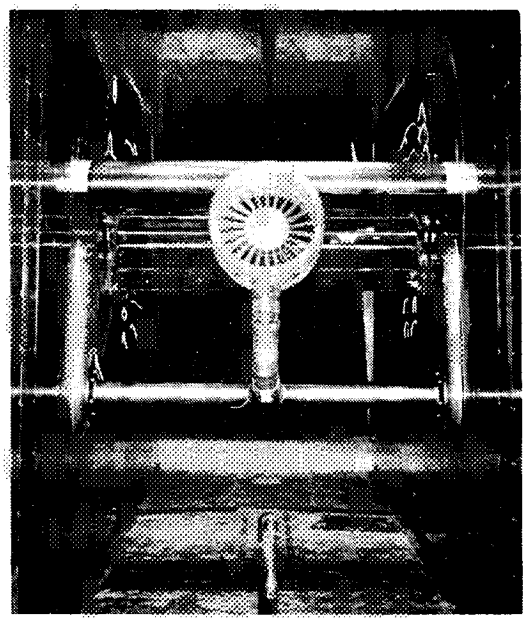

Figure 38. Installation of high-lift wing model and turbine fan between two-dimensional blowing walls (Ref. 49).

(a) Wind-tunnel installation.

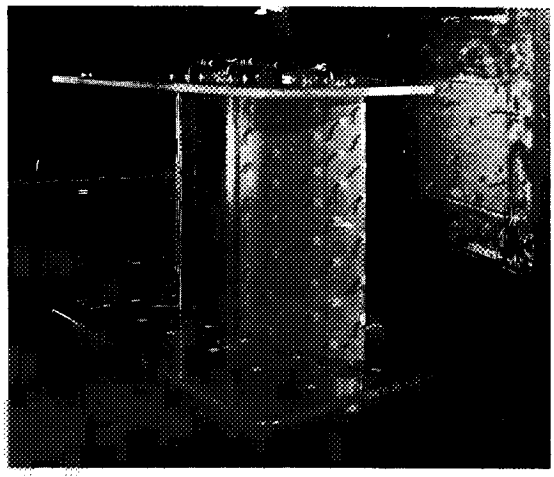

(b) Details of model.

Figure 39. A quasi-two-dimensional ejector flap model (Ref. 50).

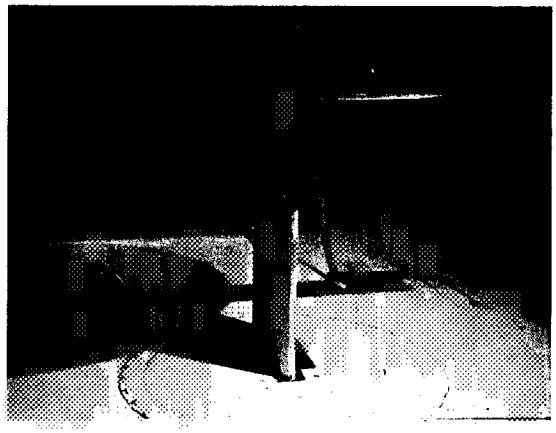

Figure 40. The cruise blowing model in the Boeing transonic wind tunnel (Ref. 52).

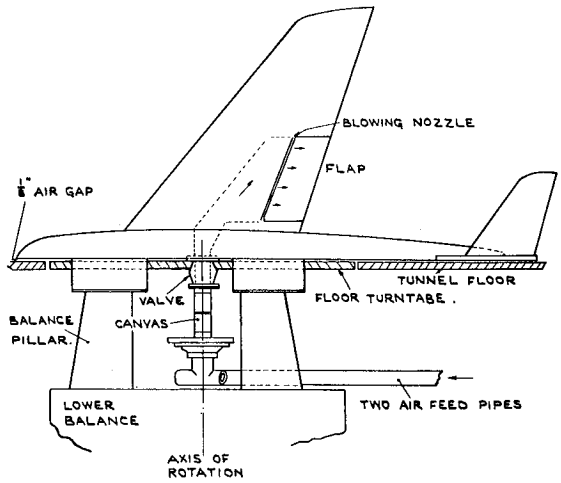

Figure 41. Semispan mount for a wing-fuselage-tail configuration (Ref. 53).

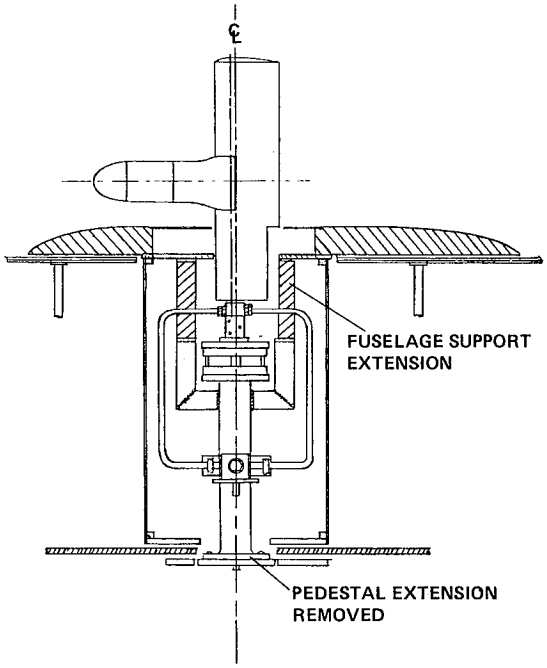

(a) Mounting details.

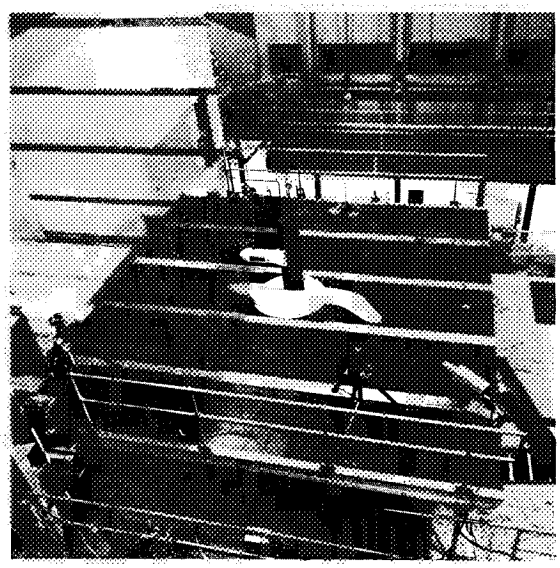

(b) View of installation in the Boeing Vertol wind tunnel.

Figure 42. Wing-fuselage semispan mount with the fuselage nonmetric (Ref. 54).

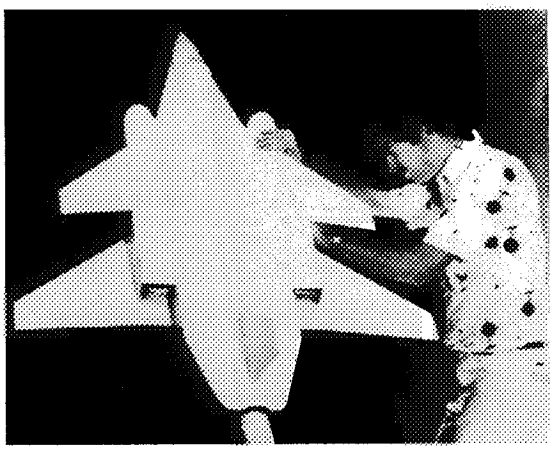

Figure 43. Twin-engine, high-speed model mounted in the Ames 12-ft tunnel (Ref. 56).

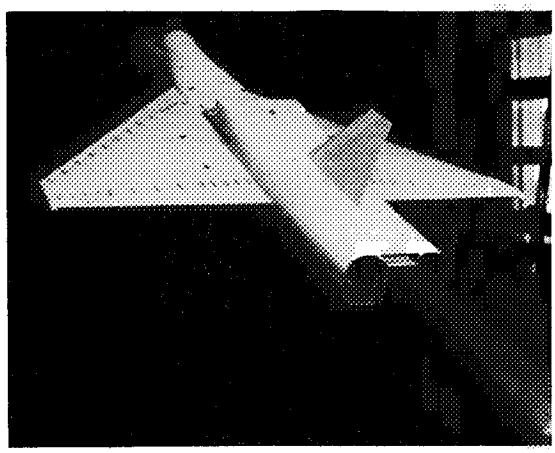

Figure 44. Sting mount of an above-the-wing inlet model in the Ames 11-ft tunnel (Ref. 43).

Figure 45. CMAPS-powered model in the Ames 11-ft transonic tunnel (Ref. 57).

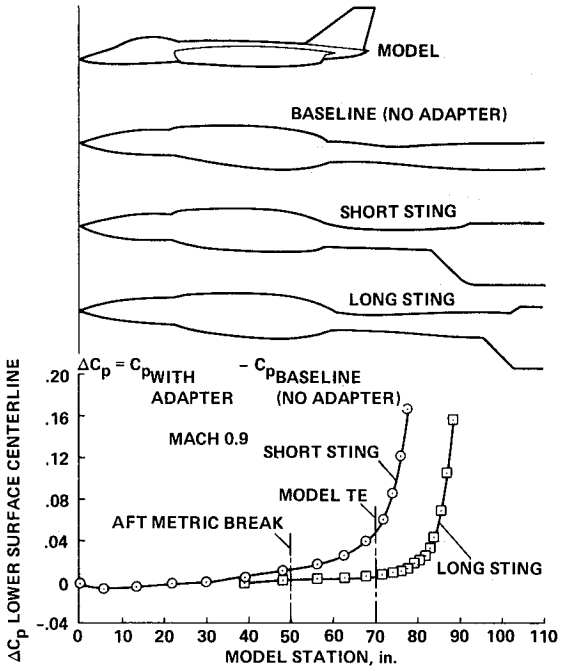

Figure 46. Sting-length effect on adapter-induced pressure increments for the CMAPS-powered model of Fig. 45 (Ref. 58).

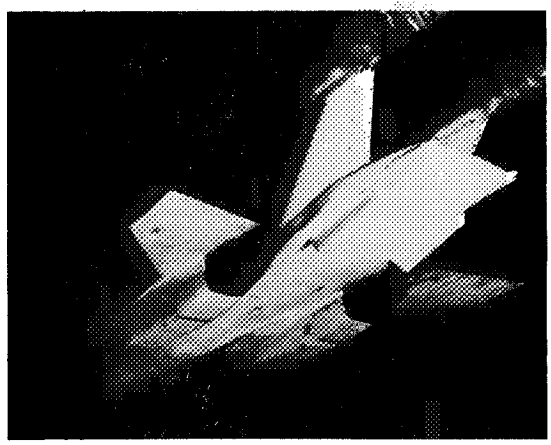

Figure 47. Twin-tail support for a generic fighter model powered by direct blowing (Ref. 59).

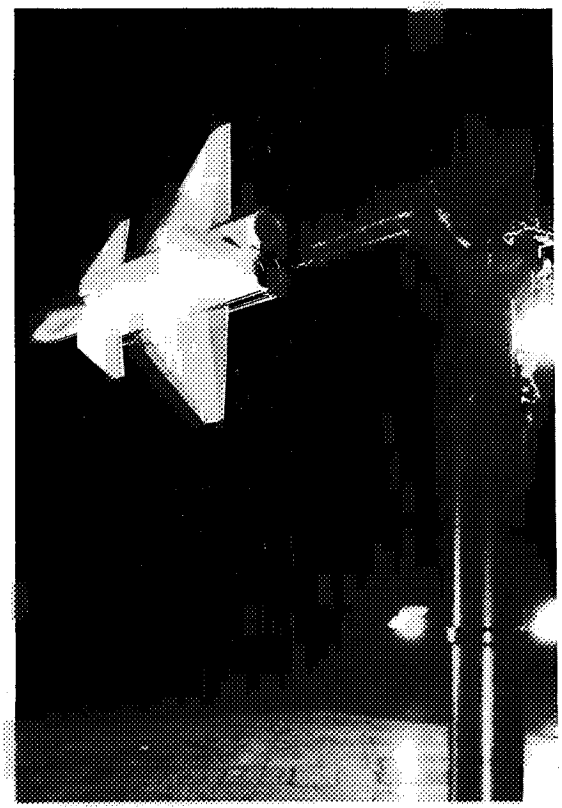

Figure 48. A sting mount installation in the Ames 40 by 80 for high-angle-of-attack studies (Refs. 60, 61).

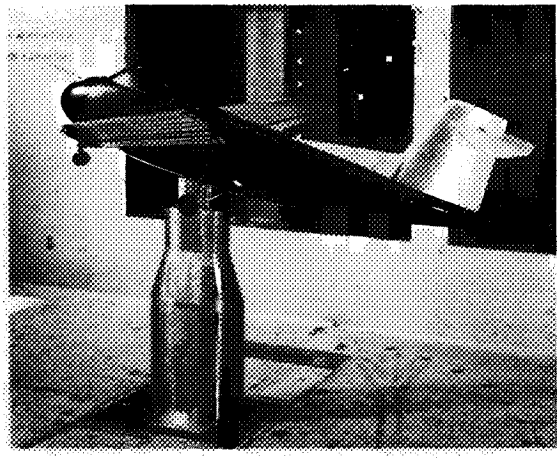

(a) Mounted in Ames-Army Air Mobility Command 7 by 10 1/7-scale (Ref. 62).

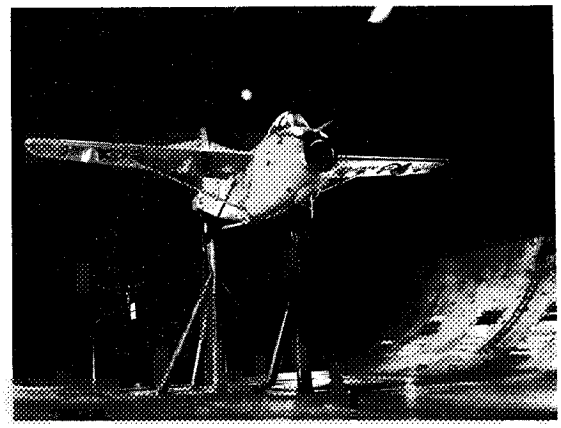

(b) The H-126 aircraft mounted in the Ames 40 by 80.

Figure 49. Wind-tunnel mounting of the H-126.

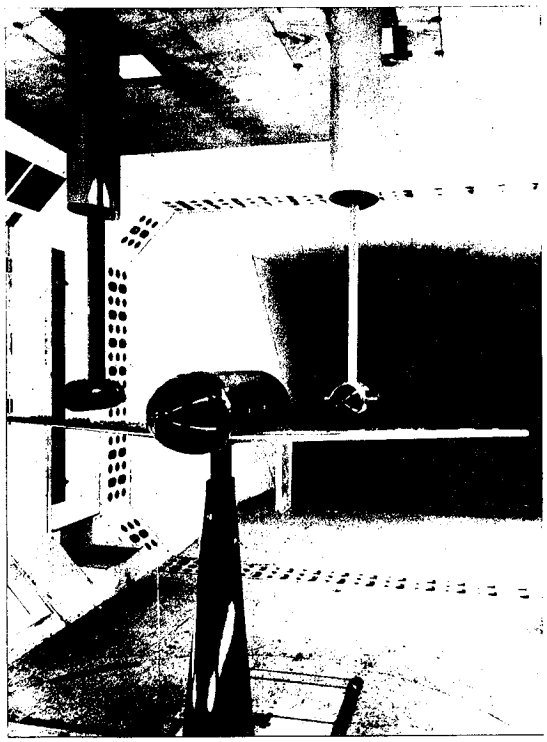

Figure 50. Composite model rig for jet-nacelle model with wing-fuselage inverted (Ref. 63).

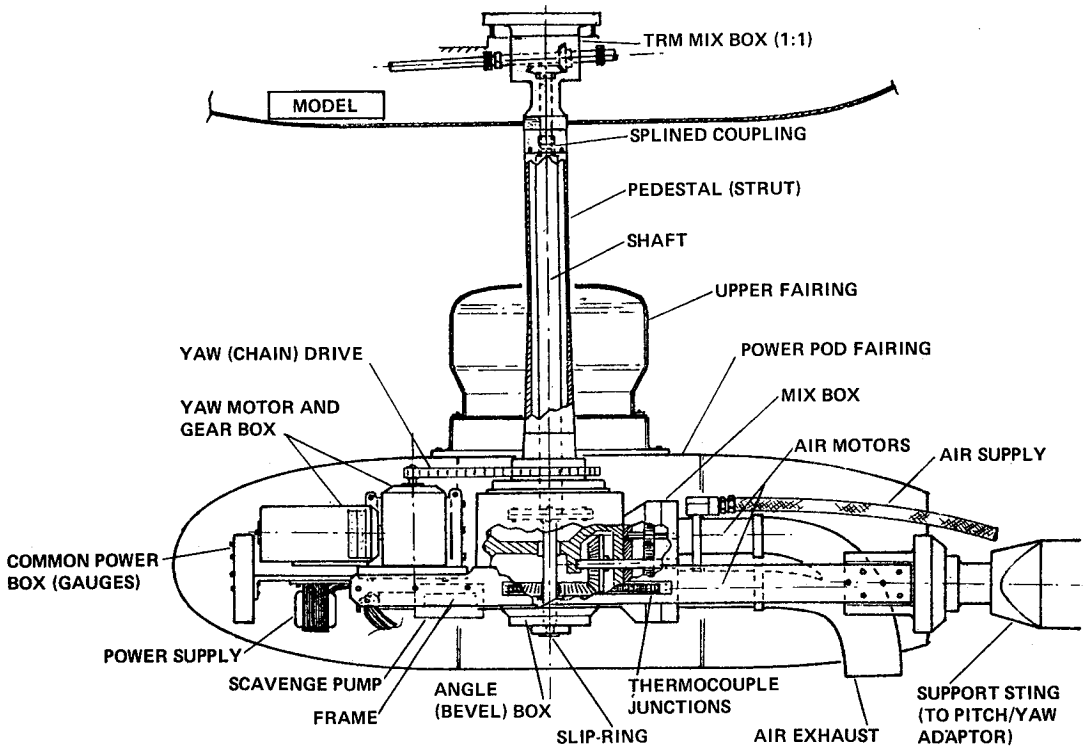

Figure 51. Pedestal-mounted model on the Vertol power pod (Ref. 28).

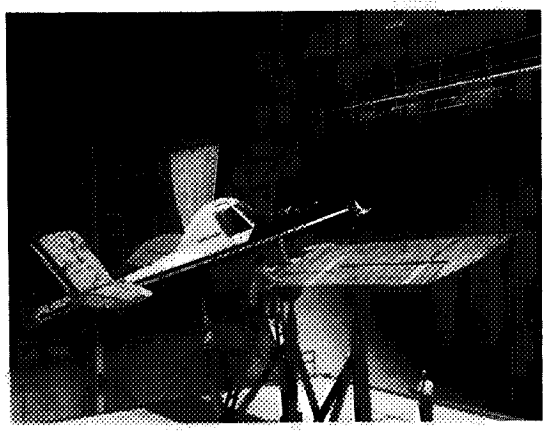

Figure 52. Aircraft installation in the Langley 30 by 60.

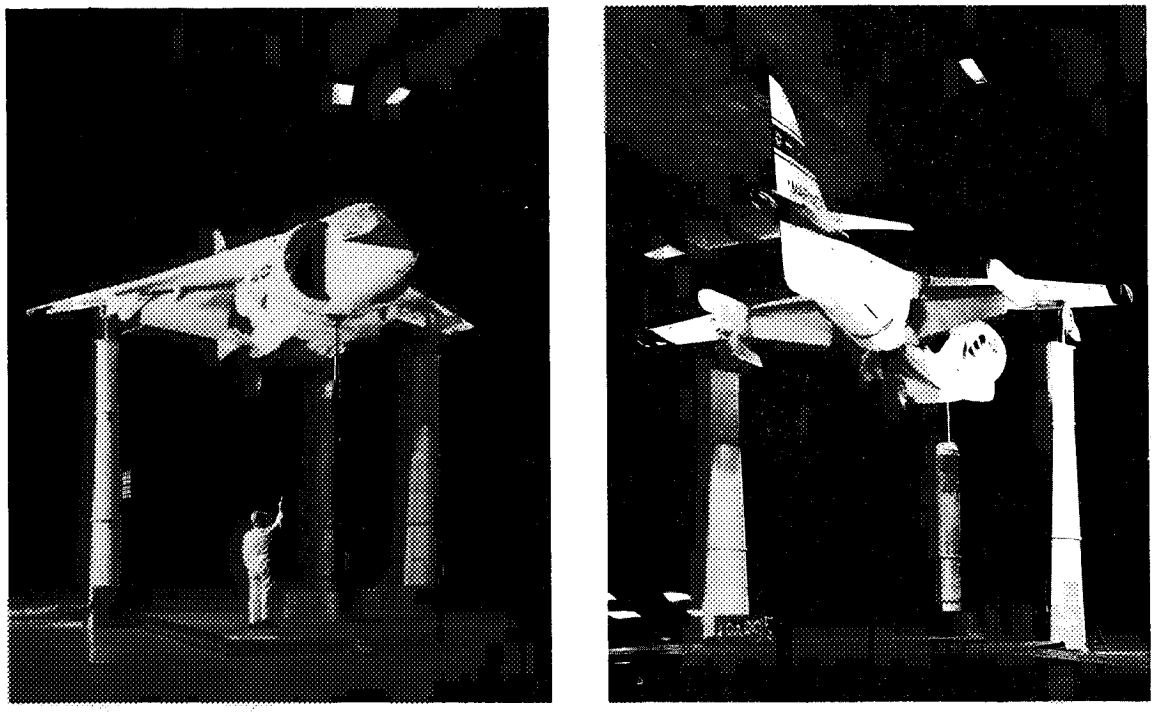

(a) 3/4 front.

(b) 3/4 rear.

Figure 53. Full-scale AV-8B model mounted in the Ames 40 by 80 (Ref. 19).

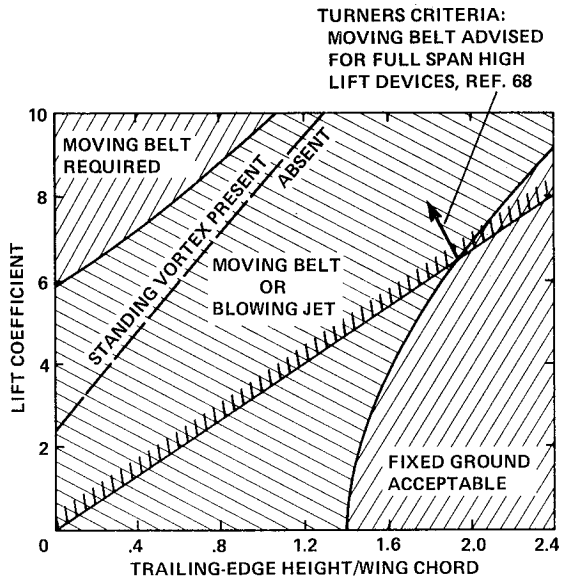

Figure 54. Criteria for ground-effect simulation (Refs. 29, 68).

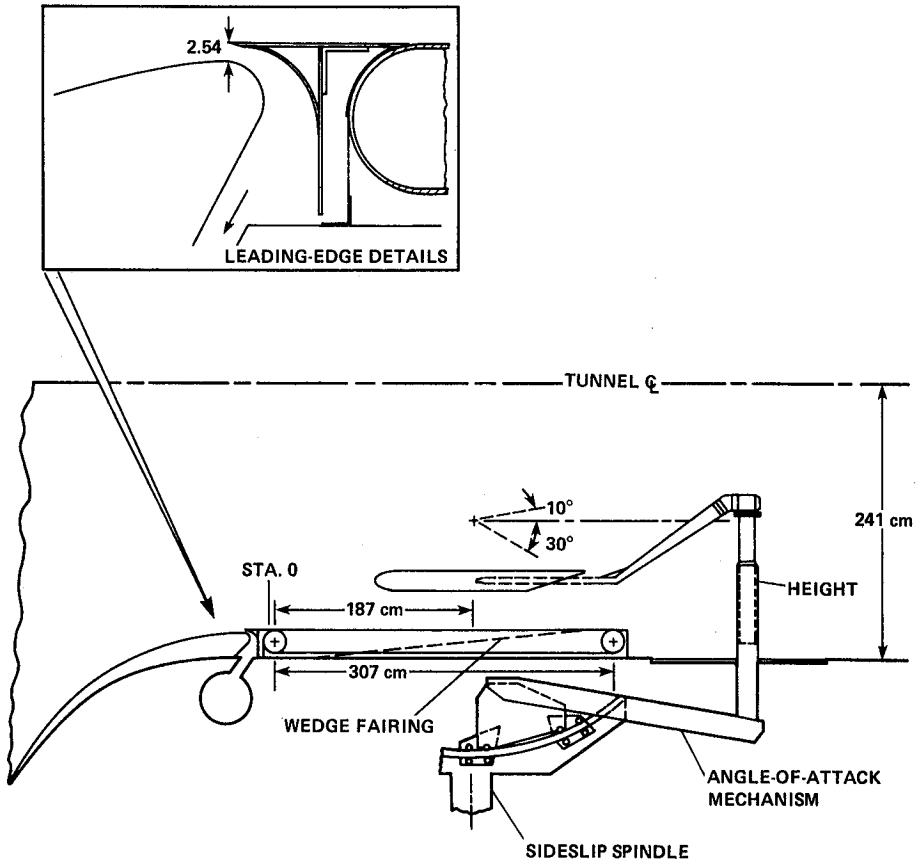

Figure 55. Turner's moving-belt installation (Ref. 68).

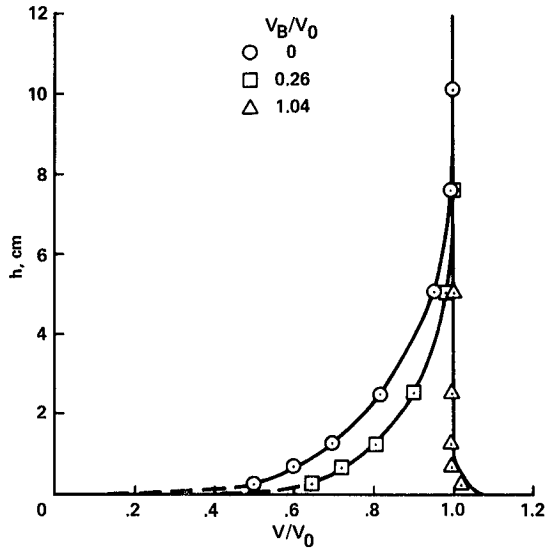

Figure 56. Effect of belt velocity on boundary-layer profiles: station 187; see Fig. 55 (Ref. 68).

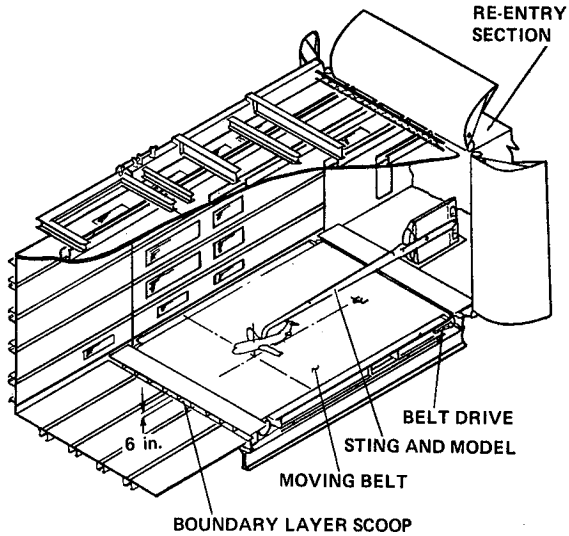

Figure 57. Moving-belt installation in the Boeing V/STOL wind tunnel (Ref. 28).

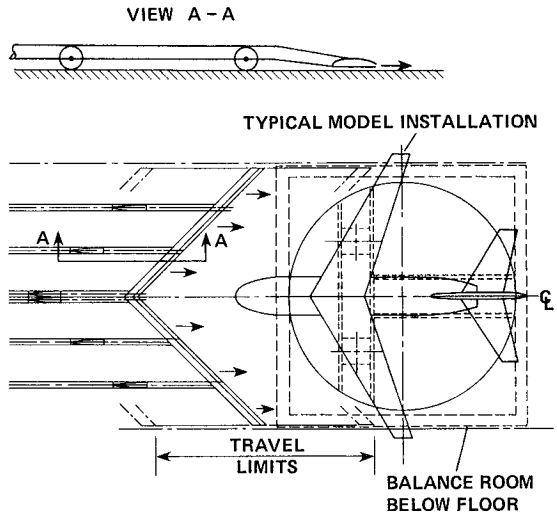

Figure 58. Ames 40 by 80 proposed floor BLC design (Ref. 70).

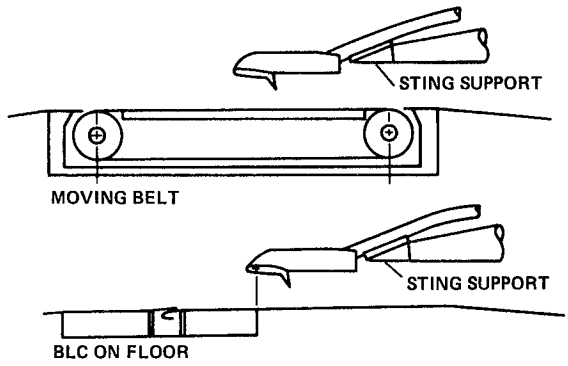

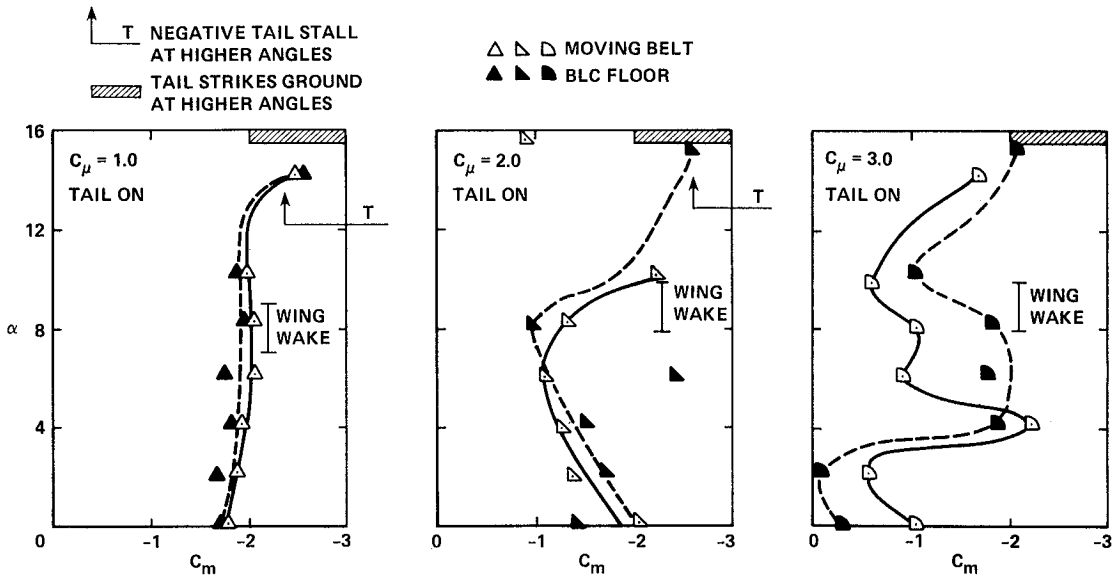

Figure 59. A sampling of data comparing the use of BLC on the wind-tunnel floor with that of a moving belt: h/c = 1.0 (Ref. 72).

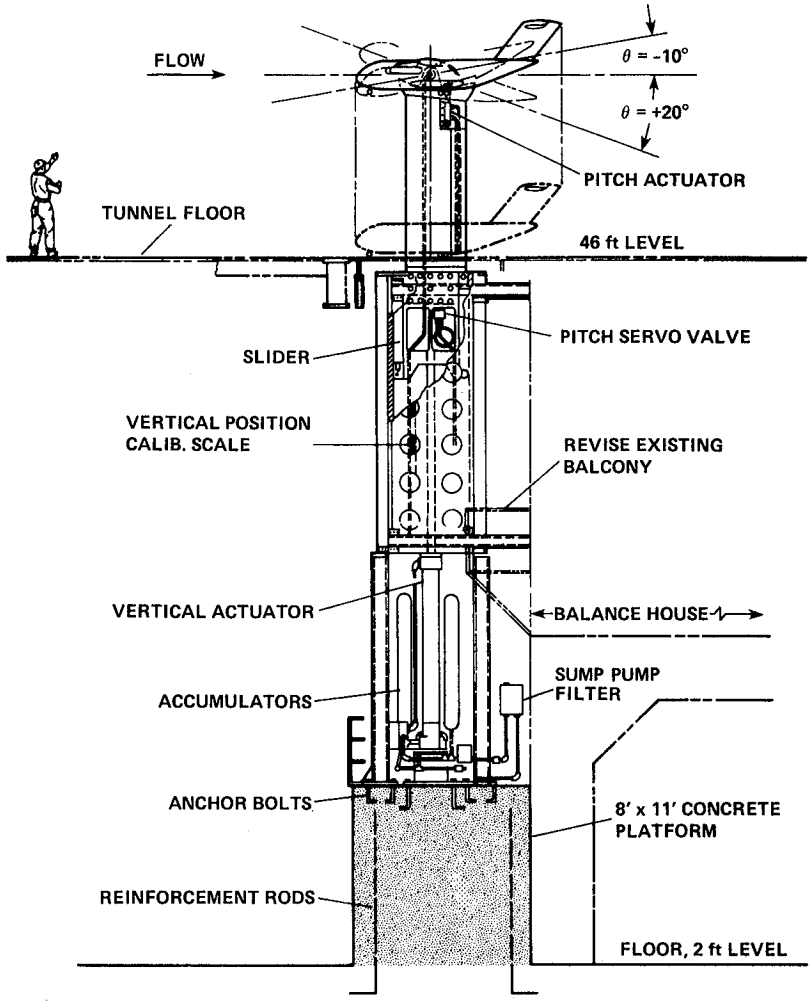

Figure 60. Transient ground-effect support design for the Ames 40 by 80 (Ref. 73).

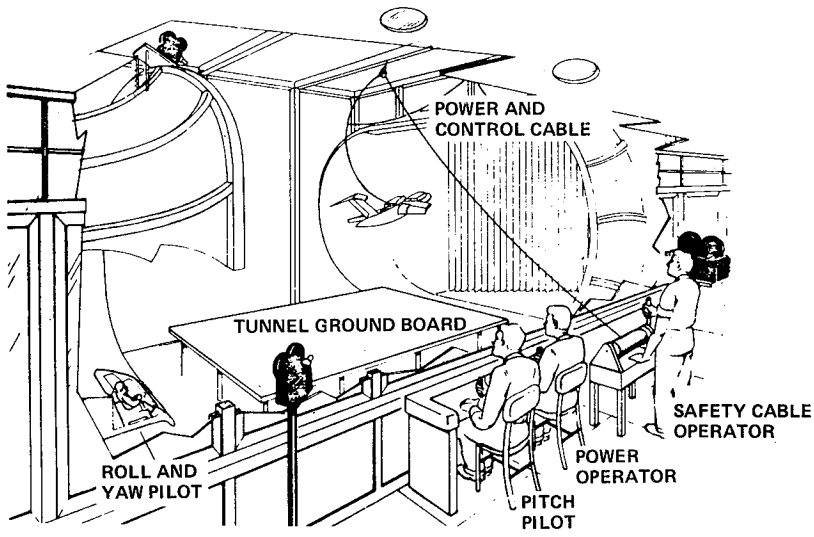

(a) Test setup in test section.

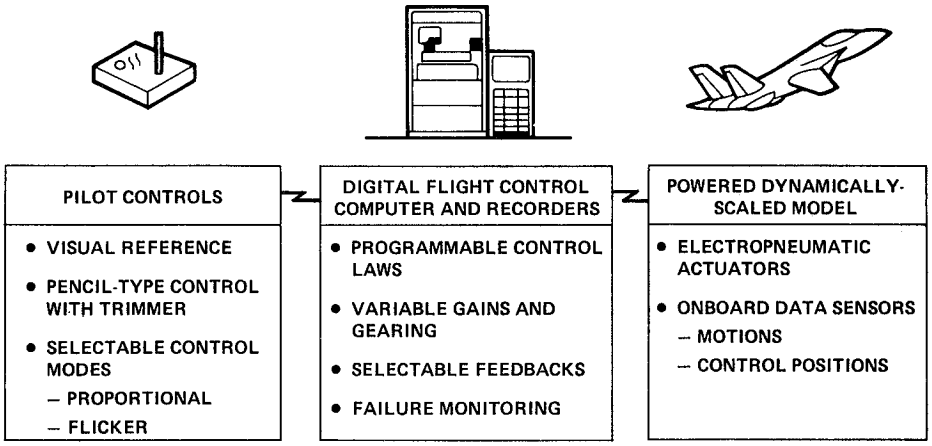

(b) Description of system features.

Figure 61. Free-flight operation in the Langley 30 by 60 wind tunnel (Ref. 74).

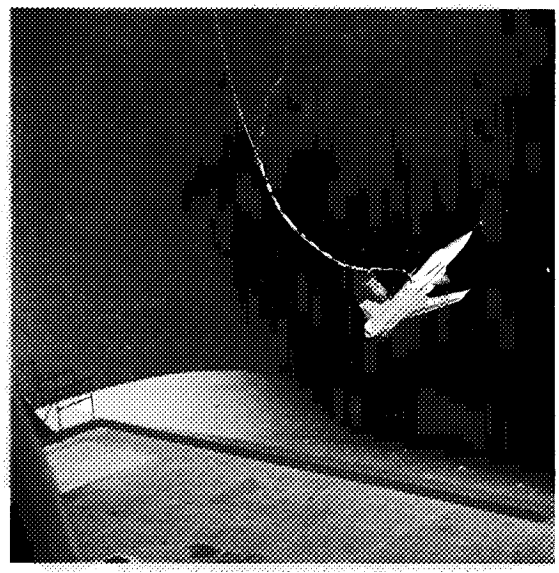

Figure 62. An X29A model in flight in the Langley 30 by 60 tunnel (Ref. 75).

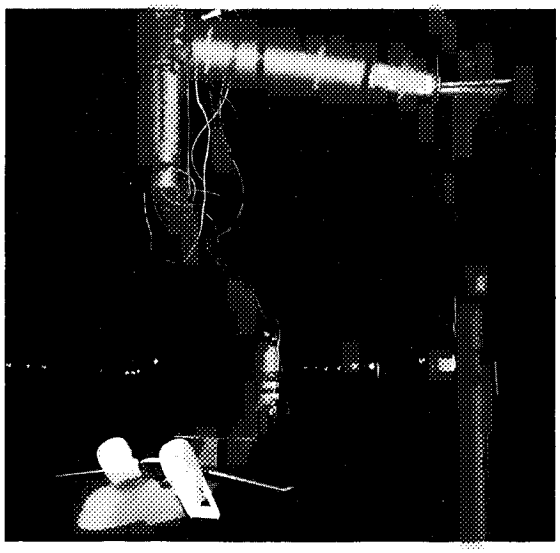

(a) Model support.

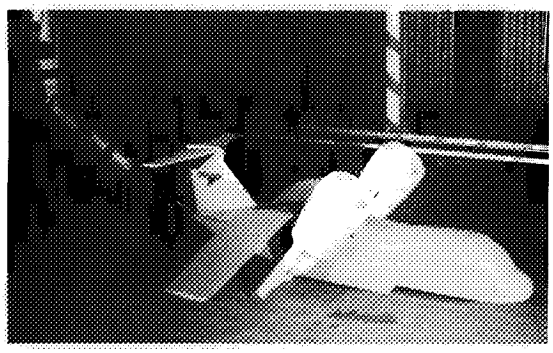

(b) Grumman 698 model at wheel height.

Figure 63. Use of the Princeton track for ground-effect tests (Ref. 78).

DATA SOURCE	i_t	h (OGE), cm (in.)	h (IGE), cm (in.)
○ DMT (PRINCETON)	20°	42 (16.5)	9.6 (3.8)
□ 40x80 TUNNEL (AMES)	20°	42 (16.5)	9.6 (3.8)
△ 7x10 TUNNEL (LANGLEY)	OFF	22.6 (8.9)	9.6 (3.8)
⍙ 7x10 TUNNEL (15x17 SECT. WITH MOVING BELT)	OFF	22.6 (8.9)	9.6 (3.8)

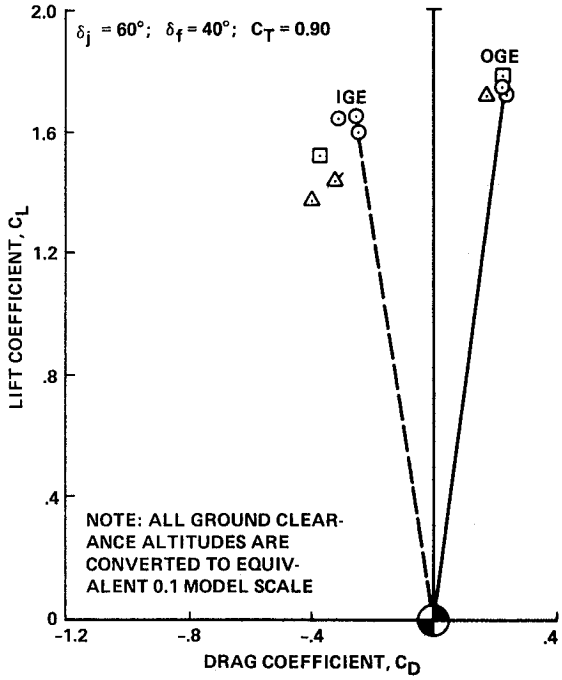

Figure 64. Comparison in ground-effect of results using the Princeton Track with that from three other facilities: tilt-wing model; h measured using Princeton model scale (Ref. 77).

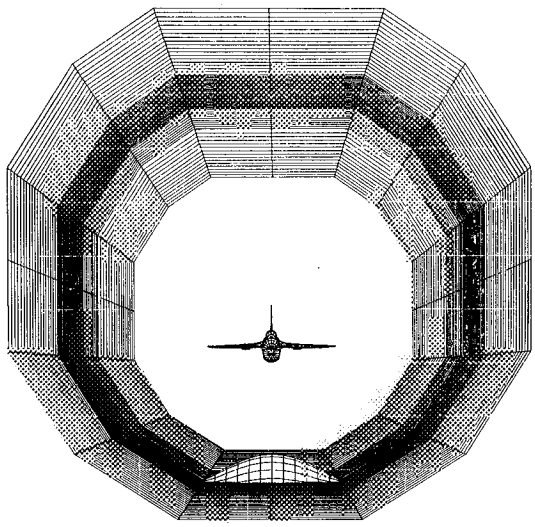

(a) PAN AIR model of Ames 12-ft tunnel (front view).

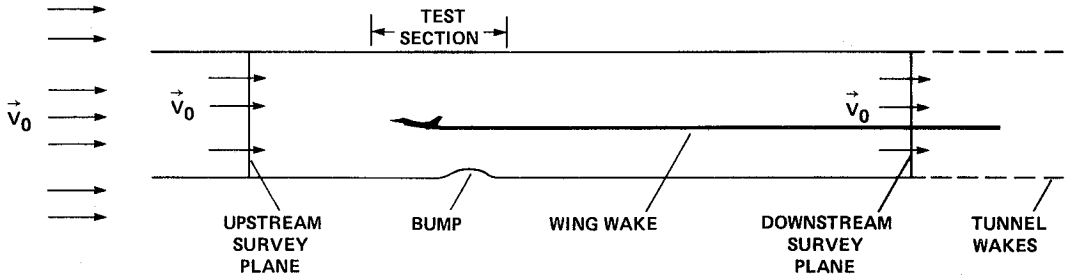

(b) Schematic of complete PAN AIR model; section shown at plane of symmetry.

Figure 65. Evaluation wall constraints using potential-flow paneling method (Ref. 84).

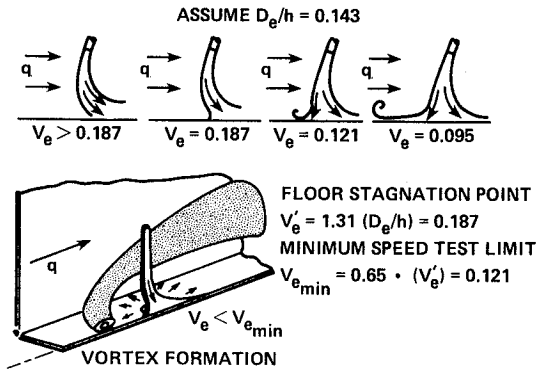

Figure 66. Minimum-speed testing limit for a configuration with two side-by-side lifting jets at $h/D_e = 7$ (Ref. 5).

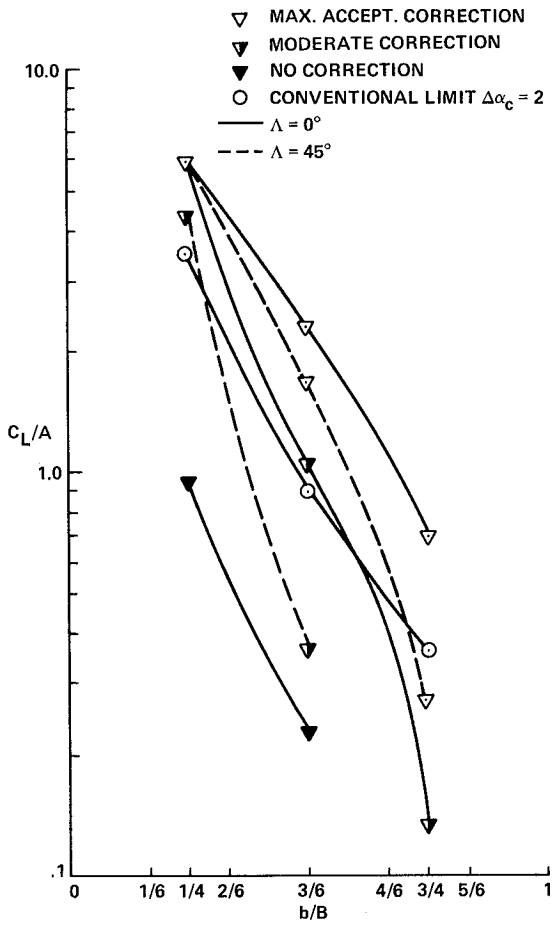

Figure 67. STOL testing limits: $D_j/L = 0$; model in center of wind tunnel; B/H = 4/3 (Ref. 88).

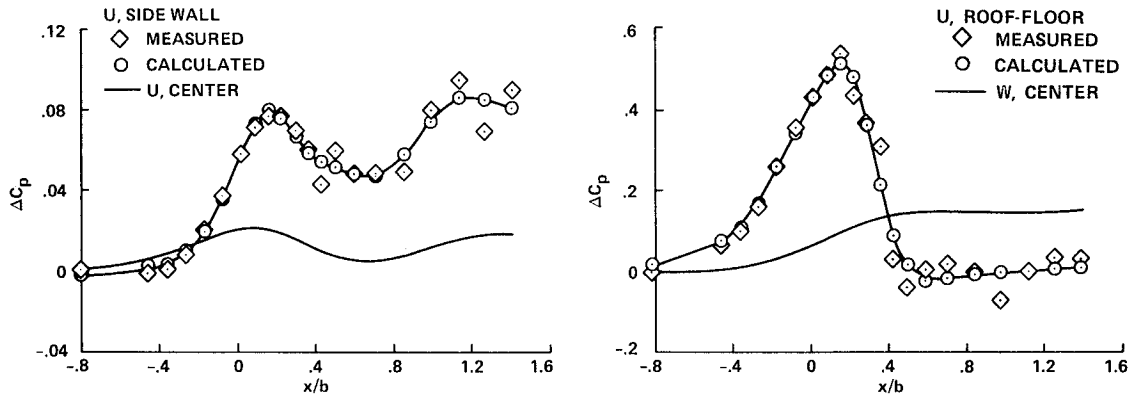

(a) Wall pressure signatures.

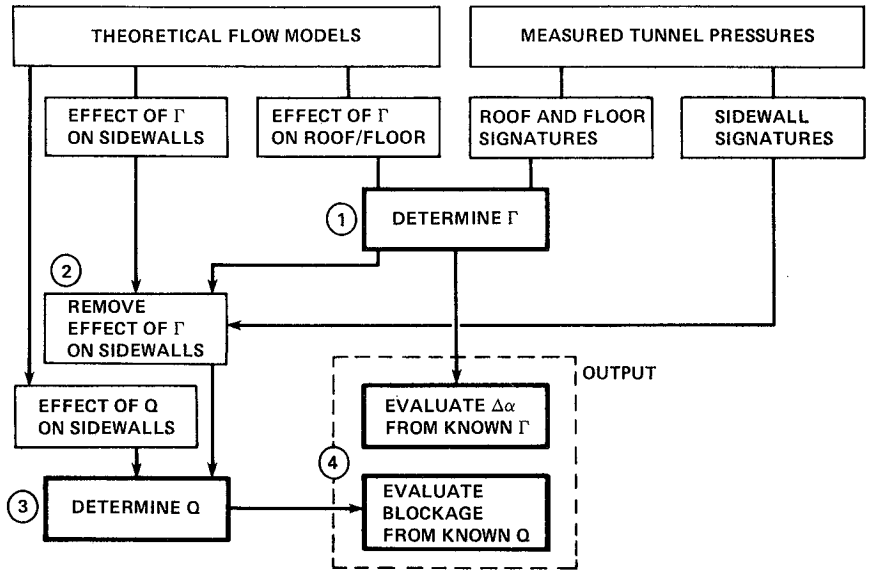

(b) Block diagram of procedure.

Figure 68. Evaluating wall corrections using wind-tunnel surface pressures (Ref. 82).

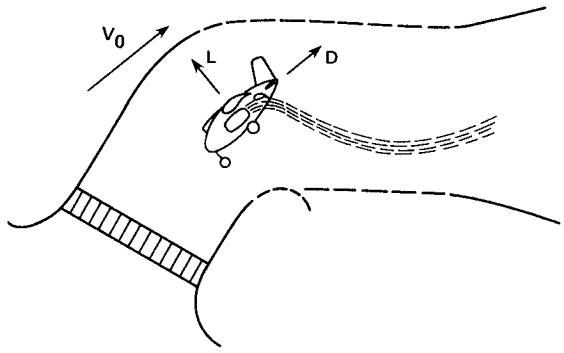

Figure 69. Adaptable wall concept for V/STOL wind-tunnel testing (Ref. 92).

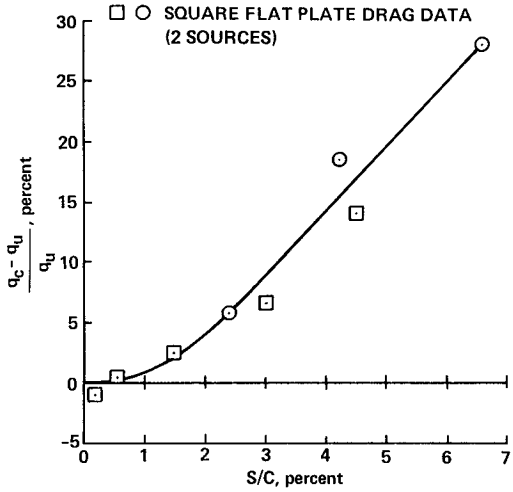

(a) Wake blockage correction to flat-plate drag data assuming $C_{D_c} = 1.17$.

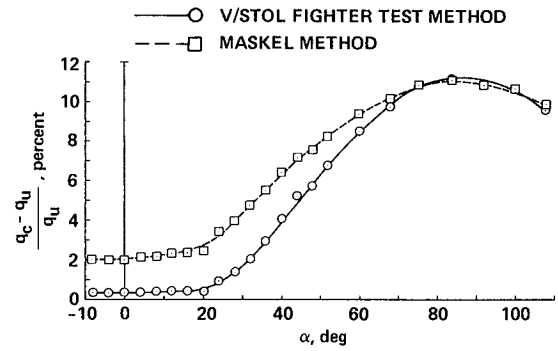

(b) Comparison of Maskell wake blockage correction with method developed for V/STOL fighter model test applied to test run.

Figure 70. Blockage corrections for high-angle-of-attack model (Ref. 60).

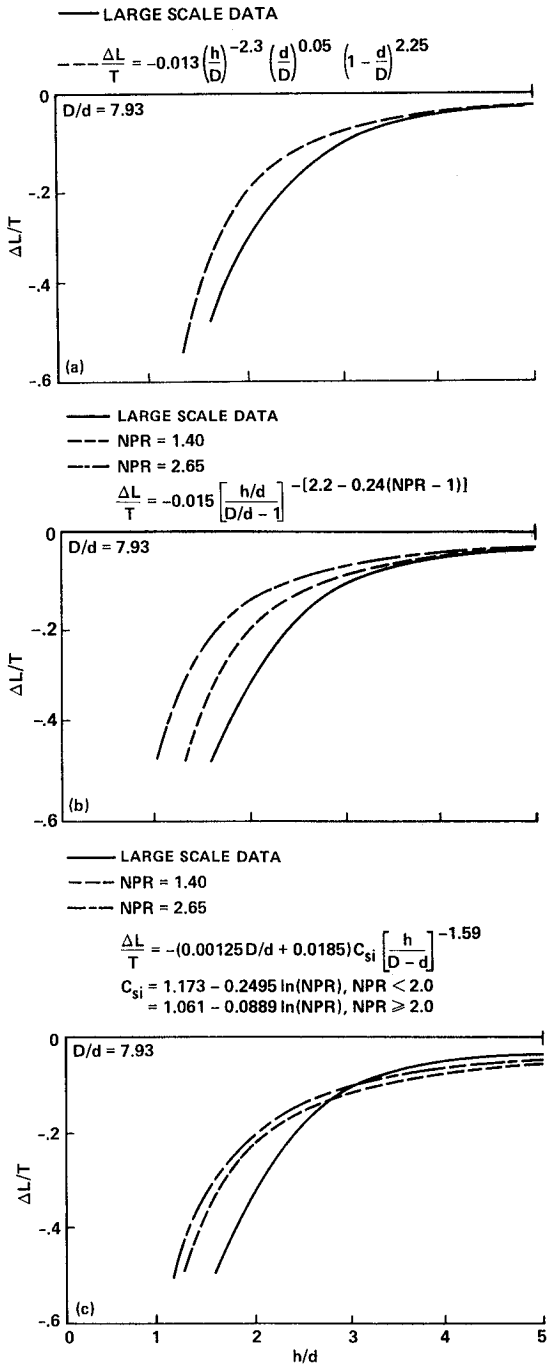

Figure 71. Comparison of large-scale data with predicted lift losses (Ref. 93).

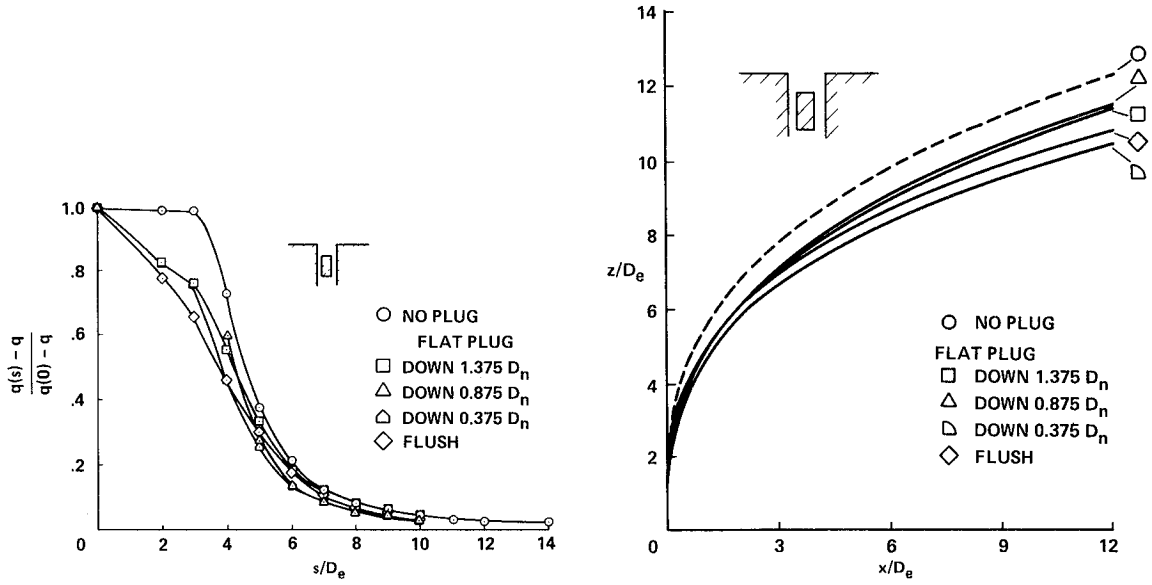

(a) Dynamic pressure decay. (b) Jet centerline trajectories.

Figure 72. Effect of a flat plug on characteristics of a round jet: R = 6 (Ref. 95).

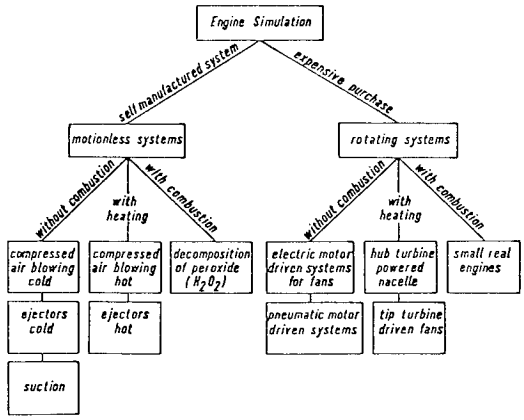

Figure 73. Classification of principal engine simulation techniques (from Ref. 97).

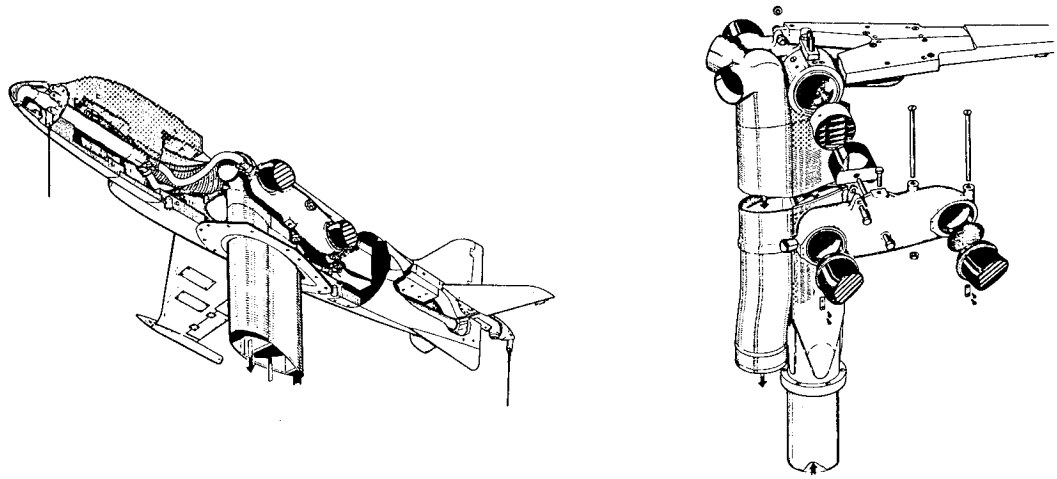

(a) General model arrangement. (b) Ducting and nozzle details.

Figure 74. Hawker P.1127, 1/10th-scale model (Ref. 63).

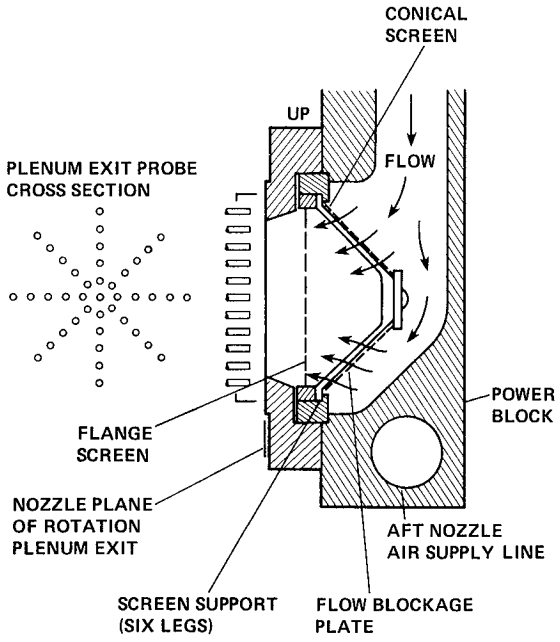

Figure 75. 15% AV-8B model nozzle air-feed design (Ref. 8).

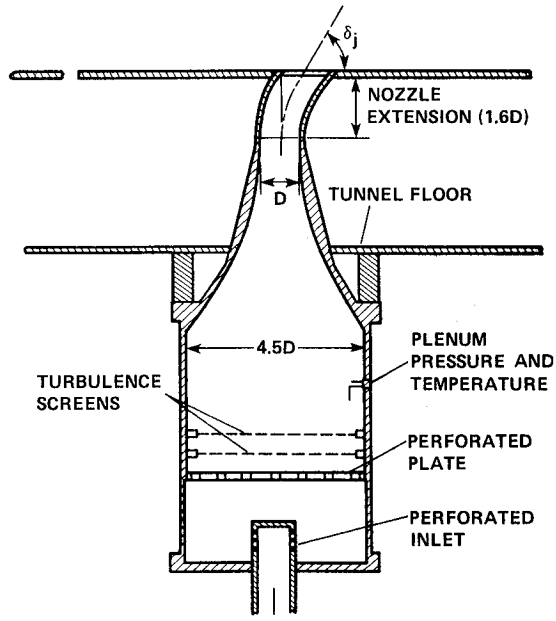

Figure 76. Nozzle and plenum chamber design to insure a jet with uniform velocity profile (Ref. 47).

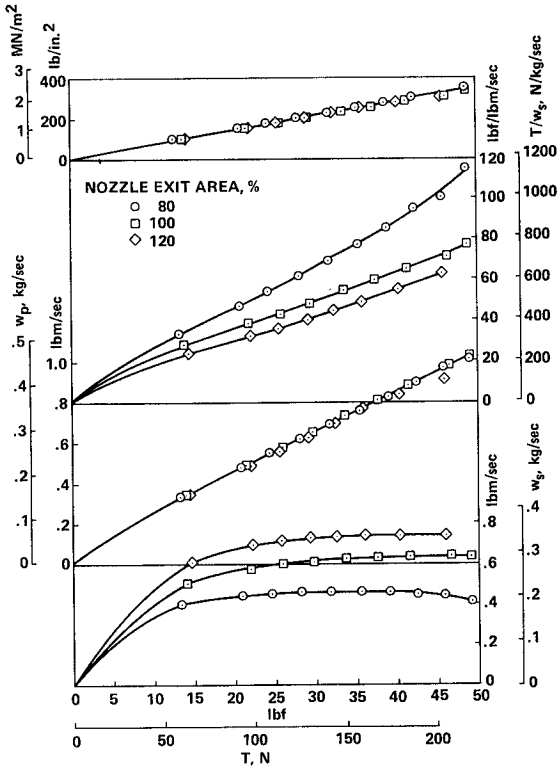

Figure 77. Effect of exit area ratio on ejector performance (Ref. 98).

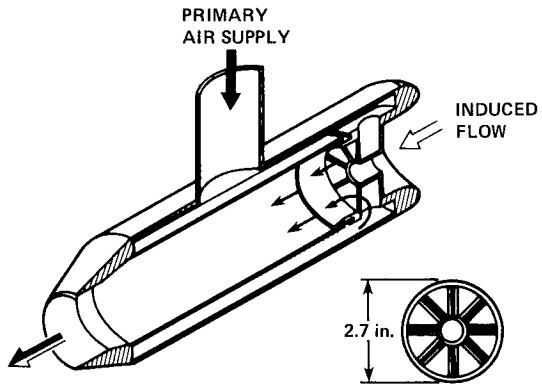

(a) Turbojet (Ref. 97).

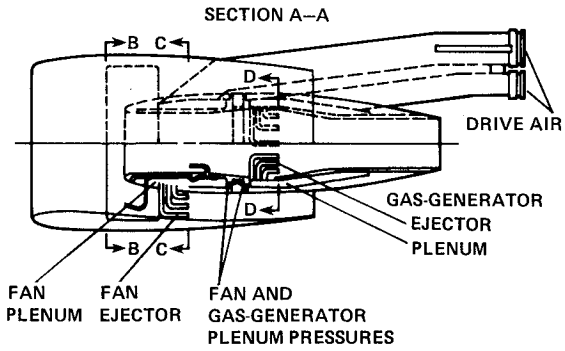

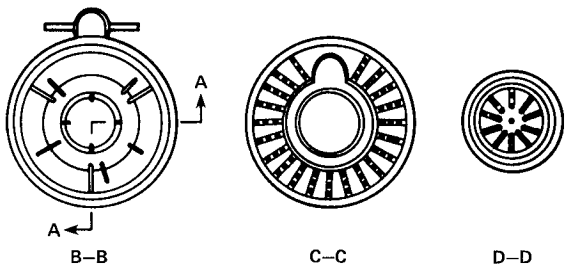

(b) Turbofan (Ref. 99).

Figure 78. Power simulation by ejectors.

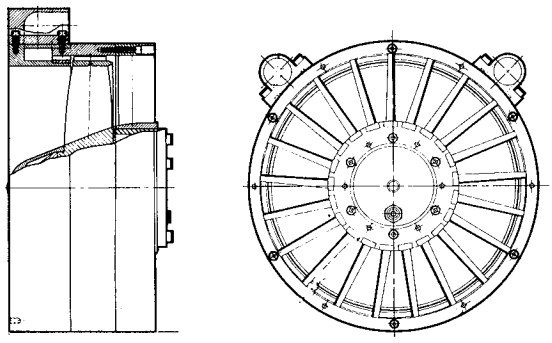

Figure 79. Tip-driven fan assembly.

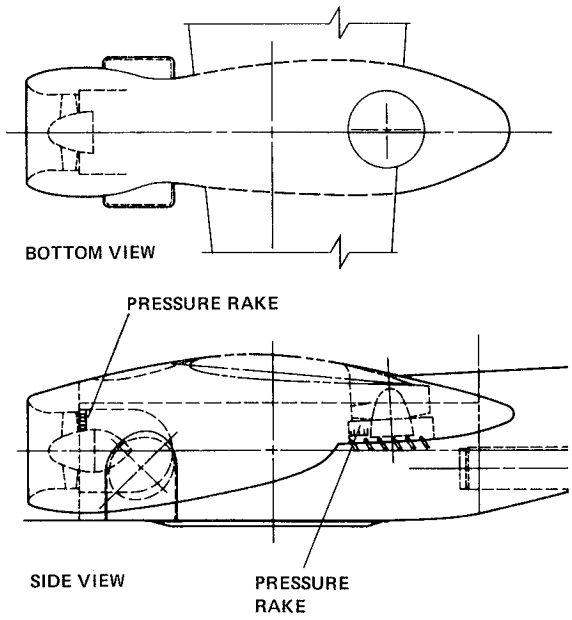

(a) Nacelle details.

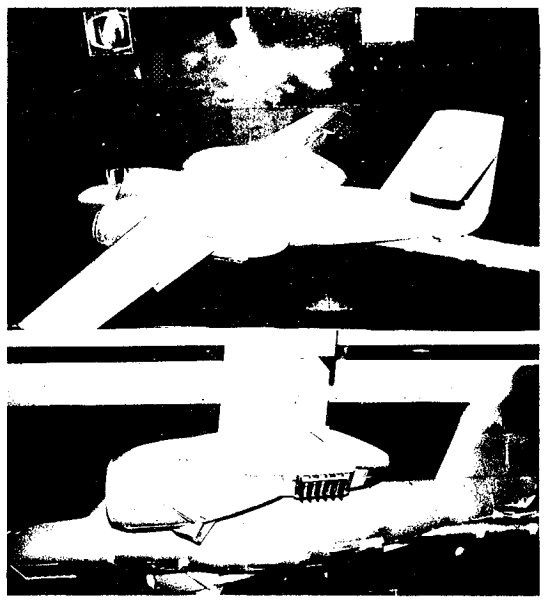

(b) Model installed in the Langley 4- by 7-m tunnel.

Figure 80. Use of tip-driven fan in a lifting-nacelle configuration (Ref. 101).

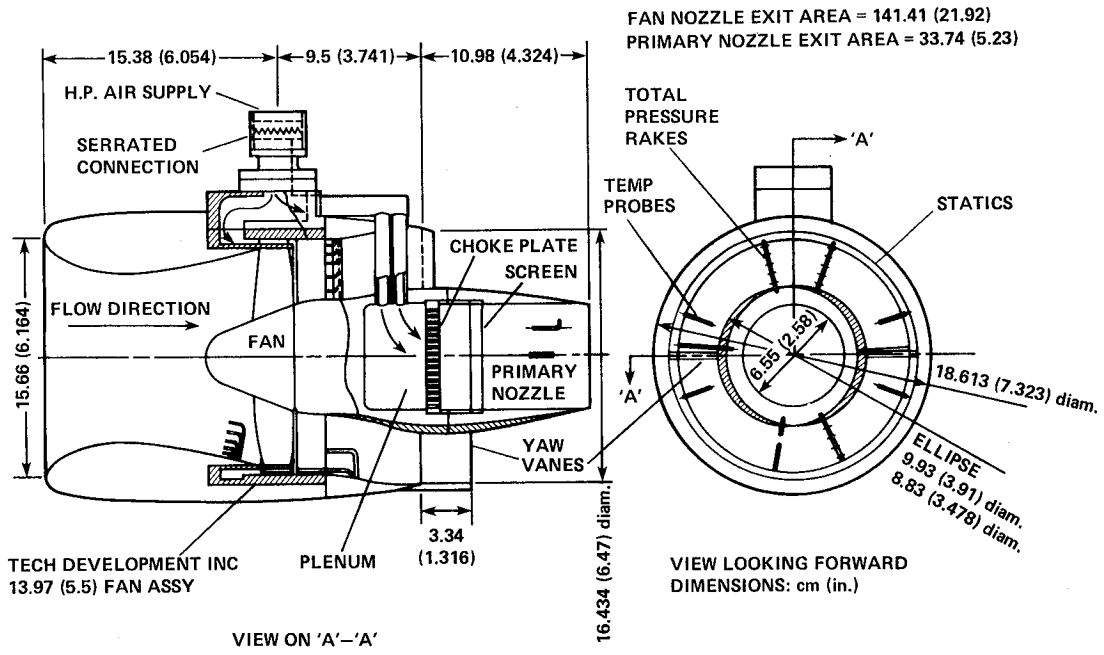

Figure 81. Use of 5.5-in. tip-driven fan in Boeing lift-cruise fan assembly (Ref. 102).

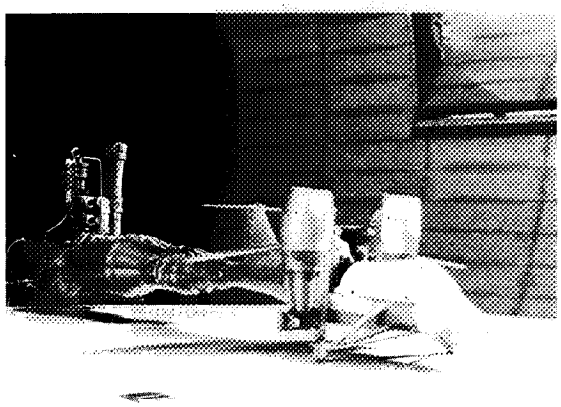

Figure 82. 11% Grumman V/STOL model in ground effect tests.

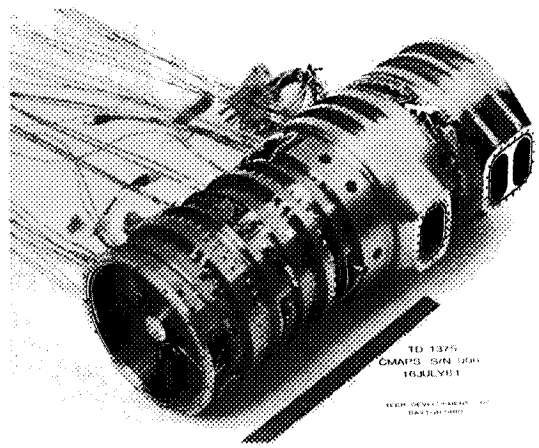

Figure 83. CMAPS before installation into a model.

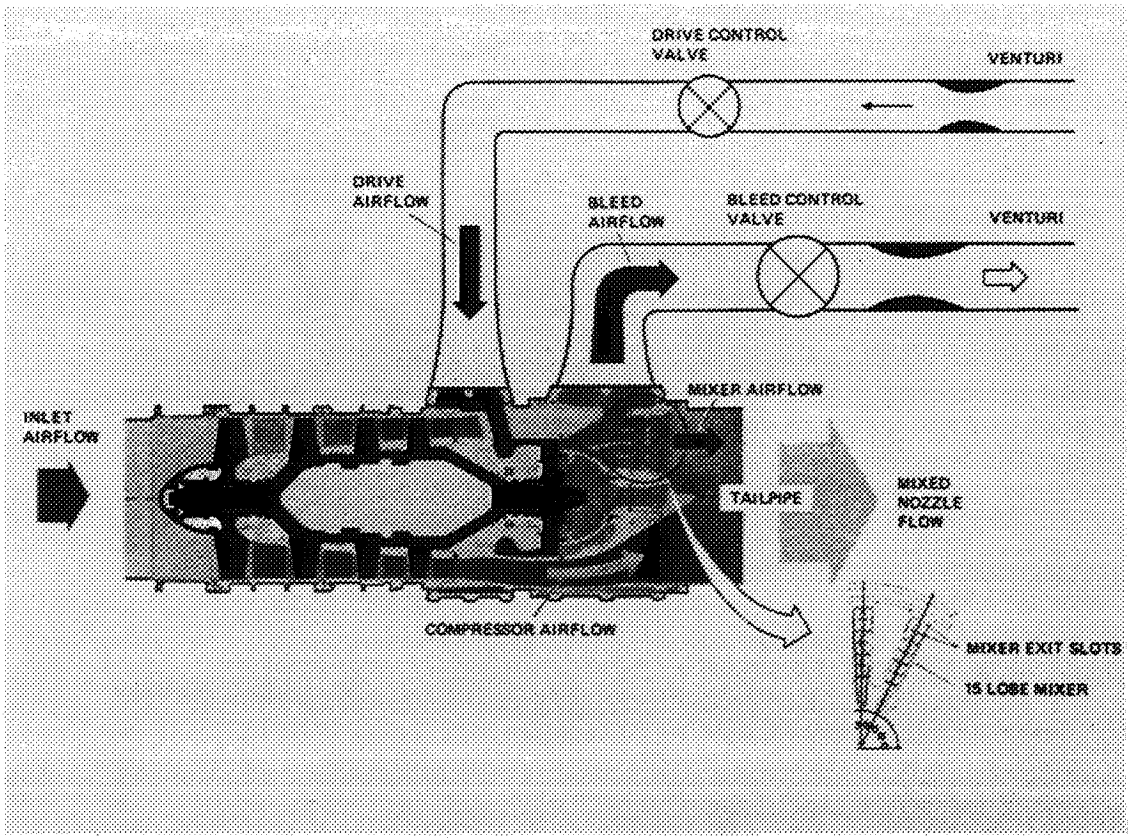

Figure 84. Schematic of CMAPS.

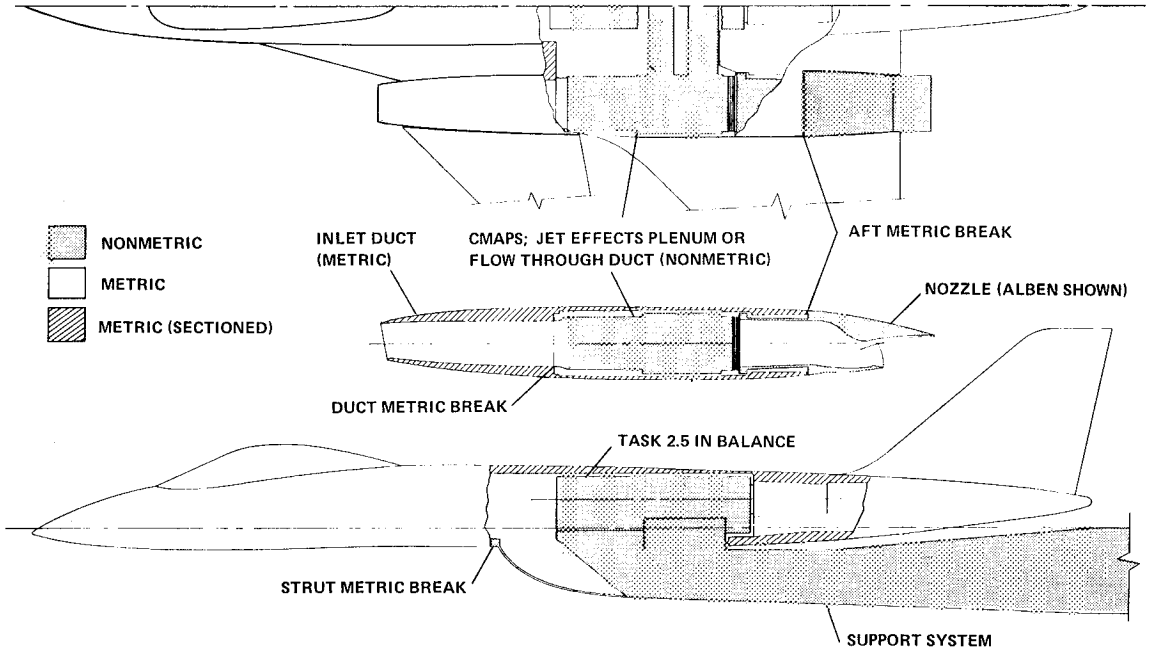

Figure 85. Support system for the CMAPS-powered model shown in Fig. 45 (Ref. 105).

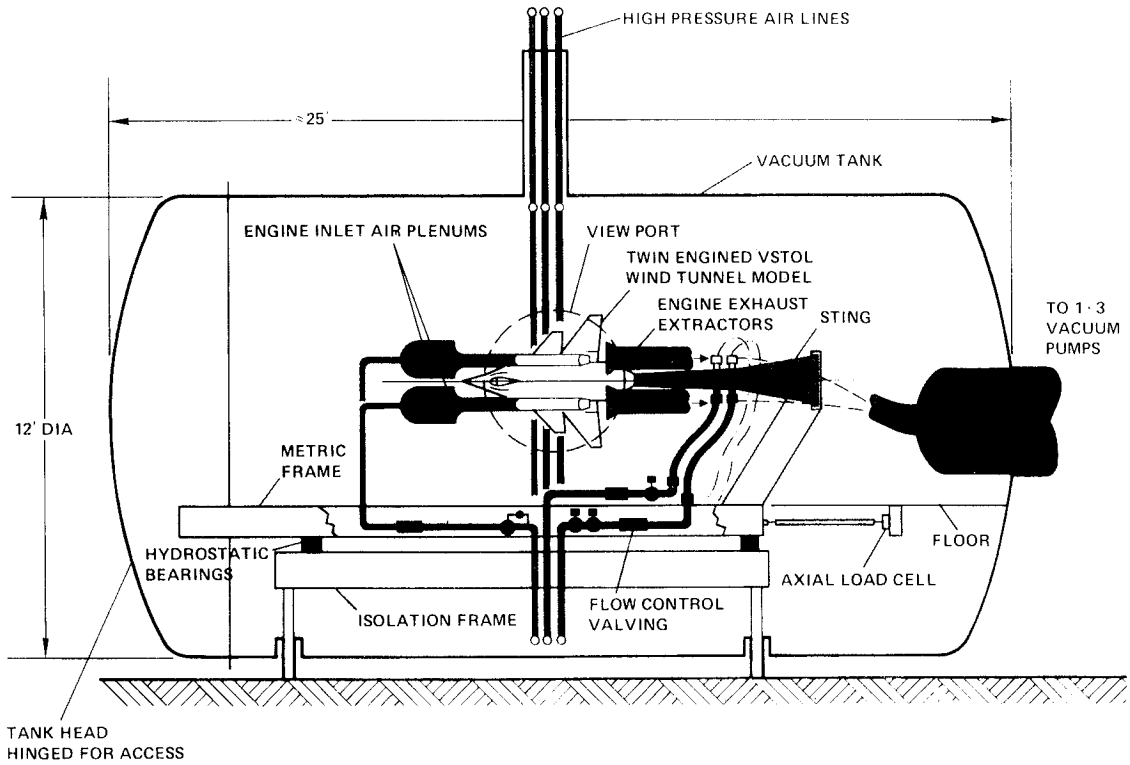

Figure 86. CMAPS calibration tank (Ref. 106).

	THRUST		W		P_T/P_O	A_e	
	N	(lb)	kg/sec	(lb/sec)		m^2	$(in.^2)$
J85-5	11,560	(2600)	19.28	(42.5)	2.24	.0742	(115)
T58	2,670	(600)	5.67	(12.5)	2.1	.0188	(29.2)
J97	20,020	(4500)	31.75	(70)	3.0	.0839	(130)
JT15-D	8,450	(1900)	34.02	(75)	1.35	.1419	(220)

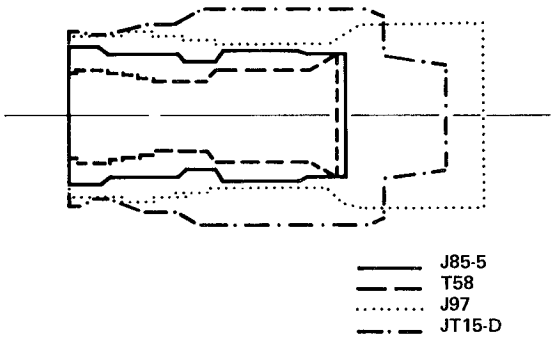

Figure 87. Relative engine sizes of small gas turbines (Ref. 4).

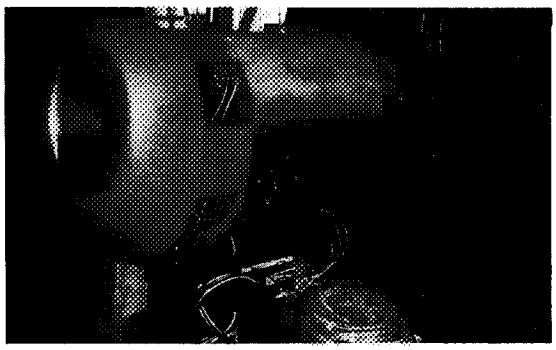

(a) 3/4 front view.

(b) 3/4 rear view.

Figure 88. A JT15D installation for an upper-surface blowing model (Ref. 104).

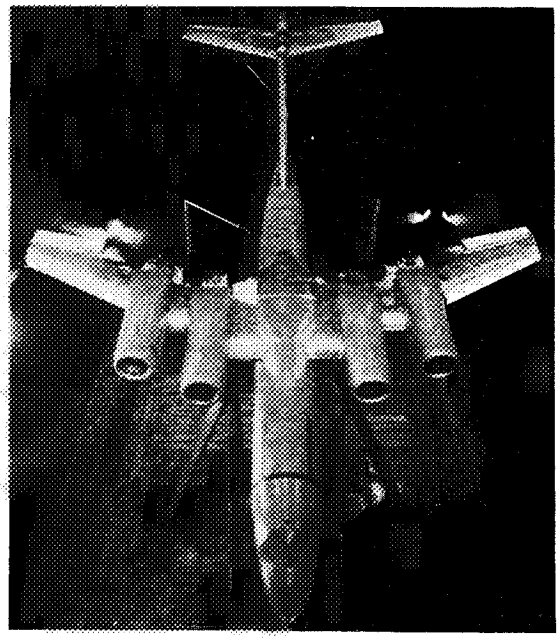

Figure 89. Large-scale upper-surface model using the JT15D engines (Ref. 15).

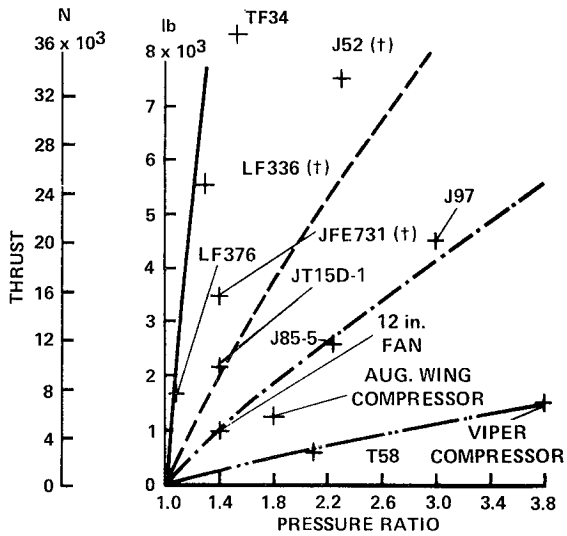

REFERENCE LINES

$Cd \cdot C_V \cdot A_N \cdot \rho_N \cdot V_j^2$

WHERE:

A_N =

m^2	$in.^2$
0.485	1045
0.102	220
0.051	110
0.014	30

Cd = .96
C_v = .95

(†) ESTIMATED

Figure 90. Thrust as a function of pressure for several candidate large-scale model engines (Ref. 4).

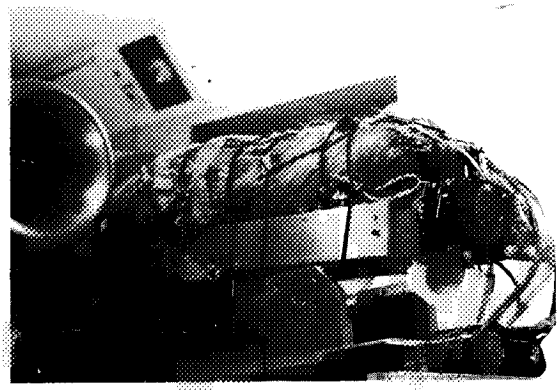

Figure 91. 11% G698 on-board instrumentation shown ready for installation of the fuselage shell.

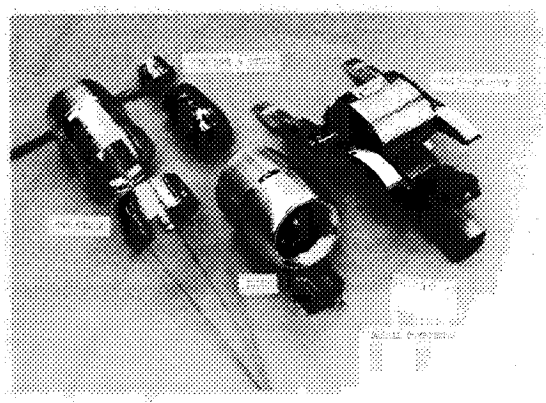

Figure 92. Nacelle components for the 11%-scale G698 model.

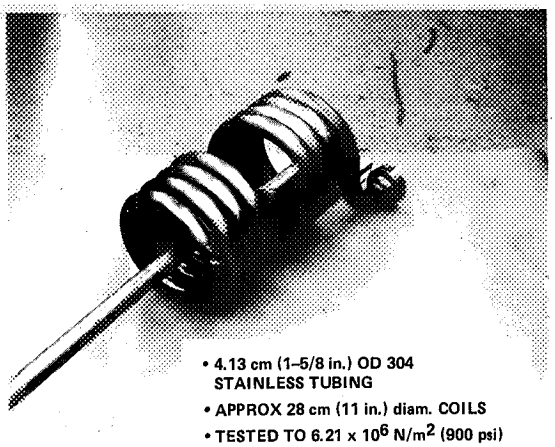

Figure 93. Drive-air force-isolation coil for the 11% G698 model.

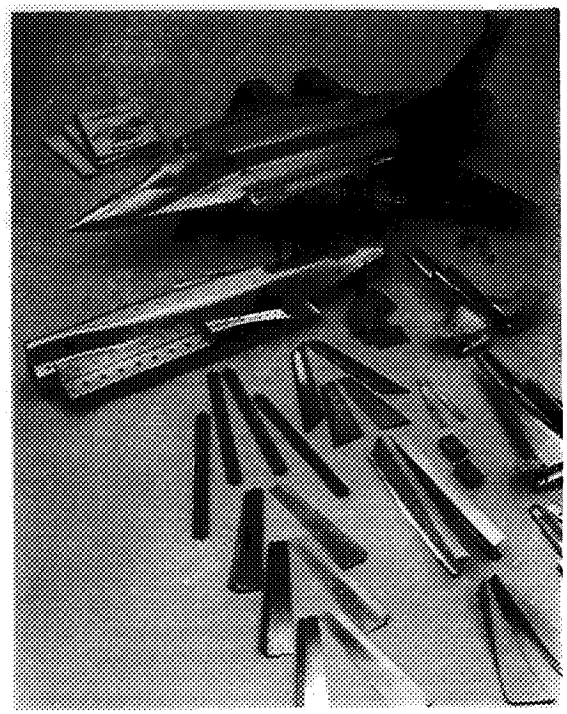

Figure 94. Model parts for the high-speed, two-engine fighter model of Fig. 43.

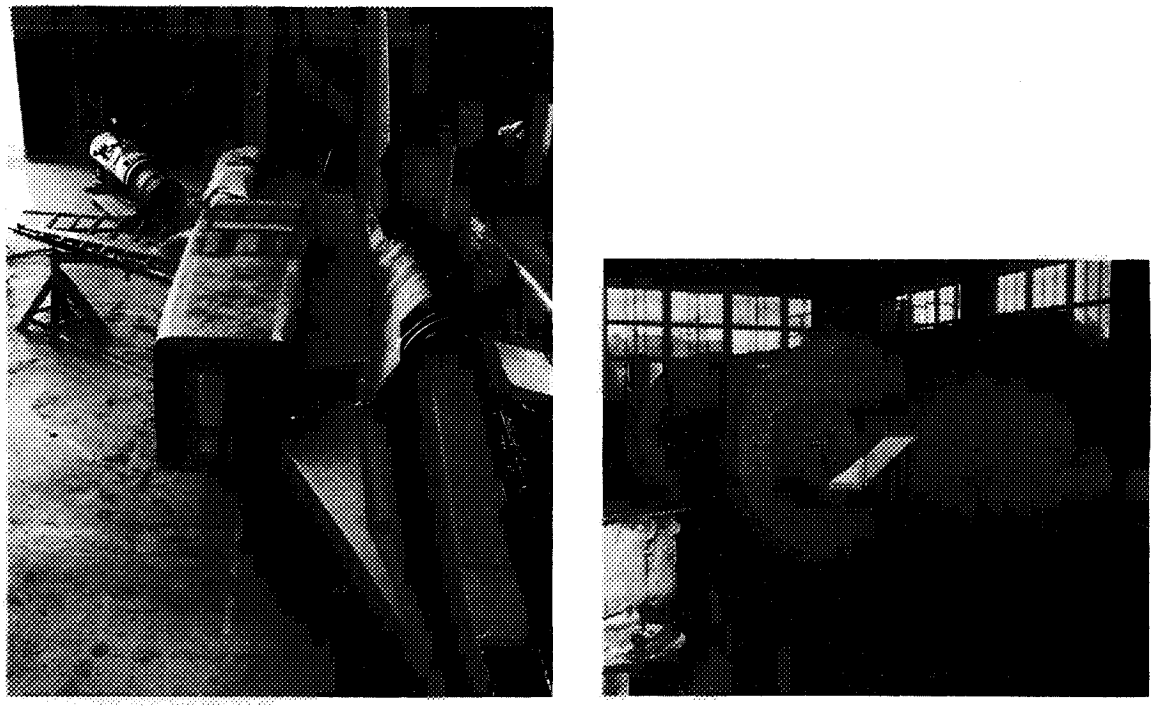

(a) Metal fabrication of model shown in Fig. 8.

(b) Soft construction use of polyurethane foam.

Figure 95. Boiler-plate model construction.

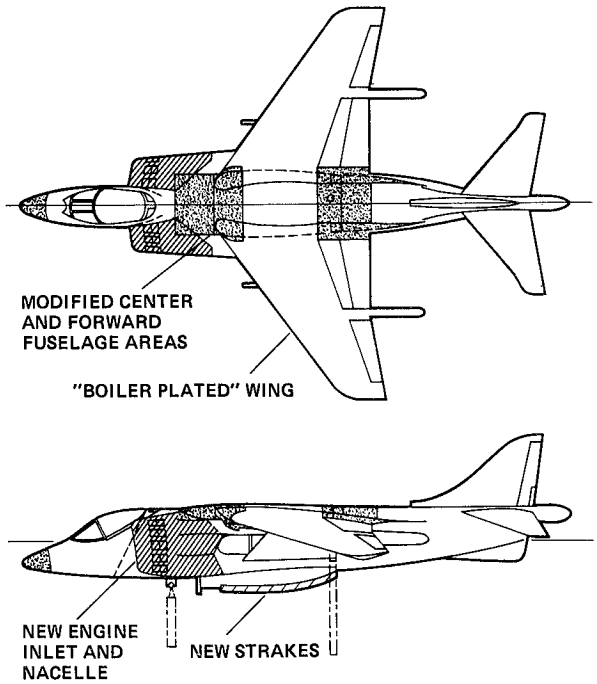

Figure 96. Boiler-plate plan for the full-scale AV-8B model (Ref. 8).

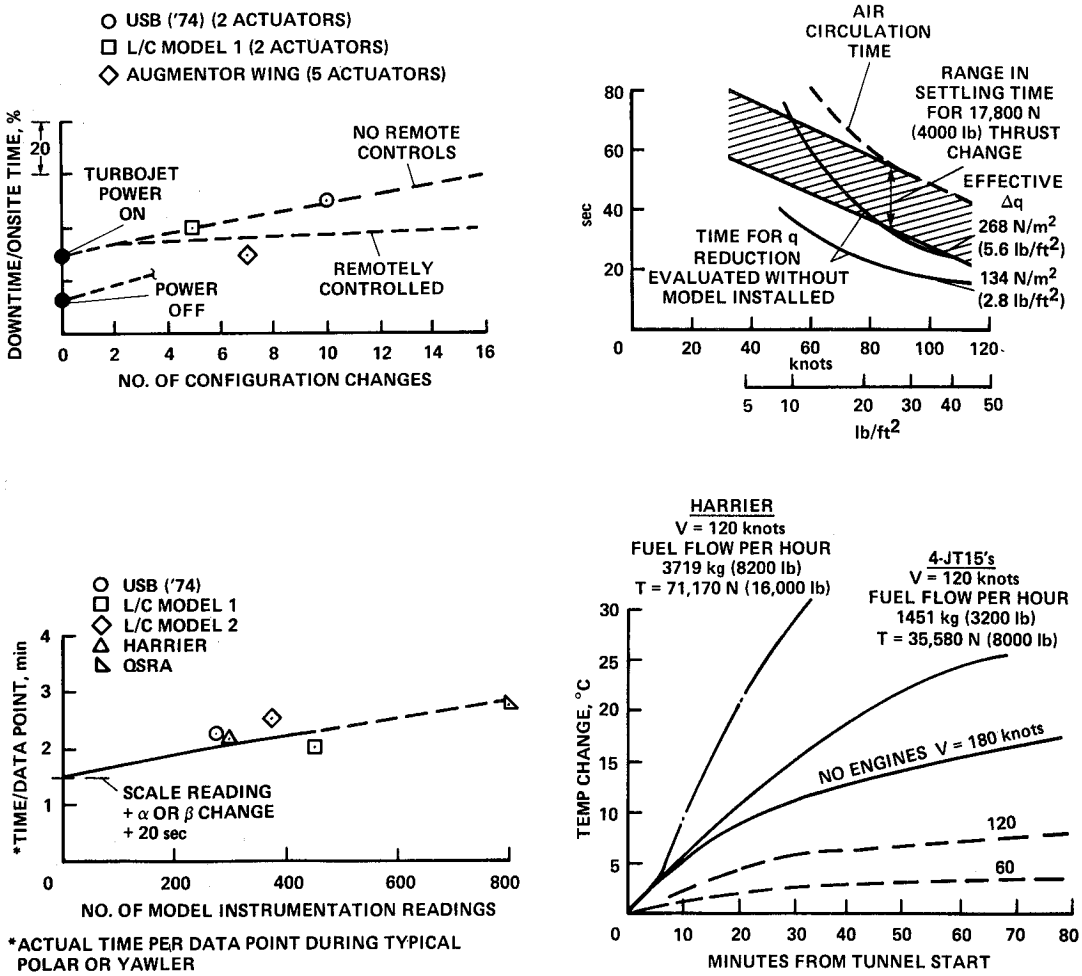

Figure 97. Factors influencing testing time for powered models in the Ames 40 by 80 (Ref. 4).

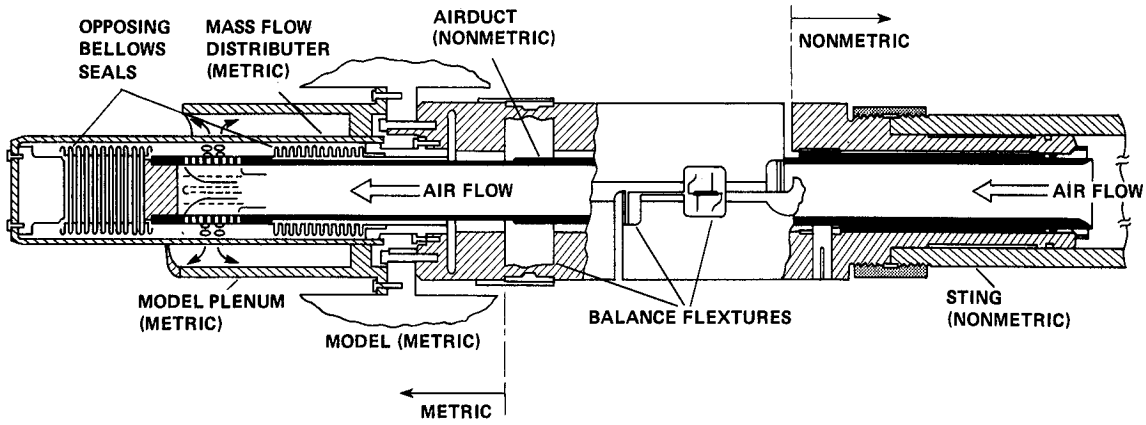

Figure 98. Schematic of flow-through internal balance (Ref. 109).

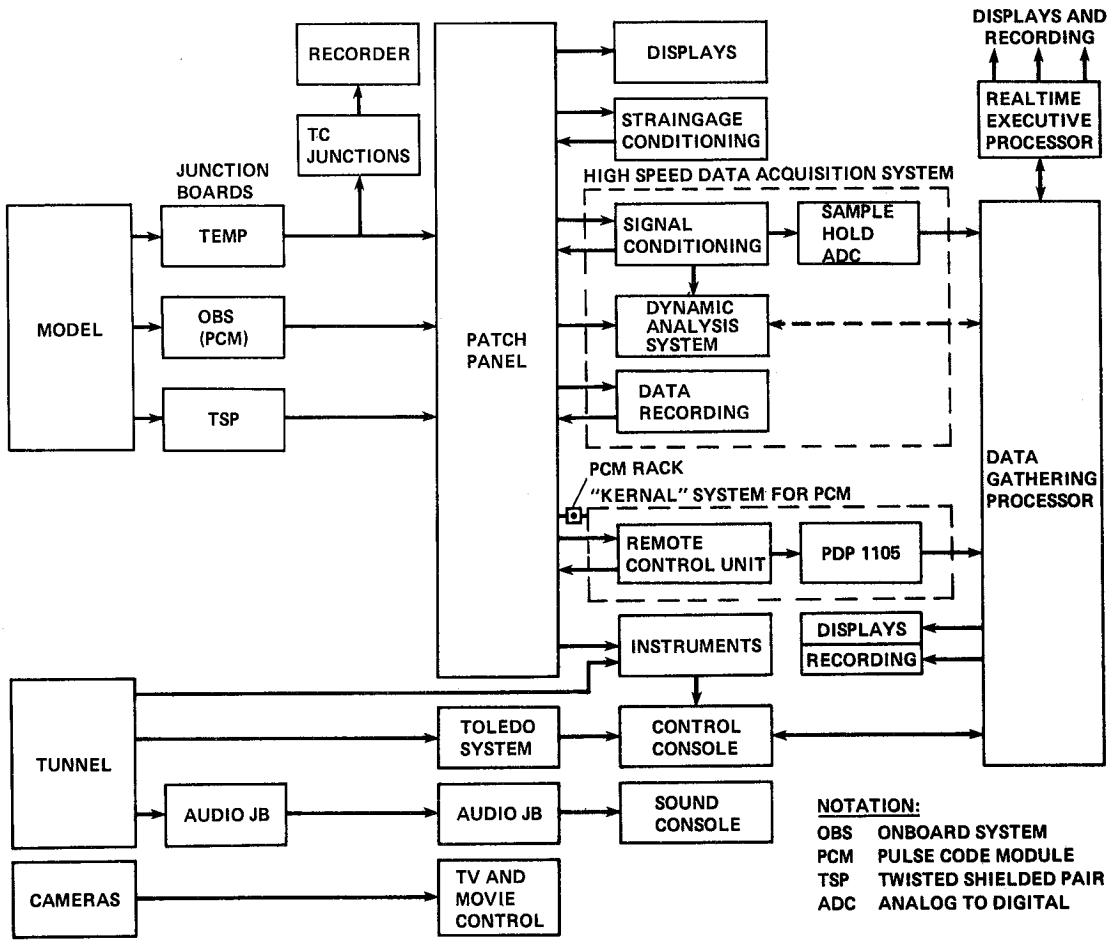

Figure 99. 40 by 80 data-acquisition system.

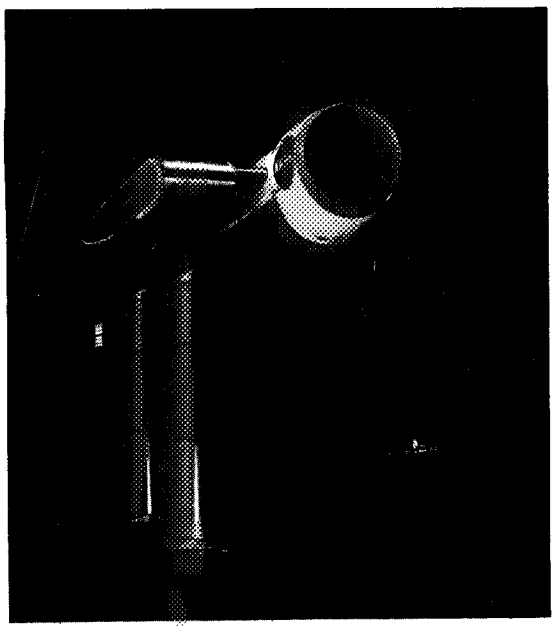

Figure 100. JT8D mounted in wind tunnel for the jet noise investigation (Ref. 114).

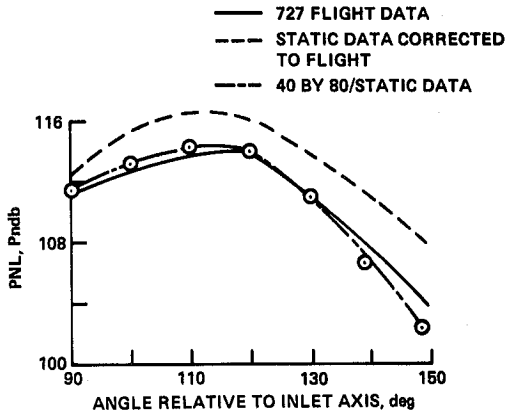

Figure 101. Comparison of 40- by 80-ft wind tunnel and flight-stand data with the 20-lobe ejector suppressor on a JT8D-17 turbofan engine (Ref. 114).

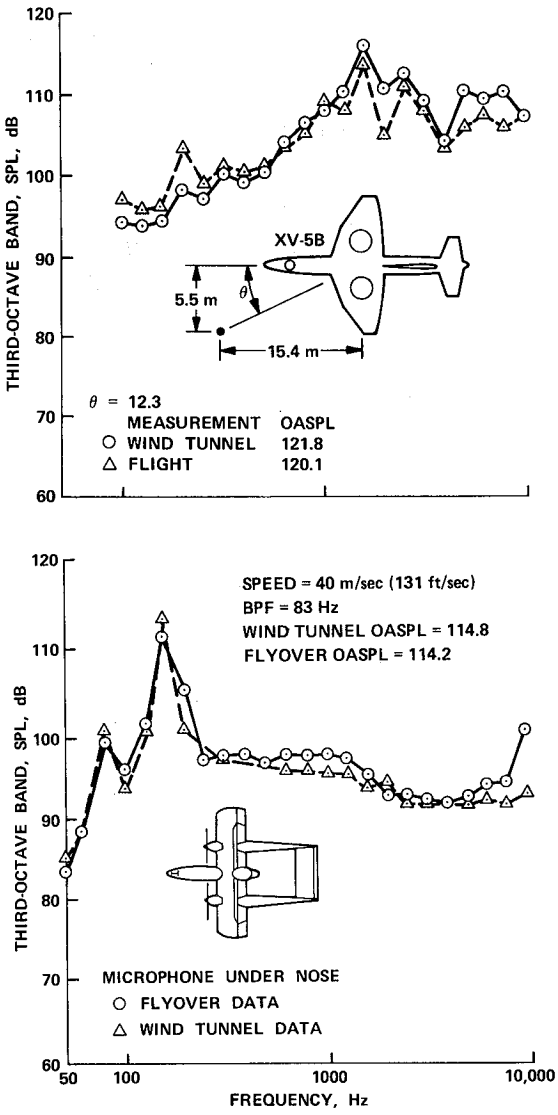

Figure 102. Comparison of corrected flyover and 40- by 80-ft wind tunnel noise data at equal distance for two aircraft (Ref. 120).

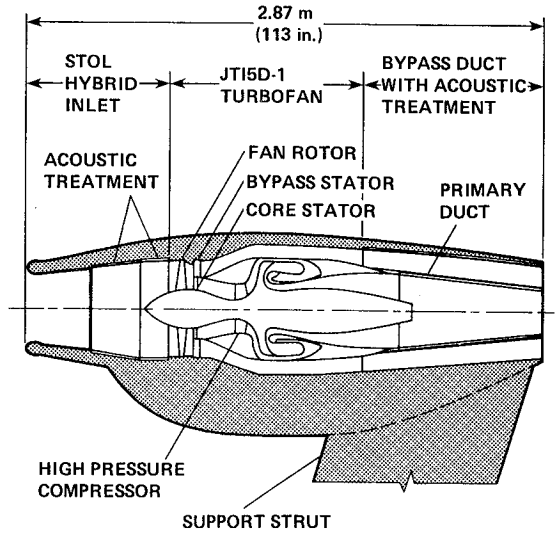

Figure 103. Hybrid inlet nacelle installation (Ref. 122).

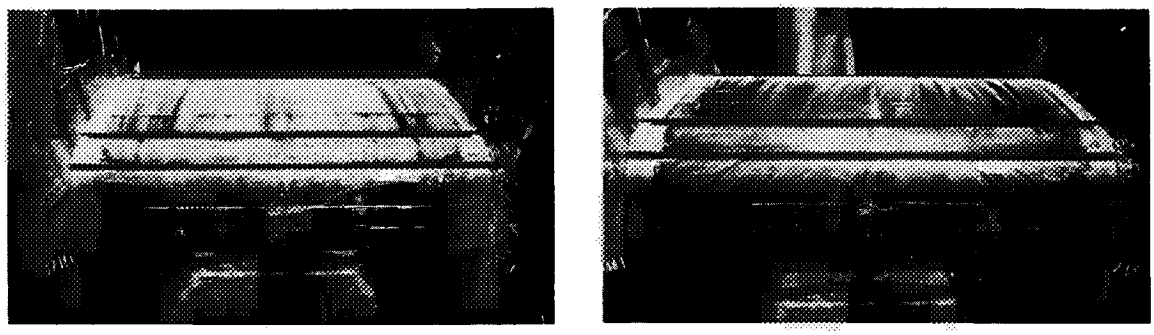

Figure 104. Oil-smear evaluation of flow on multiairfoil two-dimensional model (Ref. 49).

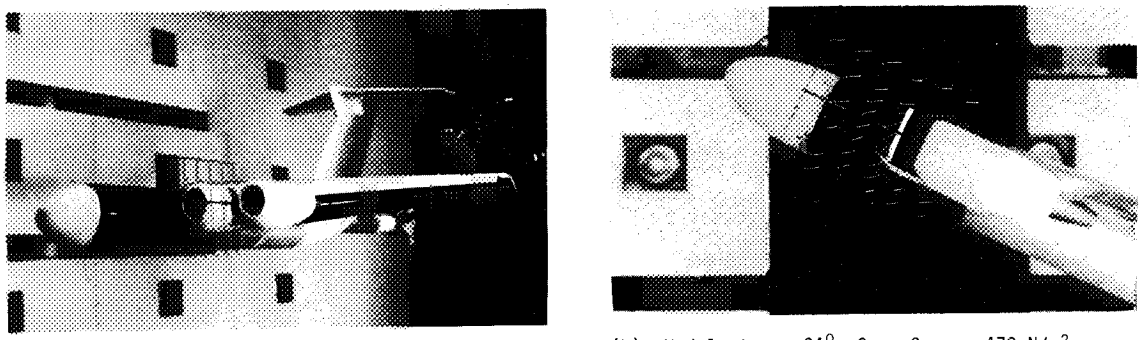

(a) Model installation.

(b) Model at $\alpha = 24^{o}$, $C_j = 2$, $q = 479$ N/m^2 (10 lb/ft^2).

Figure 105. Tuft grid study for evaluating upwash near inlet of EBF transport model (Ref. 130).

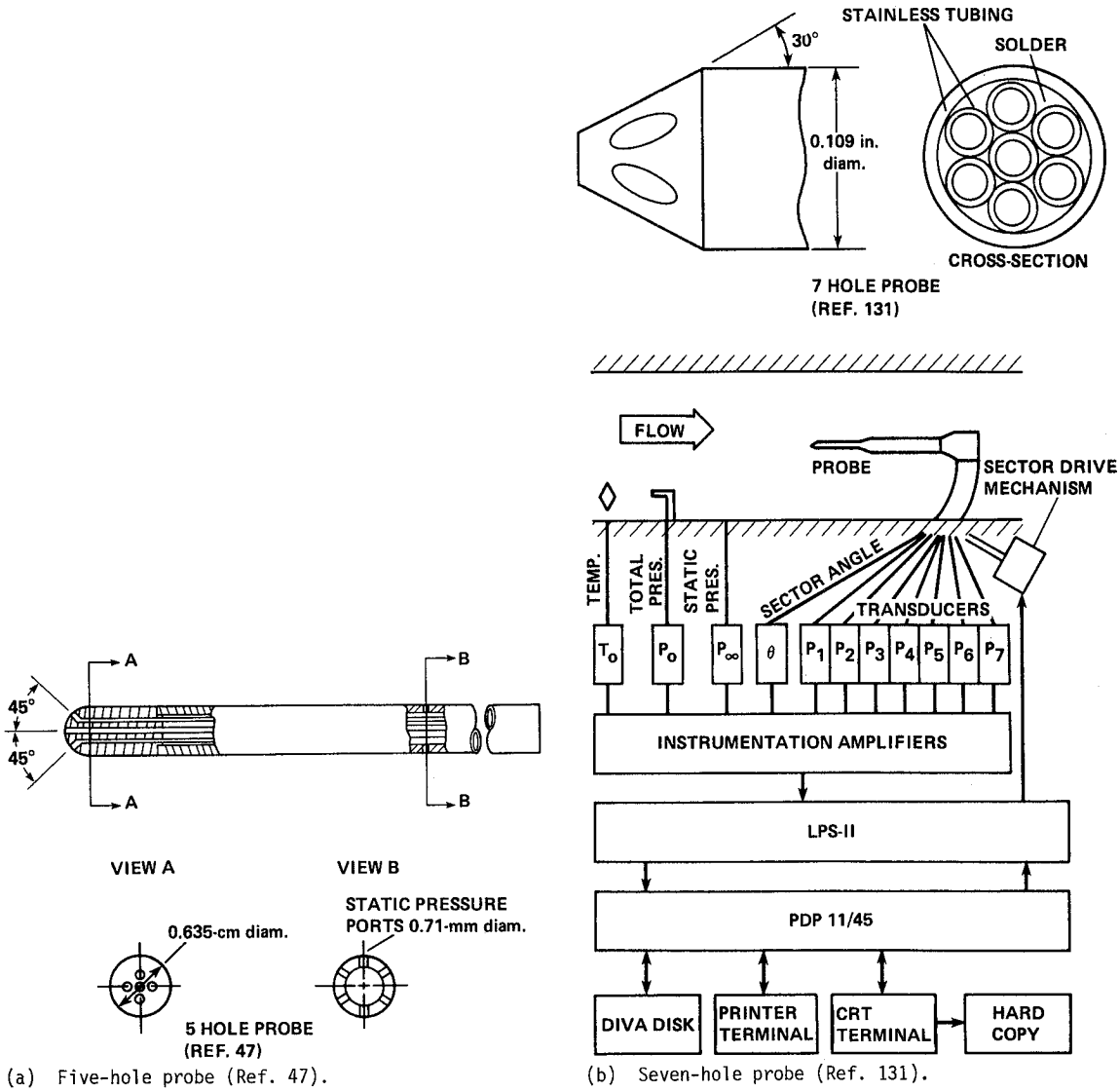

(a) Five-hole probe (Ref. 47).

(b) Seven-hole probe (Ref. 131).

Figure 106. Five- and seven-hole directional probes.

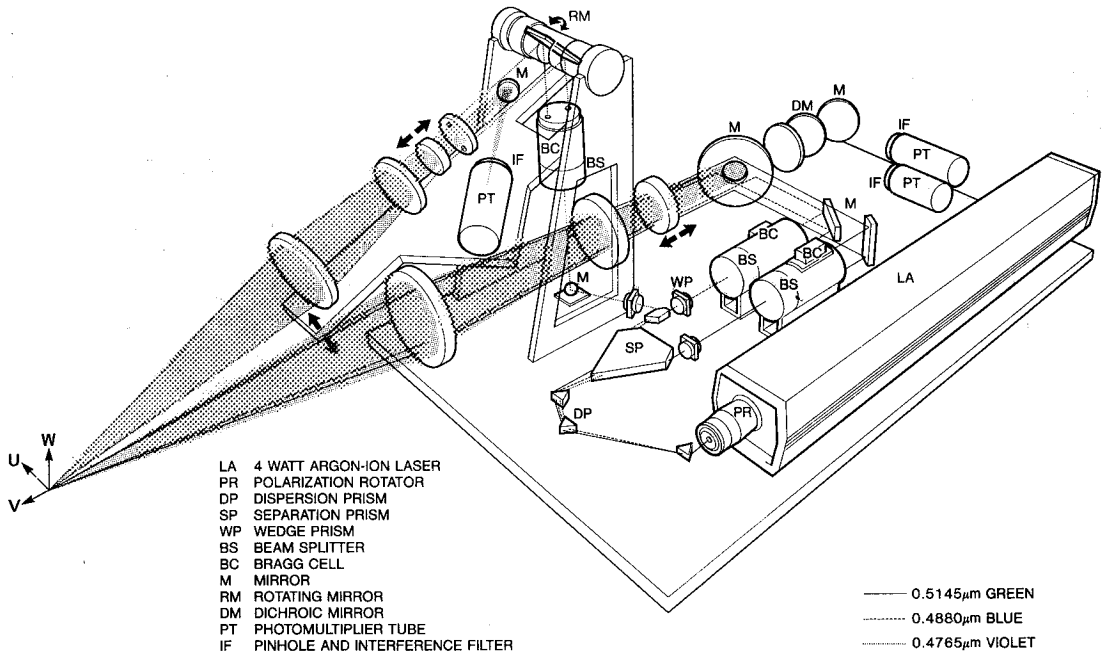

(a) Three-dimensional laser velocimeter. Uses three different colors from a single argon-ion laser to form three independent dual-scatter backscatter channels.

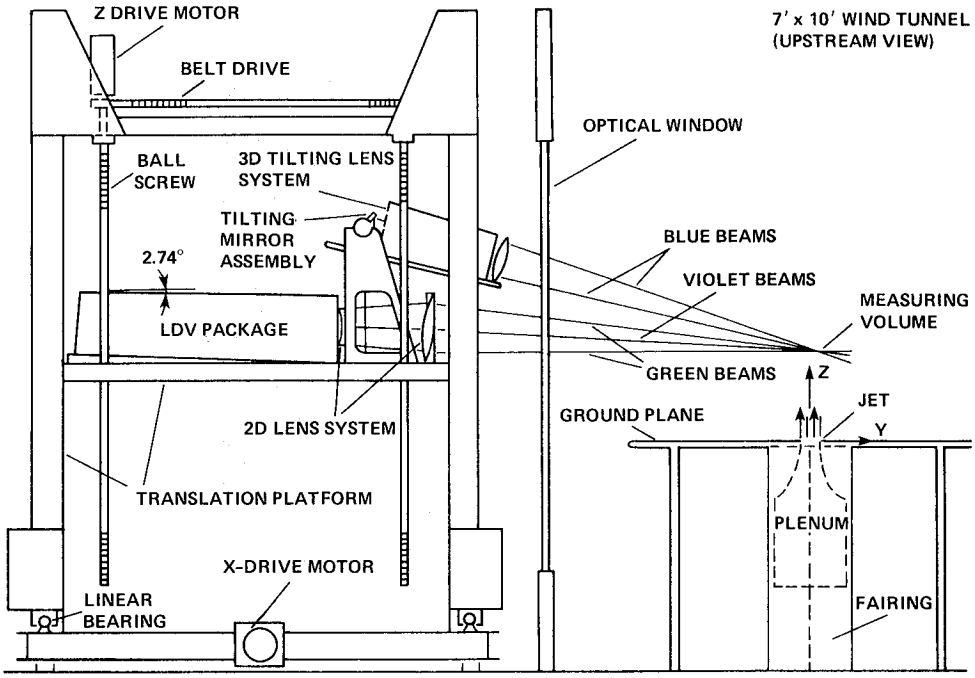

(b) Three-dimensional LDA translation platform and tunnel installation for the jet-in-a-cross-flow test.

Figure 107. Three-dimensional laser velocimeter (Ref. 132).

Figure 108. Three-dimensional laser velocimeter operating in the Ames 7 by 10 wind tunnel; jet-in-cross-flow test.

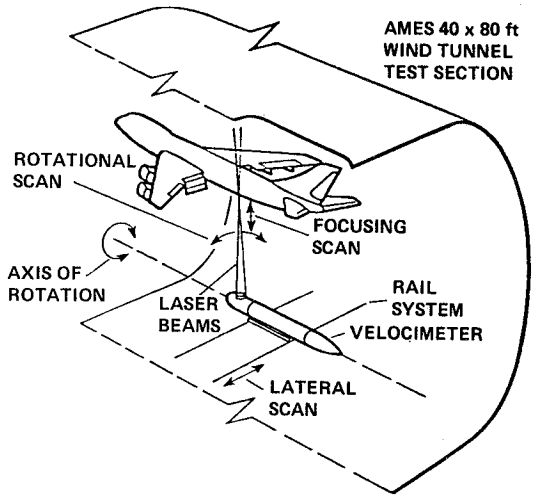

Figure 109. Use of two-dimensional laser velocimeter in large wind tunnel (40 by 80 shown) (Ref. 135).

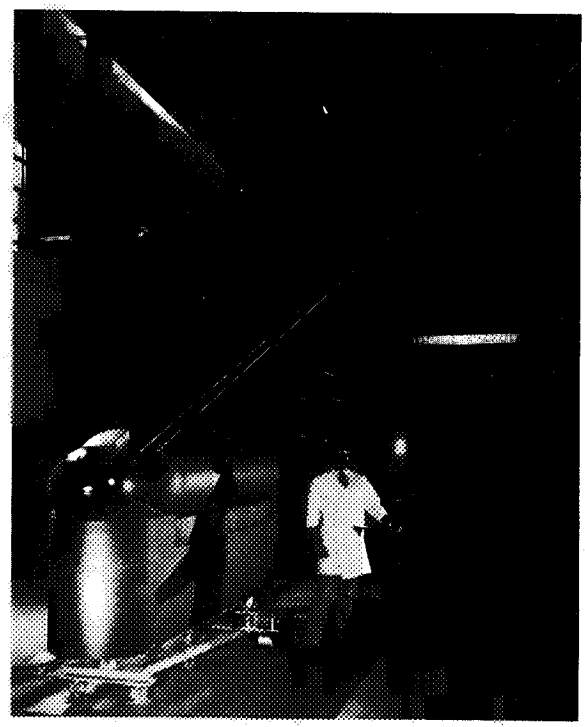

Figure 110. Large laser velocimeter in operation.

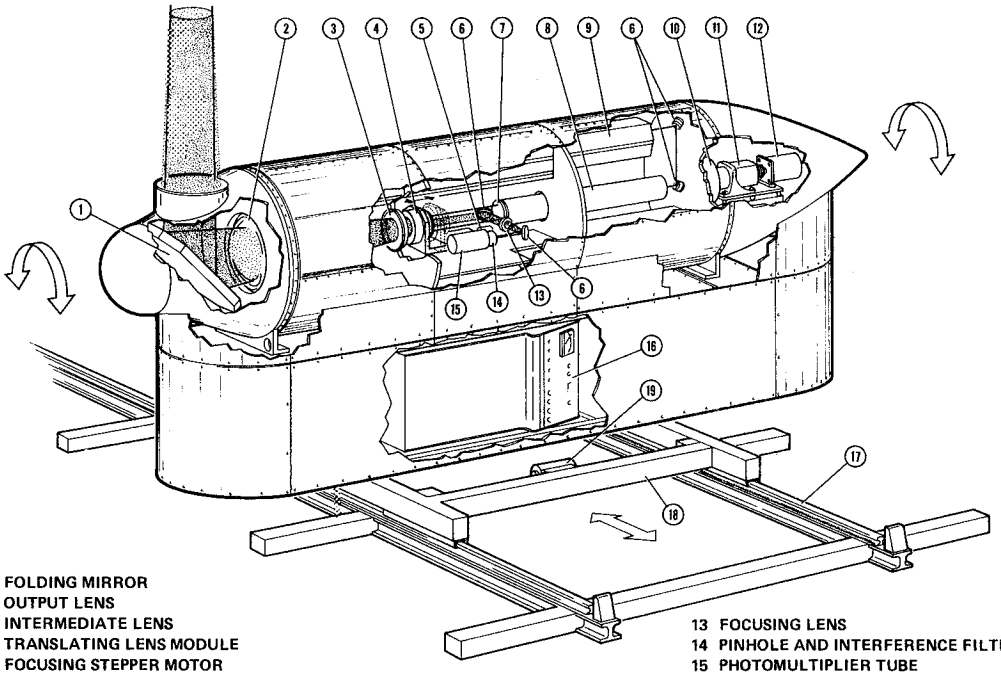

Figure 111. Laser-velocimeter system shown mounted on lateral traversing rails; insert shows alternative method of receiving for extended-range configuration (both beam pairs are shown in the insert (Ref. 135).

1. Report No.	2. Government Accession No.	3. Recipient's Catalog No.
NASA TM-85936		

4. Title and Subtitle	5. Report Date
V/STOL WIND-TUNNEL TESTING	May 1984
	6. Performing Organization Code
7. Author(s)	8. Performing Organization Report No.
David G. Koenig	A-9694
	10. Work Unit No.
9. Performing Organization Name and Address	T-3514
Ames Research Center Moffett Field, CA 94035	11. Contract or Grant No.
	13. Type of Report and Period Covered
12. Sponsoring Agency Name and Address	Technical Memorandum
National Aeronautics and Space Administration Washington, DC 20546	14. Sponsoring Agency Code
	505-43-01

15. Supplementary Notes

Point of Contact: David G. Koenig, Ames Research Center, MS 247-1, Moffett Field, CA 94035 (415) 965-5047 or FTS 448-5047

16. Abstract

Factors influencing effective program planning for V/STOL wind-tunnel testing are discussed. The planning sequence itself, which includes a short checklist of considerations that could enhance the value of the tests, is also described. Each of the considerations, choice of wind tunnel, type of model installation, model development and test operations, is discussed, and examples of appropriate past and current V/STOL test programs are provided. A short survey of the moderate to large subsonic wind tunnels is followed by a review of several model installations, from two-dimensional to large-scale models of complete aircraft configurations. Model sizing, power simulation, and planning are treated, including three areas in test operations: data-acquisition systems, acoustic measurements in wind tunnels, and flow surveying.

17. Key Words (Suggested by Author(s))	18. Distribution Statement
Wind-tunnel testing Powered-lift testing Propulsion simulation V/STOL aircraft	Unlimited Subject Category - 01

19. Security Classif. (of this report)	20. Security Classif. (of this page)	21. No. of Pages	22. Price*
Unclassified	Unclassified	74	A04

*For sale by the National Technical Information Service, Springfield, Virginia 22161